PROPERTIES OF THE NUCLEOTIDE BINDING SITES OF THE Ca^{2+}-ATPase OF SARCOPLASMIC RETICULUM

This thesis is presented in partial fulfillment for the degree of Master of Science in the Faculty of Medicine, University of Cape Town

by

David Richard Jeans, B.Sc. (Med)(Hons).(Cape Town)

September 1988

TO STEPHANIE

ABBREVIATIONS

AcP	Acetyl Phospate
ATP	Adenosine triphosphate
E	The Ca^{2+}-ATPase
E_1, E_2	Conformational forms of the enzyme
EGTA	[ethylene-bis(oxyethylenenitrilo)]tetraacetic acid
EP	Phosphoenzyme
FITC	Fluorescein isothiocyanate
IAEDANS	5-(2-((iodoacetyl)amino)ethyl)aminonaphthalene-1-sulfonic acid
LDH	Lactate dehydrogenase
LSR	Light sarcoplasmic reticulum
Mops	3-(N-morpholino) propanesulfonic acid
NEM	N-ethyl maleimide
Pi	Inorganic phosphate
PK	Pyruvate kinase
RR	Ruthenium red
SDS-PAGE	Sodium dodecyl sulphate polyacrylamide gel electrophoresis
SRV	Sarcoplasmic Reticulum Vesicles
TC	Terminal cisternae
TEMED	N, N, N′, N′ -tetramethylenediamine
TNP-ATP	2′-3′-O-(2,4,6-trinitrophenyl)adenosine 5′-triphosphate
Tris	Tris (hydroxymethyl)aminomethane

ACKNOWLEDGEMENTS

I wish to thank

Professor M.C. Berman for creating the opportunity to work in his research unit and for his patient guidance and supervision.

The members of the Biomembrane Research Unit for their valuable discussions and interest.

Norma Linton for her expert assistance.

Mr J. Dale and Mr D. Radmeyer for their help in the preparation of the electron micrographs.

Messers R.D. Alexander, J. Ferreira and M. Smith for help in the preparation of sarcoplasmic reticulum vesicles.

Nadiema Jackson for typing this manuscript and Richard Goold for help with final printing.

This work was financed by a CSIR FRD postgraduate bursary.

CONTENTS

ABSTRACT

Properties of the nucleotide binding site of the Ca^{2+}-ATPase of skeletal muscle sarcoplasmic reticulum have been investigated. The study centred around interaction of the high affinity ATP analog, 2′-3′-O-(2,4,6-trinitrophenyl)adenosine 5′-triphosphate, (TNP-ATP), with the Ca^{2+}-ATPase.

Defined fractions of the sarcoplasmic reticulum (SR), corresponding to the terminal cisternae (TC) and light SR (LSR), were isolated. The TC were shown to have distinctive morphological characteristics that differ from the LSR. The TC vesicles contained electron dense intravesicular material representative of Ca^{2+} binding proteins, and visible membranous "feet" structures, which are reported to interconnect with the transverse tubule. Functional characterisation of the isolated fractions provided evidence for the predominant localisation of Ca^{2+} release channels in TC, and concentration of Ca^{2+}-ATPase molecules in LSR. These conclusions were based on the following observations: (a) decreased Ca^{2+} transport of TC versus LSR; ruthenium red, a Ca^{2+} channel blocker, enhanced Ca^{2+} transport and pumping efficiency in TC, (b) higher Ca^{2+}-ATPase activity for LSR in the presence and absence of ionophore, (c) rapid Ca^{2+} efflux from TC which is inhibited by ruthenium red. Of special interest was the characterisation of the TC and LSR with respect to turnover-dependent TNP-ATP fluorescence. Fluorescence observed for TC was approximately 65% of that for LSR. This phenomenon may be attributable to either the decreased Ca^{2+}-ATPase content of the TC vesicles or open Ca^{2+} release channels. Hence the TNP-ATP fluorescence characteristics appear to reflect the morphological and functional subspecialisation of the defined SR fractions.

TNP-ATP binding to the Ca^{2+}-ATPase in a conventional 'mixed' SR preparation was monitored by differential absorption spectroscopy. The difference spectrum of TNP-ATP bound to the non-phosphorylated enzyme is altered upon ATP hydrolysis, consistent wilth conformationl changes occuring at the nucleotide binding site during turnover. The addition of KCl decreased the magnitude of the TNP-ATP difference spectrum of the turning-over enzyme consistent with K^+-induced changes in the affinity of TNP-ATP bound. Titration studies also indicated that K^+ diminished the stoichiometry of TNP-ATP binding. However, the reappearance of a decreased TNP-ATP absorbance peak upon exhaustion of ATP provides evidence for binding of TNP-ATP to the E_1 species in the presence of K^+.
The effects of TNP-ATP on enzyme turnover in a 'mixed' SR preparation was measured by the pH stat and coupled enzyme assays. TNP-ATP stimulated Ca^{2+}-ATPase activity in the pH stat assay with $K_{0.5}$ (apparent) = 0.80 μM. Maximum stimulation (49%) was observed with 5.0 μM nucleotide, and higher concentrations produced lower levels of activation. Stimulatory effects of TNP-ATP and millimolar ATP were shown to be complementary, and may represent secondary enzyme activation via interaction with the regulatory nucleotide site. However, with the coupled assay, TNP-ATP only inhibited Ca^{2+}-ATPase activity, with $K_{0.5}$ (apparent) = 24 μM, consistent with competitive inhibition of Mg.ATP binding to the catalytic nucleotide site. Investigation into the apparent discrepancy between TNP-ATP effects as measured by the two assays precluded possible TNP-ATP inhibition of the coupling enzymes. Significantly, however, the coupling enzyme pyruvate kinase (PK) was shown to stimulate Ca^{2+}-ATPase activity when included in the pH stat assay reaction medium, with $K_{0.5}$(apparent) = 47 μg/ml. TNP-ATP acceleration of turnover was detected over and above the PK effect,

indicating separate activation mechanisms. PK was subsequently shown to enhance ADP quenching of AcP-induced TNP-ATP fluorescence. This finding was interpreted in terms of an increase in the apparent affinity of the Ca^{2+}-ATPase for ADP induced by PK. $K_{0.5}$ (apparent) was decreased 4-fold, from 36 μM to 9 μM. Kinetic parameters for ADP binding to PK were measured by the NADH-linked absorbance assay. ADP binding was non-cooperative (n_H = 0.89), with K_m = 210 μM and V_{max} = 253 μmol/mg/min. These calculated parameters were used in the determination of predicted reaction velocites from the measured [ADP]free at different flux rates in the coupled enzyme assay. Reaction velocities were greater than predicted, indicating that ADP transfer may not involve dissociation and diffusion through the aqueous environment, but may occur via direct interaction between PK and the Ca^{2+}-ATPase. A postulated PK : ADP ligand may function as a kinetically competent substrate for the Ca^{2+}-ATPase. The experimental observations of PK effects on the Ca^{2+}-ATPase are interpreted in terms of a direct metabolic transfer mechanism (Srivastava and Bernhard, 1986a). ADP binding and release may be facilitated by the formation of an intermediate enzyme-enzyme complex.

It is postulated that in the intact cell, high concentrations of cytosolic enzymes may favour protein-protein interaction. Direct transfer of nucleotides to and from the active site of the Ca^{2+}-ATPase may be physiologically relevant.

1.0 INTRODUCTION

1.1 THE SARCOPLASMIC RETICULUM OF SKELETAL MUSCLE

1.1.1 Function

The skeletal muscle sarcotubular system controls Ca^{2+} release and uptake, which, in turn, regulates muscle contraction and relaxation. The sarcotubular system consists of two main components, the transverse tubules (T-system), and the sarcoplasmic reticulum (SR). The transverse tubules are invaginations of the surface membrane (sarcolemma) which allow contact between the lumen and extracellular fluids (Huxley, 1964; Franzini-Armstrong and Porter, 1964; Peachey, 1965). The SR is an extensive internal membranous network which surrounds the myofibrils (Bennett and Porter, 1953; Porter and Pallade, 1957; Franzini-Armstrong et al., 1975), (see Fig. 1).

The SR consists of two defined regions, continuous longitudinal tubules or 'light' SR (LSR) and the terminal cisternae (TC) or 'heavy' SR. The TC are junctionally associated with the T-system in characteristic structures called triads (Porter and Palade, 1957). In the triad, two TC are connected to an intervening transverse tubule via electron-dense bridging "feet" structures (Somlyo, 1979; Franzini-Armstrong, 1980; Eisenberg and Eisenberg, 1982). These feet structures span the reported 120-140 Å gap between the TC and the T-system (Franzini-Armstrong, 1970). The TC and LSR regions of the SR show characteristic morphological features which reflect their subspecialisation. LSR consists of a single type of membrane which is comprised largely of Ca^{2+}-pump protein (Meissner, 1975; Saito, 1984). The TC consists of two types of membrane, the Ca^{2+}-pump containing membrane, and the junctional face membrane which

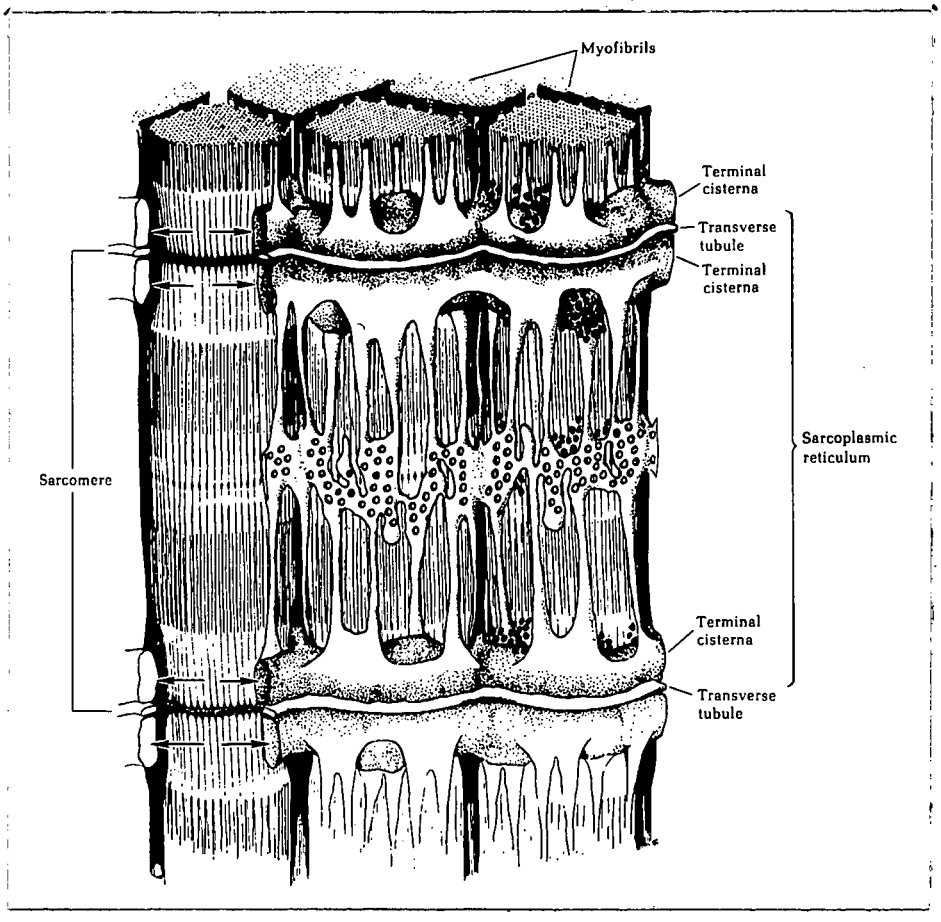

Figure 1: Schematic representation of the sarcotubular system of mammalian skeletal muscle (Lehninger, 1975).

carries the feet structures. In addition, Ca^{2+} binding proteins are contained within the lumen of the TC (Saito et al., 1984), and the Ca^{2+} release channels have been identified in the TC membrane (Lai et al., 1988). This subspecialisation of TC and LSR allows the SR membrane network to play a major role in controlling muscle contraction and relaxation (see Fig. 2).

Muscle contraction is initiated by the rapid release of Ca^{2+} from the TC at the triadic junction, in response to a nerve impulse propogated into the cell through the T-system. Released Ca^{2+} binds to the Ca^{2+}-binding subunit of troponin (troponin c), which induces an interaction between myosin and actin, and subsequent muscle contraction (Inesi, 1972; Taylor, 1979). The translocation of Ca^{2+} into the SR lumen, mediated by the Ca^{2+}-pump protein, results in detachment of myosin from actin, and enables the muscle to relax.

Winegrad (1970) suggests that the LSR and TC may represent the "relaxation" and "release" sites of SR respectively. Accordingly, muscle relaxation would involve the preferential uptake by LSR of released Ca^{2+}. This Ca^{2+} would then slowly diffuse to the TC region which is enriched in Ca^{2+}-binding protein. The TC region therefore acts as a reservoir for Ca^{2+} accumulated in the LSR, and represents the region of Ca^{2+} release, which triggers muscle contraction. In support of this, electron probe analysis of skeletal muscle cells indicates that the majority of Ca^{2+} released from the SR membrane during muscle contraction originates in the TC (Somlyo et al., 1981). The precise physiological mechanism of Ca^{2+} release remains an unsolved issue. Various stimuli including induction by Ca^{2+}, depolarisation of SR membrane, alteration in pH, changing membrane surface charge, and drugs, have been reported to trigger Ca^{2+} release from SR (Endo et al., 1977; Shoshan et al., 1981; Winegrad, 1982; Kim et al., 1983; Palade, 1987).

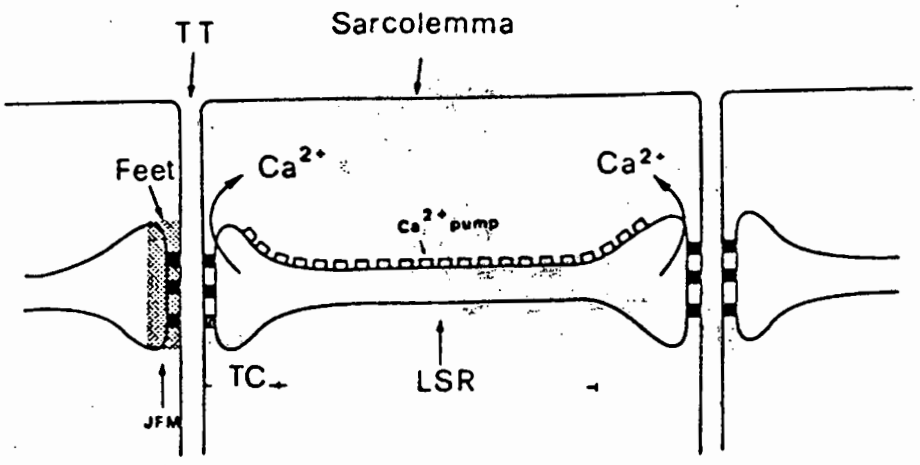

Figure 2: Schematic representation of the sarcoplasmic reticulum, showing the relationship between the transverse tubule (TT), junctional face membrane (JFM), terminal cisternae (TC), and light sarcoplasmic reticulum (LSR), (Volpe et al., 1987).

The reaccumulation of Ca^{2+} into the SR is against a concentration gradient of up to 100 000 : 1, and this active transport of Ca^{2+} is ATP-dependent, being the function of the membrane-bound Ca^{2+}-ATPase.

1.1.2 Structure and composition

Vigorous homogenisation of rabbit skeletal muscle causes fragmentation of the SR membrane, which then reseals in the form of vesicles (Nagai et al., 1960; Ebashi and Lipmann, 1962). These vesicles retain the appropriate in vivo orientation in that the outer vesicular surface corresponds to the cytoplasmic surface of the sarcoplasmic reticulum. Microsomal fractions of SR membrane vesicles can be isolated by differential centrifugation (Eletr and Inesi, 1972). The main SR vesicular membrane protein components are the Ca^{2+}-ATPase (Mr $\simeq$ 110 kD), calsequestrin (Mr $\simeq$ 63 kD) and two intrinsic glycoproteins (Mr $\simeq$ 53 kD and 160 kD). Campbell and Maclennan (1983) report the presence of a proteolipid (Mr $\simeq$ 12 kD) which constitutes a small percentage of the total protein mass. Other minor proteins exist in the SR membrane, but their properties are not clearly defined.

Although Racker and Eytan (1975) reported that the proteolipid improved the coupling efficiency in reconstituted vesicles, its mechanism of action and physiological role is largely unknown. Calsequestrin is confined to the SR lumen, and is the predominant intracellular component of the SR terminal cisternae (Saito et al., 1984). Purification of calsequestrin was first described by Maclennan and Wong (1971). The molecular weight of calsequestrin has been estimated at 44 kD - 65 kD, the differences being attributable to sensitivity to electrophoretic conditions (Maclennan and Wong, 1971; Ikemoto et al., 1972; Meissner, 1973;

Inesi and Scales, 1974). Calsequestrin is water soluble and highly acidic, which renders it suitable for sequestering and storing Ca^{2+} within the SR lumen (Meissner, 1975). In the original preparations, calsequestrin constituted approximately 7% of the total SR protein, and bound up to 50 Ca^{2+} ions/calsequestrin molecule (Maclennan and Wong, 1971). Isolated calsequestrin exhibits substantial conformational changes upon Ca^{2+} binding (Ikemoto et al., 1974; Ostwald et al., 1974). Maurer et al. (1985) have demonstrated crystallisation of calsequestrin by complex formation with divalent cations, and suggest that a specific "crystallisation cycle" may be physiologically relevant in the mechanism of Ca^{2+} storage and release.

Ostwald and Maclennan (1974) isolated a second acidic protein, the Ca^{2+}-binding or M55 protein (Mr $\simeq$ 55 kD). The M55 protein bind Ca^{2+} with a high affinity but low capacity (16-22 nmoles/mg). M55 and calsequestrin have a similar internal location (Maclennan and Holland, 1975), and it appears likely that they have related functions. The physiological role of the 160 kD and 53 kD glycoproteins remains unresolved. The glycoproteins are transmembranous, and a large proportion of the molecule is located on the cytoplasmic surface of the SR (Campbell and Maclennan, 1981). From reconstitution studies, Racker (1972) proposed that the glycoprotein may form an anion selective channel in the SR membrane. Chiesi and Carafoli (1982) have shown that both transport and ATPase activity are inhibited by binding of trifluoperazine to the 53 kD glycoprotein, and suggest that SR may be regulated by a glycoprotein-dependent process. The glycoproteins appear to contain high affinity nucleotide binding sites, as they can be covalently labelled with the photoaffinity probe 8-N_3-[γ-^{32}P] ATP (Campbell and Maclennan, 1983). Leonardo and Kutchai (1985), using

reconstituted SR vesicles, have postulated that the 53 kD glycoprotein may be involved in the coupling of Ca^{2+} transport to ATP hydrolysis.

The lipid portion of the SR membrane provides a barrier to the diffusion of intravesicular Ca^{2+}, and lipid-protein interaction appears to play a significant role in maintaining membrane protein structure and function (de Meis, 1981; McIntosh and Ross, 1985). Phospholipids comprise approximately 90% of the total lipid content of the SR membrane (Meissner and Fleischer, 1971; Owens et al., 1972). The main phospholipid component is phosphatidylcholine (50-70%) and the remainder comprises of phosphatidylethanolamine, phosphatidylinositol, phosphatidylserine and sphingomyelin (de Meis, 1981).

The neutral lipid fraction consists predominantly of cholesterol, with smaller amounts of triglycerides and free fatty acids (Marai and Kuksis, 1973; Tada et al., 1978).

1.2 ACTIVE CALCIUM TRANSPORT BY THE Ca^{2+}-ATPase OF SARCOPLASMIC RETICULUM

1.2.1 The catalytic cycle of the Ca^{2+}-ATPase

The Ca^{2+}-adenosine triphosphatase (Ca^{2+}-ATPase) of skeletal muscle actively transports Ca^{2+} from the cytoplasm into the lumen of SR, using the chemical energy derived from ATP hydrolysis. The overall chemical reaction catalysed by the Ca^{2+}-ATPase may be represented as follows:

$$ATP + HOH + Ca^{2+}_{out} \xrightarrow[Ca^{2+}\text{-ATPase}]{Mg^{2+}} ADP + P_i + Ca^{2+}_{in}$$

The stoichiometry of the above reaction is two Ca^{2+} ions translocated per ATP hydrolysed, under optimal conditions (Meissner 1973; Inesi et al., 1980). However, the Ca^{2+}-ATPase is reported to exhibit variable stoichiometry under changing conditions of pH, external [Ca^{2+}] and temperature (Meltzer and Berman, 1985).

SR vesicles exhibit two distinct types of ATPase activities - Ca^{2+} independent (basal) and Ca^{2+}-dependent (extra). Basal ATPase activity requires only Mg^{2+} for full activation, whereas extra ATPase activity requires both Ca^{2+} and Mg^{2+} and is related to the uptake of Ca^{2+} into SR vesicles (Hasselbach and Makinose, 1961; Tada et al., 1978). Ca^{2+} uptake and ATP hydrolysis is activated by the free Ca^{2+} concentration in the medium, and experimental values for half-maximal activity vary from 0.1-2.0 μM Ca^{2+} (Ikemoto, 1975; Hasselbach, 1978; Tada et al., 1978; Inesi et al., 1980). Initial evidence for phosphoenzyme formation during ATP hydrolysis resulted from the observation that SR vesciles, incubated in the presence of Ca^{2+}, Mg^{2+}, ATP and [^{14}C]ADP, were able to catalyse rapid phosphate exchange between ADP and ATP (Ebashi and Lipmann, 1962). This ATP⇌ADP exchange exhibits the same

Ca^{2+} concentration dependence as Ca^{2+}-uptake and ATP hydrolysis ($K_{0.5}$ = 0.1-2.0 μM), which suggests that a phosphoprotein is formed as a reaction intermediate (Hasselbach, 1964). Subsequent studies showed that the ATPase is phosphorylated by ATP during enzyme catalysis, and that an acid-stable phosphoenzyme intermediate could be isolated (Martonosi, 1967; Degani and Boyer, 1973). The phosphoryl group of the phosphoprotein is covalently attached to the β-carboxyl of an aspartyl residue (Dagani and Boyer, 1973).

The mechanism of action of the Ca^{2+}ATPase of SR has been extensively characterised, and it constitutes one of the most experimentally accessible coupled vectorial systems (de Meis and Vianna, 1979). The active transport of Ca^{2+} into the SR vesicular lumen involves three main steps:

a) Recognition and subsequent binding of Ca^{2+} at the high-affinity, externally-orientated Ca^{2+} binding sites.

b) Ca^{2+} translocation across the SR membrane.

c) Release of Ca^{2+} from the low-affinity, internally-orientated Ca^{2+}-binding sites into the SR vesicular lumen.

Ca^{2+} transport is facilitated by a conformational change of the ATPase which occurs upon phosphorylation with ATP (Ikemoto, 1974, 1975). Following hydrolysis, the enzyme returns to its initial conformation so as to initiate a new Ca^{2+} transport cycle (de Meis and Vianne, 1979).

Based on the available steady-state and kinetic studies, the catalytic cycle of the Ca^{2+}-ATPase has been described in terms of an 8 intermediate reaction (de Meis and Vianna, 1979). This reaction scheme (see Fig. 3) serves to explain the coupling of Ca^{2+} transport to substrate hydrolysis, and appears to be widely accepted. According to this model, the enzyme exists in two major

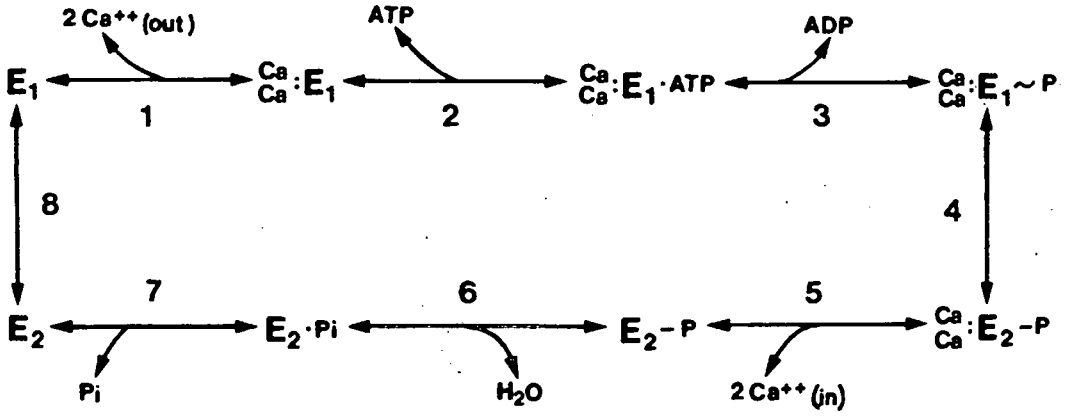

Figure 3: The catalytic cycle of the Ca^{2+}-ATPase (de Meis and Vianna, 1979).

functional states, designated E_1 and E_2. In the E_1 form, Ca^{2+}-binding sites are orientated towards the cytoplasm, and two Ca^{2+} ions are bound with high affinity (K_m = 0.1-0.3 μM at pH 7.0), (step 1). Binding of nucleotide triphosphate (step 2) is followed by transient phosphorylation, whereby the γ-phosphate is transferred to the β-carboxyl group of an aspartyl residue in the active site (Degani and Boyer, 1973), (Step 3). Ca^{2+} is entrapped in the $2Ca.E_1{\sim}P$ phosphoenzyme species, which is sensitive to ADP (Kanazawa et al., 1971; Shigekawa and Dougherty, 1978). An enzyme conformational change (step 4) results in the conversion of the ADP-sensitive phosphoenzyme to an ADP-insensitive species, corresponding to $2Ca.E_2$-P (Bastide et al., 1973). In this ADP-insensitive form the Ca^{2+}-binding sites face the vesicular lumen, and Ca^{2+} is bound with low affinity (K_m = 0.6-1 mM at pH 7.0) (Ikemoto, 1975; Takisawa and Makinose, 1983). This marked decrease in affinity represents the Ca^{2+} translocation step (Verjovski-Almeida and de Meis, 1977), and satisfies the thermodynamic requirements for intravesicular Ca^{2+} accumulation (Martonosi et al., 1987). The internalised Ca^{2+} site is inaccessible to ethyleneglycol-bis-(β-amino-ethyl-ether) N, N′-tetraacetic acid (EGTA), (Takisawa and Makinose, 1981). Ca^{2+} is released inside the vesicle (step 5), followed by Mg^{2+}-dependent dephosphorylation, where the acyl phosphoenzyme reacts with water, releasing inorganic phosphate to the exterior (steps 6 and 7). The reaction cycle is concluded by a second and relatively slow conformational change, in which the E_2 form reverts to the E_1 form (Masuda and de Meis, 1980), (step 8). The Ca^{2+}-binding sites again face the cyoplasmic side of the membrane, and the ATPase reaction cycle can be repeated.

Jencks (1980, 1983) has described certain rules that strictly define coupling of vectorial and chemical events in the reaction system. These rules are concerned with the affinity and mechanism of ligand binding, and specifically prevent one process from occuring without the other. All of the enzyme intermediates must be involved for the efficient coupling of ATP hydrolysis to Ca^{2+} transport.

Makinose and Hasselbach (1971) and Barlogie et al.,(1971) originally discovered that the process of Ca^{2+} transport could be reversed, in that the Ca^{2+}-ATPase can synthesise ATP from ADP and P_i in the presence of a transmembrane Ca^{2+} gradient. When SR vesicles, previously loaded with Ca^{2+}, are incubated in the presence of EGTA, a slow rate of Ca^{2+} efflux is observed due to membrane permeability. However, this Ca^{2+} efflux is greatly increased upon addition of ADP, P_i and Mg^{2+}, and is coupled to the synthesis of ATP (Makinose, 1972; Hasselbach, 1978). A stoichiometry of 2 moles of Ca^{2+} released per mole of ATP synthesised is observed, consistent with the forward reaction (Hasselbach, 1978). Both ATP and Ca^{2+} inhibit reversal of the Ca^{2+} pump, by impairing P_i-induced enzyme phosphorylation (Barlogie et al., 1971; Masuda and de Meis, 1973; Katz et al., 1977). Yamada et al., (1972) report that the steady-state level of P_i-induced phosphoenzyme increases progressively with the magnitude of the Ca^{2+} gradient formed across the vesicular membrane. The above findings suggest that the osmotic potential energy derived from the formation of the Ca^{2+} gradient may be involved in the reversal of the SR Ca^{2+} pump, which results in ATP synthesis.

The reversibility of the Ca^{2+} pump, has also been demonstrated from ATP$\rightleftharpoons P_i$ exchange reactions, which suggest that the enzyme functions forwards (ATP hydrolysis) and backwards (ATP synthesis)

simultaneously (Makinose, 1971; de Meis and Sorenson, 1975; Carvalho et al., 1976). Accordingly, at steady-state, the Ca^{2+} gradient is sustained by the energy derived from ATP hydrolysis, and ATP synthesis is in turn mediated by the osmotic energy of the Ca^{2+} gradient.

It has been subsequently found, however, that ATP formation can occur in the absence of a transmembrane Ca^{2+} gradient (Knowles and Racker, 1975; de Meis and Tume, 1977). This discovery has lead to a new interpretation, which can also be reconciled with the previous data, in that the energy provided from ligand (ADP, P_i, Ca^{2+}) binding plays an important role in ATP synthesis (de Meis, 1981). Fernandez-Belda and Inesi (1986) have recently characterised the stoichiometries and kinetics of the individual phosphorylation reactions, and they conclude that ATP formation, in the absence of a Ca^{2+} gradient, can be attributed to the reequilibration of intermediate enzyme states which is induced by ligand binding.

Several approaches have been used in order to elucidate the kinetics of the postulated Ca^{2+} translocation step (step 4 in Fig. 3), which results in the conversion from an ADP-sensitive to an ADP-insensitive phosphoenzyme (Sumida and Tonomura, 1974; Dupont, 1980; Ikemoto et al., 1981; Takisawa and Makinose, 1981). These studies indicate a biphasic mechanism of Ca^{2+} accumulation, in that the initial phase of phosphoenzyme formation coupled with Ca^{2+} occlusion is fast, but subsequent Ca^{2+} release to the vesicular lumen is slow. Froehlich and Heller (1985) report that internalCa^{2+} release is delayed with respect to E_2P formation, and postulate that Ca^{2+} remains occluded following E_1P-E_2P isomerisation, therefore indicating that intravesicular Ca^{2+} release is rate-limiting during Ca^{2+} translocation.

Stahl and Jencks (1987) have recently proposed an alternative reaction pathway for the Ca^{2+}-ATPase, which is reportedly followed when ATP binds first, or ATP plus Ca^{2+} are added simultaneously to the enzyme. The properties of this pathway are distinct from those of the widely accepted de Meis model (Fig. 3), and these workers suggest that this could be the pathway adopted in vivo, where millimolar ATP concentrations are present (Veech et al., 1979).

1.2.2 Ca^{2+} binding sites of the Ca^{2+}-ATPase

The Ca^{2+}-ATPase reaction pathway as proposed by de Meis and Vianna (1979) does not address the mechanism of Ca^{2+} binding and internalisation, which is inherent to understanding the active transport of Ca^{2+} across the SR membrane. The conventional alternating access model of de Meis and Vianna infers an ATP-dependent interconversion of high and low affinity Ca^{2+} binding sites. Accordingly, the externally-orientated high-affinity Ca^{2+}-binding sites re-orientate to face the vesicular lumen following enzyme phosphorylation. A number of studies have provided evidence for conformational changes occuring within the Ca^{2+}-ATPase upon Ca^{2+} binding, including:

a) Sulphydryl group reactivity is reported to be modified in the presence of Ca^{2+} (Thorley-Lawson and Green, 1977; Ikemoto et al., 1978).

b) The electron spin resonance spectrum of iodoacetamide labeled SR vesicles is altered following Ca^{2+} binding (Coan and Inesi, 1977).

c) Ca^{2+}-binding to the enzyme produces a detectable increase in intrinsic tryptophan fluorescence (Dupont and Leigh, 1978; Gullain et al., 1981).

d) Altered properties of the fluorescent probes, fluorescein isothiocyanate (FITC), (Pick and Karlish, 1980), and anilinonaphthalenesulphonate (ANS), (Arav et al., 1983), are observed upon Ca^{2+} binding.

The above observations indicate that protein structural changes are induced by Ca^{2+} binding to the postulated external high affinity sites.

Equilibrium dialysis studies using the radioactive tracer $^{45}Ca^{2+}$ initially indicated two classes of Ca^{2+}-binding sites on the Ca^{2+}-ATPase (Chevallier and Butow, 1971). Inesi et al. (1980) demonstrated from equilibrium experimentation that Ca^{2+} binding occurs via a cooperative mechanism, indicating the involvement of two interacting sites. The positive cooperative effect is attributable to sequential Ca^{2+} binding. Watanabe et al. (1981) report that Ca^{2+} affinity and the cooperativity of binding increases at alkaline pH. Hill and Inesi (1982) analysed the pH modulation of cooperative binding, using a theoretical model consisting of four interacting subunits representing a dimeric enzyme configuration. They postulated competitive binding between protons and Ca^{2+}, with Ca^{2+} binding cooperativity being inversely proportional to $[H^+]$. Direct measurements of the rate of Ca^{2+} binding using rapid Millipore filtration (Dupont, 1982) were consistent with a mechanism involving sequential Ca^{2+} binding to two interacting sites. These studies indicate that the two Ca^{2+} binding sites in the E_1 enzyme conformation are not equivalent; occupation of one site of low apparent affinity induces a slow conformational change which unveils a second site of high apparent affinity. This proposed model is in accordance with the phenomenon of equilibrium Ca^{2+} binding cooperativity. Champeil et al., (1983) investigated the effects of Mg^{2+} on the kinetics of Ca^{2+} binding

using stopped flow fluorescence. They found that at pH 7.0, in the absence of Mg^{2+}, addition of Ca^{2+} to a Ca^{2+}-deprived enzyme produced a monophasic intrinsic fluorescence rise. However, this intrinsic fluorescence rise was observed to be biphasic (at high Ca^{2+} concentrations), following preincubation of the Ca^{2+}-deprived enzyme with Mg^{2+}. They suggest that Mg^{2+} induces an enzyme configuration with a readily accessible low-affinity (K_d = 25 μM) Ca^{2+}-binding site, and occupancy of this site triggers a conformational change which reveals a second high affinity Ca^{2+} site. Therefore the presence of Mg^{2+} appears to drive the Ca^{2+}-ATPase towards a conformational state which is capable of relatively fast Ca^{2+} binding.

Recent studies have provided a definitive demonstration of sequential Ca^{2+} binding and subsequent translocation following enzyme phosphorylation with ATP (Inesi, 1987; Khanashvili and Jencks, 1988) Two Ca^{2+}-binding domains are predicted, and there appears to be a sequential internalisation of Ca^{2+}, in that the first bound Ca^{2+} ion is the first to be released to the vesicular lumen. Tanford *et al*. (1987) propose a similar model in which the E_1 Ca^{2+} uptake state is divided into substates with differing Ca^{2+}-binding domains. The model is consistent with equilibrium Ca^{2+}-binding cooperativity, and also incorporates the structural specificity of functional domains as proposed by Maclennan *et al*. (1985). In this respect, the enzyme conformational change induced by binding of the first Ca^{2+} ion is explained in terms of a relatively minor and rapid "hinge-bending" mechanism. This differs from the postulated slow and major Ca^{2+}-induced conformational

change of previous models (Dupont, 1982; Fernandez-Belda et al., 1984). The Tanford model provides an explanation for:

a) A fixed transport stoichiometry of two for Ca^{2+} binding to active Ca^{2+}-ATPase units.

b) "Occlusion" of bound Ca^{2+} ions.

c) The observation that two Ca^{2+} ions must be bound before enzyme phosphorylation can occur.

An additional advantage of this model is that it does not postulate any specific changes to the conventional model as proposed by de Meis and Vianna (1979). Ordered Ca^{2+} binding is suggested, but the main $E_1 \rightarrow E_2$ translocation step is unaffected.

1.2.3 Structure of the Ca^{2+}-ATPase

The Ca^{2+}-ATPase is an asymetrical transmembrane protein, and elucidation of the various functional domains within the enzyme has provided insight into the molecular mechanism of energy transduction and Ca^{2+} translocation. The primary structure of the Ca^{2+}-ATPase has been deduced from nucleotide sequence analysis of cloned DNA (Maclennan et al., 1985; Brandt et al., 1986, 1987). These studies show the Ca^{2+}-ATPase polypeptide chain to consist of 997 amino acid residues, with a calculated Mr of 109 763 daltons.

Following the determination of the complete primary amino acid sequence, a hypothetical model of the secondary and tertiary structure of the Ca^{2+}-ATPase was proposed by Maclennan et al., (1985), (see Fig. 4). According to this model, the protein consists of five major domains:

a) Three distinct globular cytoplasmic domains corresponding to the regions for ATP-binding, phosphorylation, and energy transduction. The ATP-binding domain is separated from the phosphorylation domain by a hinge region.

b) An intramembranous section which anchors the enzyme in the lipid bilayer. This section is reported to be comprised of eight to ten transmembrane helices (Maclennan et al., 1985; Brandt et al., 1986; Squire et al., 1987), containing predominantly negatively charged groups which form the transmembrane Ca^{2+} channel.

c) A penta-helical stalk region, which is enriched with negatively charged aspartyl residues, creating a favourable environment for Ca^{2+} binding. This stalk section links the cytoplasmic domains to the intramembranous region.

The membrane bound Ca^{2+}-ATPase has two sensitive tryptic cleavage sites, designated T_1 and T_2. Limited digestion with trypsin initially cleaves the Ca^{2+}-ATPase at the T_1 site (residue 514), producing fragments A (Mr = 55 kD) and B (Mr = 54 kD). Subsequent tryptic cleavage of fragment A at the T_2 site yields subfragments A_1 (Mr = 33 kD) and A_2 (Mr = 22 kD), (Thorley-Lawson and Green, 1973; Stewart and Maclennan, 1974; Maclennan and Reithmeier, 1982). These tryptic cleavage sites approximately delimit the proposed cytoplasmic domains of the hypothetical structural model of Maclennan et al. (1985).

The migration of covalent ^{32}P with the A_1 species during SDS-gel electrophoresis indicates that the phosphorylation site is located on this subfragment (Thorley-Lawson and Green 1973; Green et al., 1980). The aspartic residue that becomes phosphorylated in the E_1-P intermediate has been identified as Asp-351 (Maclennan et al., 1985).

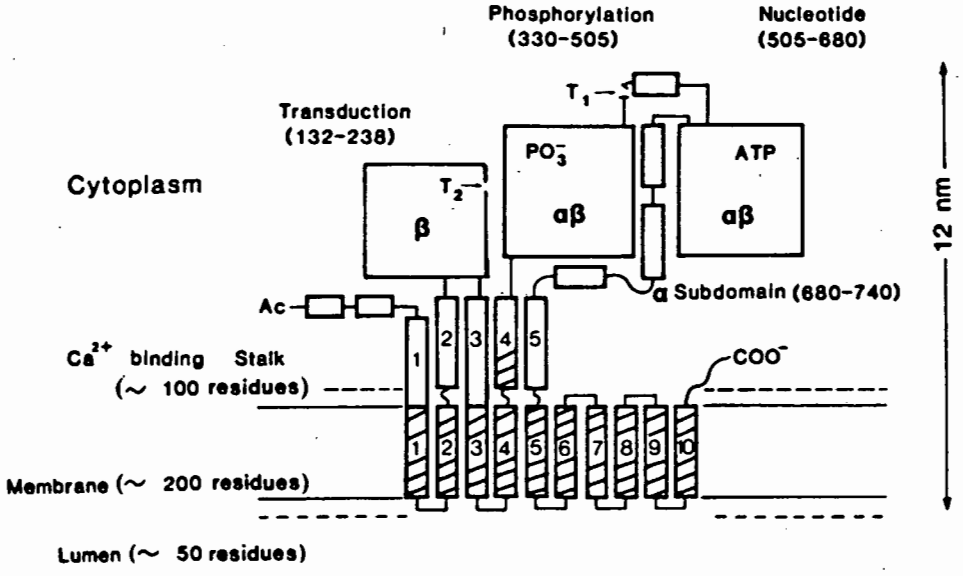

Figure 4: Proposed structural domains of the Ca^{2+}-ATPase (Maclennan et al., 1985).

Modification of a lysyl residue by fluorescein-5′-isothiocyanate (FITC) inhibits ATP-dependent catalytic activity (Mitchinson et al., 1982; Pick, 1981). This lysyl residue has been located on the B fragment at position 514 (Maclennan et al., 1985). Other amino acid residues have also been shown to be involved in the nucleotide binding domain. Pyridoxal-5′-phosphate (PLP) inhibits ATPase activity by altering an unidentified lysyl residue, which is located on the A_1 subfragment (Murphy, 1977). Lys-684 has recently been identified as the target site of adenosine triphosphopyridoxal (AP_3PL), an affinity label directed toward the ATP binding domain (Yamamoto et al.,1988).

The A_2 subfragment is proposed to contain the energy transduction domain (Maclennan et al., 1985). The inclusion of the A_2 species in planar lipid membranes confers increased Ca^{2+} permeability to the membrane, providing evidence that the Ca^{2+} transport channel is located on this subfragment (Shamoo et al., 1976). Pick and Racker (1979) showed that reaction of the carboxyl reagent dicyclohexylcarbodimide (DCCD) with the Ca^{2+}-ATPase inhibits Ca^{2+} binding, Ca^{2+}-ATPase activity and Ca^{2+} transport. The inclusion of Ca^{2+} prevented the observed inhibition, which suggests that DCCD is binding to the Ca^{2+} sites. The DCCD binding site was identified on the A_2 subfragment. Maclennan and Reithmeier (1985) report that the anion transport inhibitor, 4-4′-diisothiocyano-2-2′-stilbene (DIDS), inhibits Ca^{2+} transport through modification of a residue located on the B fragment.

Modification of specific thiol groups with N-ethylmaleimide (NEM) has been shown to inhibit intermediary steps of the Ca^{2+}-ATPase catalytic cycle (Yamada and Ikemoto, 1978; Kawakita et al., 1980). NEM treatment of SR vesicles results in alteration of those thiol groups involved in E-P formation from ATP (designated SH_P).

Phosphoenzyme decomposition is inhibited by NEM modification of the thiol groups responsible for the E_1~P to E_2 - P transition (designated SH_D). In SH_D derivitisation, the presence of the non-hydrolysable ATP analog AMP-P(NH)P is required to protect the SH_F group and hence specifically modify SH_D. SH_D labelling has been located on the A_1 subfragment (Saito et al., 1984). The characterisation of these functionally relevant thiol groups has been exploited in the identification of E_2P as the phosphoenzyme species responsible for enhanced TNP-ATP fluorescence (Davidson and Berman, 1987).

From the above modification studies, sites of functional importance have been located on the proposed domains. However, knowledge of the actual folding of the peptide and the exact relationship between nucleotide and transport sites is limited. Changes in tertiary structure and the relative spatial arrangement of functional domains may play an important role in the mechanism of energy transduction. Fluorescence energy transfer experiments have proved useful in providing information on the tertiary structure of the Ca^{2+}-ATPase (Scott, 1985; Hermann et al., 1986). Studies with the fluorescent probe 5-(2-((iodoacetyl)amino)ethyl) aminonaphthalene-1-sulfonic acid (IAEDANS), which binds to the B fragment, have provided an estimation of its apparent distance relative to site specific probes situated at both the nucleotide and Ca^{2+} binding sites (Squier et al., 1987). The results of these studies are interpreted in terms of a tertiary structural model in which the cytoplasmic section of the B fragment is folded behind the A_1 subfragment, thereby forming a cleft for nucleotide binding (Squier et al., 1987). Tanford et al. (1987) have postulated a model for cooperative Ca^{2+} binding which is consistent with the proposed structural arrangement of the functional domains

(Maclennan et al., 1985). Accordingly, a "hinge" region at the bottom of the Ca^{2+}-binding cavity may be equivalent to the suggested "hinge" which links the ATP-binding and phosphorylation domains (Maclennan et al., 1985). Hinge movement closes the Ca^{2+}-binding cavity and simultaneously induces movement of bound ATP, which results in transferal of the terminal phosphate group to the phosphorylation site. Therefore this model describes a possible molecular mechanism for the efficient coupling of enzyme phosphorylation with the vectorial transfer of Ca^{2+}. From circular dichroism studies, Csermely et al. (1987) report that the $E_1 \rightarrow E_2$ transition occurs without significant changes in secondary structure or any major rearrangement of the polypeptide chain. Therefore this provides evidence that the transition probably occurs by rearrangement of functional domains through hinge-type movements, similar to those suggested by Tanford et al. (1987).

The Ca^{2+}-ATPase forms two defined types of 2-D crystal which are presumed to correspond to the E_1 and E_2 enzyme conformations (Dux and Martonosi, 1983 and ; Taylor et al., 1986; Varga et al., 1987). The exposure of SR vesicles to Ca^{2+} or lanthanides results in the formation of the E_1-type crystals, which consist of chains of ATPase monomers. Lanthanides and Ca^{2+} are presumed to bind to the E_1 form of the enzyme, and the E_1 structural unit is a monomer. The E_2-type crystals are induced by vanadate or inorganic phosphate in the absence of Ca^{2+}. These E_2-type crystals are comprised of characteristic helical ATPase dimer chains, consistent with a dimeric structural unit. Analysis of the electron micrograph structure of the 2-D E_2-type crystals indicates the apposition of two Ca^{2+}-ATPase molecules linked together by a bridged structure in the cytoplasm to form a dimeric unit. The space below the bridged

structure is presumed to be accessible to substrates in the native SR membrane.

Although the E_1-type and E_2-type crystalline aggregates reflect the possible existence of distinct types of ATPase interactions in the two major enzyme conformations, there is conflicting evidence as to the precise spatial organisation and minimum functional unit of the Ca^{2+}-ATPase. The concentration of Ca^{2+}-ATPase is high in the SR membrane (3-6 mM), (Martonosi et al., 1987), which would be expected to favour monomeric subunit interaction. Electron microscope studies (Jilka et al., 1975), chemical cross-linking (Murphy, 1976; Kosk-Kosicka et al., 1983), radiation inactivation experiments (Hymel et al., 1984), and fluorescence energy transfer techniques (Vanderkooi et al., 1977; Fagan and Dewey, 1986; Highsmith and Cohen, 1987) have provided evidence for association between Ca^{2+}-ATPase monomers, and the results are consistent with postulated dimeric or tetrameric structures.

Several lines of evidence indicate that the functional unit is actually an independent monomeric Ca^{2+}-ATPase. Secondary structural predictions based on the primary amino acid sequence (Maclennan et al., 1985; Brandt et al., 1986, 1987) suggest that the monomeric unit is functionally competent. Solubilisation of SR vesicles, using non-ionic detergents (particularly $C_{12}E_8$ and triton X-100), causes delipidation and subsequent formation of Ca^{2+}-ATPase monomers in detergent micelles (McIntosh and Ross, 1985). The detergent-activated monomeric enzyme shows full Ca^{2+}-dependent ATPase activity (Dean and Tanford, 1978, Moller et al., 1980; McIntosh and Ross, 1985). Although the vectorial transport of Ca^{2+} has not been directly demonstrated, the interconversion of high and low affinity Ca^{2+}-binding sites following phosphorylation is indicative of Ca^{2+} translocation in the solubilised monomer

(Anderson et al., 1985). However, the solubilised monomer displays several properties which reflect that differences exist between it and the native membranous Ca^{2+}-ATPase. In particular, the detergent-solulised enzyme is more unstable in the absence of Ca^{2+} (Moller et al., 1980; Kosk-Kosicka et al., 1983; McIntosh and Ross, 1985), shows a more rapid, Mg^{2+}-independent rate of dephosphorylation (Anderson et al., 1982; Yamamoto and Tonomura, 1982) and appears to have a lower affinity for Ca^{2+} (McIntosh, 1984). McIntosh and Ross (1985) have postulated that these discrepancies may be attributable to substitution of detergent for endogenous phospholipids, and that specific phospholipid-protein interactions contribute to the maintenance of enzyme structure and catalytic activity.

The precise structural and functional unit of the Ca^{2+}-ATPase remains a controversial issue. Martonosi et al. (1987) suggest that the Ca^{2+}-ATPase of SR may constitute a self-associating complex in which dimers and tetramers exist in equilibrium with monomers.

1.2.4 Ligand Binding to the Ca^{2+}-ATPase

a) The effects of K^+

The results from initial investigations into the effects of K^+ and monovalent cations on the catalytic cycle of the Ca^{2+}-ATPase were conflicting . K^+ was reported to compete with Ca^{2+} for the active site, therefore inhibiting formation of the phosphoenzyme (de Meis, 1971; de Meis and de Mello, 1973). In direct contrast to this, other investigators showed that K^+ has an activating effect on enzyme turnover (Rubin and Katz, 1967; Yamada et al., 1970). Duggan (1977) clarified the effects of monovalent cations on Ca^{2+}-ATPase activity, and attributed the apparent K^+-induced inhibition to

contamination of the isolated SR vesicles with varying amounts of myosin, actomyosin, and mitochondrial fragments. Incorporation of inorganic cations in the suspension medium may also contribute to the apparent inhibition of enzyme activity.

K^+ stimulates calcium uptake with half-maximal stimulation at 11 mM K^+ (Shigekawa and Pearl, 1976; Duggan, 1977). The ratio of Ca^{2+} transported to P_i released is 2, and remains unaltered in the presence of K^+, despite an increase in nett Ca^{2+} uptake. This suggests that K^+ increases the rate of Ca^{2+} transport, as apposed to an indirect effect which would increase the efficiency of uptake (Duggan, 1977).

K^+ affects the kinetic parameters of a number of the intermediary reactions of the Ca^{2+}-ATPase reaction pathway. K^+ stimulates activity by increasing the rate-limiting hydrolysis of the ADP-insensitive phosphoenzyme (steps 6 and 7, Fig. 3), (Shigekawa and Pearl, 1976; Gullain et al., 1984). Chaloub and de Meis (1980) report that K^+ decreases levels of phosphoenzyme formed by P_i. Steady-state E-P levels from ATP are unaffected by K^+ (Shigekawa and Akowitz, 1979). K^+ modifies the relative distribution of phosphoenzyme species, in that it inhibits conversion of the ADP sensitive into the ADP-insensitive phosphoenzyme at low Mg^{2+} and high Ca^{2+} (Shigekawa et al., 1978). KCl affects ATP formation from E-P and added ADP, in that it causes an 11-fold decrease in the apparent affinity of E-P for ADP. However, this may not be due specifically to K^+, as other anions of K^+ salts show similar effects (Shigekawa and Kanazawa, 1982).

K^+ decreases turnover-induced TNP-ATP fluorescence (see section 1.2.5) in a manner that is consistent with binding to the monovalent cation site ($K_{0.5}$ = 49 mM), and which results in enhanced enzyme turnover (Davidson and Berman, 1985). Acceleration of enzyme hydrolysis by K^+ would therefore favour a decrease in E_2P levels, which could account for lowered TNP-ATP fluorescence. Alternatively, decreased TNP-ATP fluorescence observed in the presence of K^+ has been attributed to K^+-induced changes in the affinity of the enzyme for TNP-ATP (Bishop et al., 1986).

b) The role of Mg^{2+}

Mg^{2+} appears to fulfill a diverse number of roles in the catalytic function of the SR Ca^{2+}-ATPase. The Ca^{2+}-ATPase uses the Mg-ATP complex as its true physiological substrate (Weber et al., 1966; Kanazawa et al., 1971; Yamamoto et al., 1979; de Meis and Vianna, 1979; Makinose and Boll, 1979). The Ca^{2+}-ATP complex can also be utilised as a substrate for active Ca^{2+}-transport, although the rates of certain intermediary reactions are slower, and the ATPase activity is low (Souza and de Meis, 1976; Yamada and Ikemoto, 1980; Shigekawa et al., 1983).

Apart from complex formation with ATP, Mg^{2+} is reported to bind to the Ca^{2+}-ATPase and stimulate conversion of the ADP-sensitive to the ADP-insensitive phosphoenzyme (Shigekawa and Dougherty, 1978; Anderson et al., 1985). Mg^{2+} binding to the enzyme accelerates the hydrolysis of the ADP-insensitive phosphoenzyme (Inesi et al., 1970; de Meis and de Mello, 1973; Garrahan et al., 1976). Mg^{2+} is also required for phosphorylation from P_i in the reverse reaction (Masuada and de Meis, 1973), which results in ATP synthesis coupled to Ca^{2+} efflux. Enzyme phosphorylation is inhibited by high concentrations of Mg^{2+} (de Meis, 1976), through possible stabilisation of the E_1 species (Loomis et al., 1982). The varied

functions of Mg^{2+} imply that the enzyme may possess more than one kind of Mg^{2+}-binding site. Makinose and Boll (1979) have postulated that the Ca^{2+}-ATPase has a Mg^{2+} site which is involved with enzyme activation, and a separate site which binds the substrate Mg.ATP. Champeil et al. (1983) report that, at pH 7.0, enzyme phosphorylation following the simultaneous addition of ATP, Ca^{2+} and Mg^{2+} was faster in vesicles which were preincubated in Mg^{2+}. This suggests that Mg^{2+} induces an enzyme conformation favourable for reaction with Ca^{2+} and ATP. Inhibition of Ca^{2+}-ATPase activity by Mg^{2+} occurs at pH values greater than 7.0 (Wakabayashi et al., 1987; Bishop and Al-Shawi, 1988). This inhibition is attributable to Mg^{2+} binding to lumenal Ca^{2+} transport sites with progressively higher affinity at higher pH values. A postulated dead-end complex is formed, and Mg^{2+} dissociation is rate-limiting during enzyme turnover (Bishop and Al-Shawi, 1988).

1.2.5 Nucleotide binding to the Ca^{2+}-ATPase

Ca^{2+}-ATPase activity is modified by ATP in a relatively complex manner. ATP binding studies reveal that the nucleotide binds as the Mg^{2+}-chelate (Meissner, 1973; Vianna, 1975), and the hydrolytic activity of the enzyme shows a biphasic substrate dependence (Yamamoto and Tonomura, 1967; Inesi et al., 1967; Dupont, 1977; Verjovski-Almeida and Inesi, 1979; Moller et al., 1980). The observed ATP modulation of Ca^{2+}-ATPase activity cannot be explained in terms of simple Michaelis-Menten kinetics. The initial velocity of enzyme turnover increases in a saturable manner in the micromolar ATP range (K_m = 2-20 μM), and the hydrolytic rate is activated by millimolar ATP concentration (K_d = 0.4-3 mM), (Bishop et al., 1987). The enhanced catalysis in the millimolar ATP range is attributable to secondary regulatory effects, and phosphoenzyme

levels remain unchanged. These effects are non-hydrolytic as evidenced by the fact that millimolar concentrations of the non-hydrolysable ATP analogs AMP-PCP (Taylor and Hattan, 1979; Cable et al., 1985) and AMP-CPP (Dupont, 1977) effectively modulate ATPase activity. Micromolar concentrations of TNP-ATP (which binds with high affinity to the enzyme as compared to ATP), have also been shown to produce the secondary activation of hydrolytic activity (Dupont et al., 1985).

Several studies have indicated that ATP regulation of Ca^{2+}-ATPase activity is related to specific effects on the partial reactions of the catalytic cycle. Millimolar ATP concentrations activate the rate-limiting E_2 to E_1 transition (step 8, Fig. 3), (Froelich and Taylor, 1975; Scofano et al., 1979). The rate of dephosphorylation and liberation of P_i is accelerated by ATP (Froehlich and Taylor, 1975). From medium $P_i \rightleftharpoons HOH$ exchange measurements, McIntosh and Boyer (1983) found that the rate constant of phosphoenzyme hydrolysis is both decreased and accelerated at particular ATP concentration ranges. High concentrations of ATP stimulate the conversion of E_1P to E_2P, and subsequent intravesicular Ca^{2+}-release (Wakabayashi et al., 1986; Champeil and Gullain, 1986).

Various models describing the spatial location of the regulatory site, have been postulated to explain the mechanism of ATP modulation. The enzyme may possess separate regulatory and catalytic nucleotide sites on the same polypeptide chain (Dupont, 1977; Verjovski-Almeida and Inesi, 1979). A dimeric functional unit may exist in which the catalytic and regulatory sites are found on allosterically-linked polypeptide chains (Dupont et al., 1985). The ATPase may contain a single nucleotide site per polypeptide chain, with the regulatory ATP binding to the phosphorylated catalytic

site following ADP liberation (McIntosh and Boyer, 1983). Bishop et al. (1987) have recently proposed that the regulatory nucleotide site is not separate from the catalytic site, but is in fact equivalent to the modified catalytic nucleotide site following enzyme phosphorylation. This transformed site is able to bind ATP with a decreased affinity to produce secondary regulation of turnover. The studies of Bishop et al. (1987) involved the use of TNP-AMP, which provides a high affinity marker for the regulatory nucleotide site. From the observed stoichiometry and kinetics of TNP-AMP binding, Bishop et al. (1987) systematically exclude the possible existence of models involving a dimeric enzyme or separate regulatory and catalytic sites. Previous studies, which demonstrated a stoichiometry of one mol/mol for ATP binding on the phosphoenzyme, also suggested the exclusion of models depicting two distinct sites on the same polypeptide chain (Cable et al., 1985). The existence of regulatory sites in a detergent solubilised monomeric enzyme preparation, provides evidence against possible dimeric interaction (Moller et al., 1980; McIntosh and Boyer, 1983).

Moczydlowski and Fortes (1981) report that the (Na^+, K^+)-ATPase also exhibits secondary regulation of activity at high ATP concentrations. They conclude that the catalytic and regulatory nucleotide binding sites may be represented by a single interconverting site on the polypeptide chain.

Other naturally occuring nucleotides besides ATP are able to support Ca^{2+} transport. The relative activity of these substrates may be graded sequentially as follows: ATP (1.0) > ITP (0.8) > GTP (0.7) > CTP (0.6) > UTP (0.3), (Makinose and The, 1965). The relative rates of hydrolysis of these substrates reflect the

affinity of the Ca^{2+}-ATPase for the nucleotides (de Meis and de Mello, 1973). Energy-yielding pseudosubstrates including acetyl phosphate (AcP) (Pucell and Martonosi, 1971; Rossi et al., 1979; Liguri et al., 1980; Bodley and Jencks, 1987), p-nitrophenyl phosphate (pNPP) (Inesi, 1971) and carbamyl phosphate (Pucell and Martonosi, 1971) are also able to promote active transport of Ca^{2+} and enzyme phosphorylation. These pseudosubstrates display slower rates of hydrolysis than ATP, although the reaction mechanism appears to be similar. Secondary activation of hydrolytic activity is observed with ITP and CTP at considerably higher concentrations than the ATP-induced effect (de Meis and Mello, 1973; Taylor and Hattan, 1979). However, with the pseudosubstrates AcP (Pucell and Martonosi, 1971) and pNPP (Inesi, 1971), this secondary regulatory phenomenon is not shown.

1.2.6 Use of TNP-ATP for studies of nucleotide binding to the Ca^{2+}-ATPase

The ATP analog, 2′-3′-O-(2,4,6, trinitrophenyl) adenosine 5′-triphosphate, (TNP-ATP), is formed from trinitrophenylation of the ATP ribose residues by 2,4,6 trinitrobenzene-1-sulphonate (TNBS), and was first synthesised by Hiratsuka and Uchida (1973). The structure of TNP-ATP is shown in Fig. 5. The microenvironmental sensitivity of this ribose modified nucleotide has proved to be useful in probing the catalytic sites of a number of enzymes, including myosin ATPase (Hiratsuki and Uchida, 1973, 1976), the (Na^+, K^+)-ATPase (Moczydlowski and Fortes, 1981 a, b), mitochondrial F_oF_1-ATPase (Grubmeyer and Penefsky, 1981), and aspartokinase I (Broglie and Takahishi, 1983). TNP-ATP was introduced to studies of the Ca^{2+}-ATPase by Watanabe and Inesi (1982) and Dupont et al. (1982), who investigated the stoichiometry

and conformational changes associated with nucleotide interaction at the catalytic site.

TNP-ATP was initially reported to be hydrolysed at relatively slow rates by SR Ca^{2+}-ATPase (Watanabe and Inesi, 1982; Dupont et al., 1982). However, it is likely that TNP-ATPase activity is "parasitic", and is probably a reflection of basal Mg^{2+}-ATPase activity (Dupont et al., 1985). TNP-ATP is bound with a higher affinity than ATP (Dupont et al., 1982), and this property of the nucleotide analog has proved to be useful in the elucidation of ATP binding sites (Dupont et al., 1985). The stoichiometry of TNP-ATP binding to the non-phosphorylated enzyme has been estimated from direct binding measurements with TNP-[γ-^{32}P] ATP, from absorbance changes and from the increase in fluorescence which occurs upon nucleotide binding (Watanabe and Inesi, 1982; Dupont et al., 1982). Absorbance measurements for TNP-ATP binding are based on the characteristic differential absorption spectrum of TNP-ATP bound to SR, with respect to free TNP-ATP, that is produced in the visible region. The number of TNP-ATP nucleotide binding sites reported varies from approximately 5 to 7 nmol/mg of SR protein, and appears to be consistent with a stoichiometry of one mol of nucleotide site/mol of Ca^{2+}-ATPase (Berman, 1986). Watanabe and Inesi (1982) report a maximum value of 8 nmol of TNP-ATP sites/mg of SR protein, which they attribute to the existence of two groups of binding sites with different apparent affinities.

A characteristic feature of TNP-ATP is that the fluorescence intensity of the bound probe is greatly enhanced following induction of enzyme turnover with ATP plus Ca^{2+} (Watanabe and Inesi, 1982). Fluorescent enhancement is also observed upon phosphorylation with P_i in the absence of Ca^{2+} and ATP (Dupont and Pougeois, 1983). Although phosphorylation from P_i occurs in the

FITC labelled enzyme, TNP-ATP binding is prevented (Wakamoto and Inesi, 1984). The increased fluorescence following phosphorylation is also observed with the nucleotide analogs, TNP-ADP and TNP-AMP. TNP-AMP is reported to produce the greatest fluorescence enhancement (Nakamoto and Inesi, 1984). Enzyme phosphorylation blue-shifts the fluorescence emission peak, and greatly enhances the fluorescence quantum yield (Nakamoto and Inesi, 1984). These observation indicate that TNP-ATP is bound to the phosphoenzyme in a site with decreased polarity. Dupont and Pougeois (1983) suggest that the enhanced TNP-ATP fluorescent state results from an increase in hydrophobicity following extrusion of water molecules from the active site. TNP-ATP therefore functions as a reporter of an enzyme conformational change that occurs in the environment of the catalytic site following phosphorylation, and which is linked to the mechanism of calcium translocation (Watanabe and Inesi, 1982).

TNP-ATP fluorescence levels have been quantitatively related to phosphoenzyme levels (Bishop et al., 1984; Nakamoto and Inesi, 1984). Bishop et al., (1986) report that the observed fluorescent enhancement is attributable to a particular conformation that is common to all phosphoenzyme species, that is all phosphoenzyme intermediates cause enhanced fluorescence. However, TNP-ATP fluorescence has been shown to be consistent with levels of ADP-insensitive phosphoenzyme at low temperatures (Anderson et al., 1985). Recent studies involving redistribution of phosphoenzyme

species by thiol group modification with NEM have lead to the identification of E_2P as the phosphoenzyme intermediate responsible for enhanced TNP-ATP fluorescence (Davidson and Berman, 1987). This finding indicates that the $E_1 \rightarrow E_2$ conformational transition is reflected in altered properties of the TNP-ATP nucleotide binding site.

Berman (1986) studied the turnover-dependent fluorescence properties of EGTA-uncoupled Ca^{2+}-ATPase. The results showed that fluorescence is decreased in parallel with the extent of uncoupling, which indicates that TNP-ATP fluorescence enhancement may be associated with energy coupling in the Ca^{2+}-ATPase.

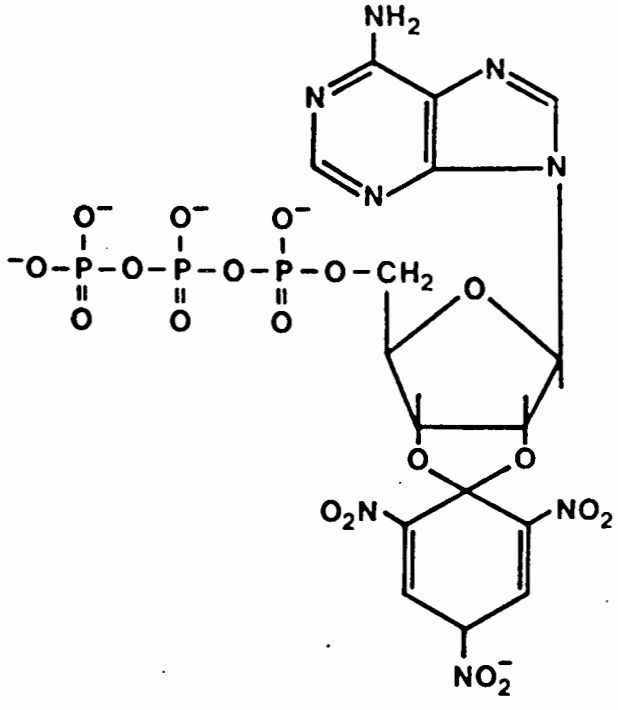

Figure 5: Proposed structure for TNP-ATP (Hiratsuka and Uchida, 1973).

1.3 METABOLITE TRANSFER VIA ENZYME-ENZYME COMPLEX FORMATION

Protein concentrations within cells are extremely high, and the cytosol cannot be regarded as a mere solution of enzymes and substrates. This is reflected in the high viscosity of cellular fluids (Mastro and Keith, 1984). Thus, within the cell, membrane and soluble proteins can interact with each other to form dynamic aggregates and multienzyme complexes. The spatial organisation of cytoplasmic and membrane-bound proteins may be regarded in terms of an equilibrium between individual proteins and assemblies of proteins formed via dynamic interaction (Kaprelyants, 1988).

There are several specific examples illustrating the existence of enzyme-enzyme interaction. Sequential pairs of enzymes in the tricarboxylic acid cycle have been shown to form characteristic complexes (Srere, 1985). The fatty acid oxidation complex (Yang et al., 1985), and the systems of tryptophan synthase (Welch, 1977) and fatty acid synthase (Wakil et al., 1983) are known examples of multienzyme complexes, which involve stable protein-protein interactions. In addition, where multienzyme complexes are not discernable, kinetic studies have revealed a number of diverse enzyme-enzyme interactions between soluble enzymes, under conditions of high localised enzyme concentrations (Srivastava and Bernhard, 1987).

The interaction and association of proteins affects the equilibrium distribution of cellular metabolites, and these equilibrium values are therefore appreciably different from those

arising by dilute enzyme catalysis. The degree to which these protein-protein interactions modulate the equilibrium partitioning of metabolites is reported to depend on four main factors (Srivastava and Bernhard, 1987):

a)The intracellular concentrations of ligands and their corresponding high affinity enzyme sites.

b)The strength of enzyme-ligand interactions.

c)The relative affinities of enzyme for reactants as opposed to products in the individual steps of the reaction.

d)The comparitive affinities of postulated enzyme-reactant and enzyme-product complexes for different enzymes and metabolites.

Srivastava and Bernhard (1986a, 1987) have recently advanced the hypothesis that the transfer of metabolites between enzyme sites may occur via direct enzyme-enzyme interaction ("direct transfer pathway"), (see Fig. 6). This theory is based upon the observation that the concentrations of high affinity enzyme sites in cells are usually higher than the concentrations of their intermediary metabolites (Srivastava and Bernhard, 1986b). This precludes the existence of substantial concentrations of intermediary metabolites outside the enzyme sites, as most of these intermediary metabolites would be expected to be confined to their respective sites, and not be present in the aqueous environment. Direct transfer may alter the optimal rate of metabolite transformation. Accordingly, intermediary metabolites may be sequestered in stable in vivo enzyme-enzyme complexes, which facilitate catalytic interconversion. The proposed "direct transfer pathway" differs from the conventionally assumed "random diffusion pathway". According to the "random diffusion pathway", an abundant metabolite pool exists in the aqueous intracellular environment, and these metabolites migrate to defined enzyme sites by random diffusion.

Following catalysis, the converted metabolites dissociate from their respective enzyme sites and re-enter the aqueous environment (Lehninger, 1975).

Appropriate models have been suggested to explain the recognition between specific enzyme pairs in the mechanism of direct transfer (Srivastava and Bernhard, 1987). The recognition signal may be encoded in the primary structure of the respective proteins, or the substrate may serve as the recognition factor, which links the enzymes together. Alternatively, neither the substrate nor the protein structure may function as the signal for enzyme-enzyme interaction - in this instance substrate interaction may induce a conformational change in one of the enzymes which is favourable for subsequent complex formation.

Srivastava and Bernhard (1986a) have described a general mechanism of direct transfer in the distribution of NADH among pairs of dehydrogenases, which exert opposite stereospecificity for hydrogen transfer to C-4 of nicotinamide. This finding is of significance because of the wide utilisation of NADH as a coenzyme substrate in several catalytic processes. The molecular basis of the direct transfer of NADH between dehydrogenase pairs has been modelled by computer graphics (Srivastava et al., 1985). However, in contrast to this proposed general direct transfer mechanism for NAD^+-dependent dehydrogenases, Ehrlich (1987) failed to detect direct transfer between isocitrate dehydrogenase and glutamate dehydrogenase, despite the fact that these enzymes displayed opposite stereospecificity for hydrogen transfer to the coenzyme. Ehrlich (1987) concluded that direct transfer of NADH between dehydrogenases may be more dependent on complementary surface interactions than on stereospecificity.

With the glycolytic kinase reactions, the internal equilibrium constants for enzyme-bound metabolites are found to be constantly near unity, which is in contrast with the magnitudes of the equilibrium constants obtained in aqueous solution (Knowles, 1980; Srivastava and Bernhard, 1987). The reactants appear to be more stable than the products, because of the stronger interaction energy for substrate binding as opposed to product binding (Huskins et al., 1982; Weber and Bernhard, 1982). The maintenance of internal equilibrium constants near unity is suggested to be the result of a selective evolutionary drive towards optimal catalytic efficiency (Srivastava and Bernhard, 1986a).

Particular reference is made to the glycolytic enzymes, including pyruvate kinase, lactate dehydrogenase and phosphoglycerate kinase, in the discussion by Srivastava and Bernhard (1986a, 1987) concerning metabolite transfer and enzyme-enzyme interaction. The glycolytic enzymes are reported to constitute the major protein component of muscle sarcoplasmic fluid (Ottaway and Mowbray, 1977). This observation is of particular relevance to this study, in that possible enzyme-enzyme interaction between pyruvate kinase and the membrane-bound Ca^{2+}-ATPase is postulated.

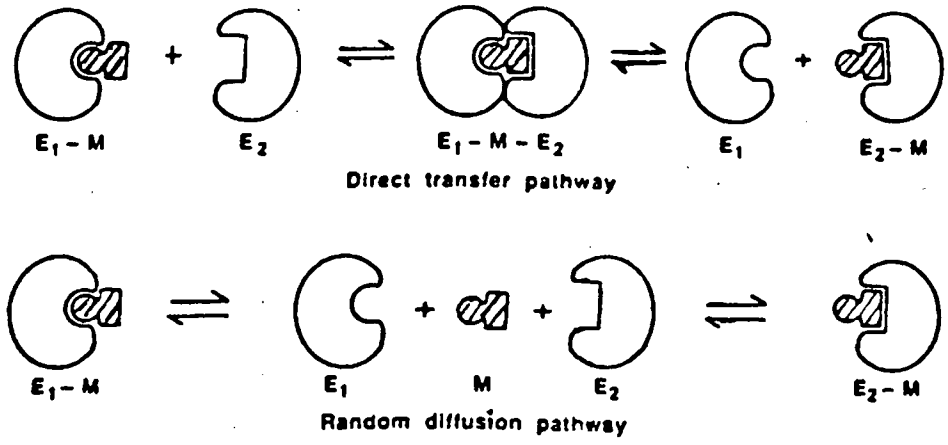

Figure 6: Schematic representation of the proposed mechanisms for direct transfer and random diffusion of metabolite (M) between two sequential enzymes (E_1 and E_2), (Srivastava and Bernhard, 1986a).

2.0 EXPERIMENTAL PROCEDURES

2.1 Materials

ATP (vanadate free), ADP, acetyl phosphate, phospho(enol)pyruvate, ruthenium red, bovine serum albumin and glutaraldehyde (grade II, 25% aqueous solution) were obtained from Sigma. Molecular weight marker proteins and all polyacrylamide gel electrophoresis chemicals were purchased from Bio-Rad. A23187 was supplied by Calbiochem and X-537A was from Roche Products. Lactate dehyrogenase, pyruvate kinase, creatine phosphate, creatine phosphokinase,and NADH were obtained from Boehringer Mannheim. $^{45}CaCl_2$ was supplied by New England Nuclear. TNP-ATP was synthesised and purified by the method of Hiratsuka (1982), and was a gift from Dr. G. Davidson. All buffers, salts, acids and solvents were of analytical grade from either BDH Chemicals (England) or Merck.

2.2 Isolation and purification of sarcoplasmic reticulum vesicles

Sarcoplasmic reticulum vesicles (SRV) were prepared according to the method of Eletr and Inesi (1972), with slight modifications.

Sarcoplasmic reticulum was isolated from white skeletal muscle excised within 15 minutes post mortem from the hind legs of a New Zealand white male rabbit, crossed with a commercial hybrid strain. Immediately after excision, the tissue was washed and cooled in 0.1 mM EDTA, pH 7.0. Trimmed muscle (200 g) was homogenised in 800 ml of medium 1 : 10 mM histidine, pH 7.0, 0.3 M sucrose, 0.1 mM EDTA for 15 seconds every 5 minutes, for 1 hour, at maximum speed in a Waring blender. During this procedure it was ensured that

the pH was maintained at 7.0 by the addition of 5% (w/v) NaOH. The homogenate was then centrifuged at 15 000 x g (9 500 rpm) for 20 minutes in rotor no. JA-14 in a Beckman J2-21 centrifuge. The supernatent was collected and filtered through glass wool (washed in medium 1) to remove low-density lipid aggregrates. The filtered suspension was centrifuged at 40 000 x g (19 000 rpm) for 90 minutes in rotor no. 19 (fixed angle) in a Beckman L4 ultracentrifuge. The resulting sediment was resuspended in 100 ml of medium 2 : 10 mM histidine, pH 7.0, 0.6 M KCl, and incubated at 0-4°C for 40 minutes to solubilise any contaminating actomyosin. The suspension was centrifuged at 15 000 x g (14 000 rpm) for 20 minutes in rotor no. JA-20 in a Beckman J2-21 centrifuge. The supernatent was retained and recentrifuged at 83 000 x g (27 000 rpm) for 60 minutes in rotor no. 30 in a Beckman L4 ultracentrifuge. This final sediment was resuspended in 5 ml of medium 3 : 10 mM histidine, pH 7.4, 0.3 M sucrose, giving a final concentration of 5-15 mg/ml SRV. The entire isolation procedure was performed at 0-4°C. Aliquots (250 µl) of the SRV preparation were quick-frozen in liquid nitrogen and stored at -70°C, where they remained stable for periods of up to 3 months.

The isolation of SRV by the method described above does not attempt to separate light and heavy fractions of SR. This "mixed" SRV preparation is commonly used in functional studies of the Ca^{2+}-ATPase, and was used in the experimental work reported in sections 3.2, 3.3 and 3.4.

2.3 Isolation and purification of sarcoplasmic reticulum terminal cisternae and longitudinal tubules

SR fractions corresponding to terminal cisternae (TC) and longitudinal tubules or light sarcoplasmic reticulum (LSR) were isolated by sucrose density gradient centrifugation based on the method of Saito et al.(1984). These TC and LSR fractions were used in the experiments described in section 3.1.

White skeletal muscle was removed from the hind legs of a New Zealand white female rabbit crossed with a commercial hybrid strain male. Ground muscle (50 g) was homogenised in 250 ml of 5 mM imidazole-HCl, pH 7.4, 0.3 M sucrose (homogenisation medium) for one minute at maximum speed in a Waring blender. The homogenate was then centrifuged at 7 020 x g (8 000 rpm) for 10 minutes in rotor no. JA-10 in a Beckman J2-21 centrifuge. The resulting pellets were rehomogenised in a further 250 ml homogenisation medium and again centrifuged at 7 020 x g (8 000 rpm) for 10 minutes in rotor no. JA-10 in a Beckman J2-21 centrifuge. The supernatent was collected and filtered through glass wool. A microsomal pellet was then obtained by centrifugation at 83 000 x g (27 000 rpm) for 120 minutes in rotor no. 30 in a Beckman L4 ultracentrifuge. The microsomes were resuspended in 10 ml of homogenisation medium using a Dounce homogeniser and then layered on top of a discontinuous sucrose gradient. The [sucrose] steps in the gradient tube consisted of 7 ml each of 1.6 M sucrose, 1.3 M sucrose, 1.1 M sucrose and 0.8 M sucrose all buffered with 5 mM imidazole-HCl, pH 7.4. These sucrose gradients were centrifuged at 70 000 x g (2 000 rpm) for 16 hours in rotor no. SW27 in a Beckman L8-M ultracentrifuge. SR membrane fractions observed at the interfaces

of the gradient steps were collected, diluted approximately 1.5 fold with 5 mM imidazole-HCl, pH 7.4, and centrifuged at 83 000 x g (27 000 rpm) for 3 hours in rotor no. 30 in a Beckman L8-M ultracentrifuge. The pellets were resuspended in 3-5 ml of homogenisation medium. Aliquots (300 µl) of the isolated fractions were quick frozen in liquid nitrogen and stored at -70°C until use.

2.4 Determination of protein concentrations

a) Lowry method

Protein concentrations of SR preparations were determined by a method based on that of Lowry *et al*. (1951).

SR protein samples (10 µl of approximately 10 mg/ml) were incubated with 10 µl of 10% sodium deoxycholate for 5 minutes and then diluted to a final volume of 1 ml with distilled water. Biuret reagent (1 ml) containing 0.025% cupric sulphate, 0.05% sodium tartrate, 2% sodium carbonate and 0.1 M sodium hydroxide was added to 0.1 ml of the SR samples, and the mixture was allowed to stand for 10 minutes. Folin-Ciocalteu reagent (0.1 ml) was then added with vigorous mixing and the colour allowed to develop for 30 minutes. SR protein concentrations were determined from changes in the absorbance at 750 nm using an HP-8450 diode array spectrophotometer. Protein standards of 2.5-25 µg bovine serum albumin (BSA) were determined in a similar way with each batch of SR samples. The unknown SR protein concentrations were then calculated from the BSA standard curve. All protein determinations were performed in triplicate and the average recorded.

b) A_{280nm} protein determination

Protein concentrations were also determined by measurement of the absorbance at 280 nm of suitable dilutions of SR protein in 10 mM Tris-HCl, pH 7.0, 1% sodium dodecyl sulphate (SDS). All A_{280nm} measurements were performed on an HP 8450 diode array spectrophotometer. Protein concentrations were calculated in terms of "serum albumin units," assuming $E_{280}^{1\%} = 6.60$ (Foster and Sterman, 1956; Kolthoff et al., 1965).

2.5 Sodium Dodecyl Sulphate Polyacrylamide Gel Electrophoresis (SDS-PAGE)

SDS-PAGE was based on the method of Laemmli (1970). Gradient gels of 4-15% acrylamide were prepared for protein analysis.

The following solutions were made for use in the preparation of the gradient gel : running gel buffer consisted of 1.5 M Tris-HCl, pH 8.8 and 0.4% SDS; stacking gel buffer, 0.5 M Tris-HCl, pH 6.8 and 0.4% SDS; acrylamide solution, acrylamide (28%) and bis (1.2%); ammonium persulphate solution (AMPS), 100 mg/ml; tank buffer, tris (6 g), glycine (28.8 g) and 10% SDS (20 ml) made up to 2 l with distilled water. The running gel was then prepared by making up 2 solutions containing 4 and 15% acrylamide respectively, as follows : running gel buffer (3.75 ml), acrylamide solution (2.0 ml and 7.5 ml), AMPS (75 µl), concentrated N.N.N′.N′-tetramethyl-ethyldiamine solution (TEMED) (9 µl), distilled water (9.166 and 3.666 ml). These 2 solutions were immediately placed in a gradient former and the gel poured by running the solutions between 2 matched glass plates, separated by spacers 1.5 mm in width, clamped in a gel casting stand. The running gel was poured intil there was a gap of approximately 4 cm from the top of the plates and then a thin

stream of water was layered on top of the gel. After approximately 30 minutes the gel was set and a clear interface could be observed between the solid gel and water layer. The water was poured off and stacking gel, consisting of stacking gel buffer (1.875 ml), acrylamide solution (0.75 ml), AMPS (35 µl), TEMED (5 µl), and distilled water (4.835 ml) was layered on top of the set running gel. A gap of approximately 2 cm was left at the top of the plate assembly, and a perspex comb containing an appropriate number of wells was fitted in the stacking gel. The stacking gel hardened in appproximately 45 minutes. A top reservoir was then fitted and a small volume of tank buffer poured into the reservoir.

Protein samples were dissolved and denatured by mixing diluted protein solutions with a solubilising buffer (0.2 M Tris-HCl, pH 6.8, 8 M urea, 2% SDS w/v, 4% ß-mercaptoethanol w/v). Bromophenol blue was added as a tracking dye. Approximately 10-20 µg of protein were applied to each well of the stacking ggel. The loaded gel was removed from the casting stand and placed in an electrophoresis tank containing tank buffer. Electrophoresis was performed at 4°C for approximately 6 hours, with a constant current of approximately 30 mA. Running was complete once the bromophenol blue tracking band was approximately 3 cm from the bottom of the gel. The gel was then carefully removed from the plate assembly and placed in fixer (30% methanol, 10% acetic acid) for about 30 minutes, to wash out the SDS. Fixer was then poured off and replaced with Coomassie blue stain (0.1% w/v Coomassie blue dissolved in 30% methanol/10% trichloroacetic acid) and the gel stained for approximately 3 hours. The gel was then destained in 30% ethanol/10% acetic acid for approximately 5 hours and then clarified by soaking in two changes of 7% acetic acid. Acetic acid was washed out by placing the gel in distilled water for approximately 30 minutes. The gel

was finally placed between appropriately cut Whatman 3M chromatography paper and photo graphic arts film, and dried at 70°C for 1 hour on a slab gel dryer.

The molecular weights of protein bands were determined by comparison with the observed mobilities of standard marker proteins.

2.6 Electron microscopy

SR cell suspensions were initially fixed in 0.5% phosphate buffered glutaraldehyde for 10 minutes. The pellet of fixed cells was then encapsulated in a 2% solution of molten agar (Ryter and Kellenberger, 1958). After the agar had set, the solidified agar containing the cells was cut into small cubes (approximately 1 mm^3).

These cubes were fixed in Palades buffered OsO_4 for 30 minutes, rinsed for 2 minute periods in 3 changes of distilled water, and then dehydrated with 0.5% uranyl acetate in 80% acetone (15 minutes). The cubes were transferred to 96% acetone for 8 minutes and washed for periods of 5 minutes in 3 changes of 100% acetone. Cubes were then placed in 50% Spurrs/50% acetone for 1 hour, and subsequently transferred to 100% Spurrs, which was changed once in 2 hours. The cell cubes were finally embedded using Spurrs resin in oven dried polythene embedding capsules and hardened by overnight incubation at 70°C. Ultra-thin sections were cut on an LKB Ultratome III, using glass knives. The sections were picked up onto 200 mesh copper grids, stained by using a saturated solution of

uranyl acetate in distilled water for 5 minutes, and rinsed with distilled water. These sections were then stained with lead citrate for 2 minutes, rinsed with distilled water and allowed to dry. The prepared sections of the SR fractions were viewed in a Hitachi H-600 electron microscope.

2.7 Assays of ATPase activities

a) NADH-coupled method

ATPase activities of SR protein preparations were measured by the NADH-coupled method as described by Horgan et al. (1972). ATP hydrolysis is coupled to the oxidation of NADH by including phospho(enol)pyruvate (PEP), pyruvate kinase (PK) and lactate dehydrogenase (LDH) in the reaction medium:

$$ATP \xrightarrow{ATPase} ADP + Pi + nH^+$$

$$ADP + PEP \xrightarrow{PK} Pyruvate + ATP$$

$$Pyruvate + NADH \xrightarrow{LDH} Lactate + NAD^+$$

NADH disappearance was monitored at 340 nm in an Aminco DW-2 dual wavelength spectrophotometer thermostated at 25°C. The reaction medium (2.5 ml) contained 20 mM histidine, pH 6.8, 100 mM KCl, 5 mM $MgCl_2$, 0.5 mM EGTA, 2.5 mM PEP, 0.1 mM NADH, 8 units/ml PK, and 8 units/ml LDH. The final concentration of SR protein was approximately 10 µg/ml and 4% (w/v) A23187 was added to render the vesicles permeable to Ca^{2+}. The reaction was initiated by the addition of ATP (concentrations indicated) and the change in absorbance per minute of basal ATPase activity was recorded. Ca^{2+}-dependent ATPase activity was then measured by the addition of 0.5 mM $CaCl_2$. The free [Ca^{2+}] was calculated to be 11.2 µM assuming a stability constant, $K_{CaEGTA} = 10^{11}$ (Schwartzenbach,

1957*). Ca^{2+}-ATPase activity in µmol/mg/min was calculated using a millimolar extinction coefficient of 6.22 for NADH.

b) pH stat method

ATPase activity was also measured by the pH stat method (Davidson and Berman, 1985). Protons released upon ATP hydrolysis by the Ca^{2+}-ATPase are neutralized by titration with a standardised solution of NaOH:

$$ATP \xrightarrow{ATPase} ADP + Pi + nH^+$$

pH stat titrations were performed with a Radiometer pHM 82 pH meter, TTT 60 titration and ABU 80 autoburette. Pulses from the latter were fed to a 10 bit D/A converter and then to a Houston omniscribe flat-bed recorder. The CO_2-free reaction medium (5 ml) contained 1 mM Mops, pH 7.4, 100 mM KCl, 5 mM $MgCl_2$, 100 µM $CaCl_2$, 30 µg/ml SR protein and 40 µM of the ionophore X-537A. The reaction medium was contained in a water-jacketed reaction vessel, thermostated at 25°C, and was continuously flushed with alkali-washed N_2 to prevent any buffering by CO_2. ATPase activities for the pH stat assay were calculated according to a calibrated value of 0.70 mol H^+ released per mol ATP hydrolysed at pH 7.4.

2.8 $^{45}Ca^{2+}$ transport assay

Calcium transport measurement of isolated SR preparations was based on the method of Martonosi and Ferretos (1964).

The transport assay medium (0.5 ml) contained 20 mM Mops, pH 6.8, 100 mM KCl, 5 mM $MgCl_2$, 5 mM K-oxalate, 0.5 mM EGTA, 0.5 mM $^{45}CaCl_2$ (3000 cpm/nmol; [Ca^{2+}] free = 11.2 µM), and 0.1 mg/ml SR protein.

* This equilibrium constant is for the reaction:
$Ca^{2+} + EGTA^{4-} = 10^{11}$

The reaction, at 25°C, was initiated by the addition of ATP (1 mM), and then terminated at 30 seconds and 60 seconds by filtering an aliquot (200 µl) of the assay medium through a Millipore filter (type HA, 0.45 µ pore size), and then washing with 15 ml wash buffer (20 mM imidazole, pH 6.0, 20 mM KCl, 5 mM $CaCl_2$). The filters were dried, placed in 5 ml of Instagel (Packard Ltd.), and assayed for radioactivity in a Beckman LS-233 liquid scintillation counter. The amount of radioactive calcium transported into the vesicular lumen was determined from the radioactivity remaining on the filter.

2.9 $^{45}Ca^{2+}$ efflux assay

Measurement of Ca^{2+} efflux from isolated SR fractions was based on the method of Shoshan-Barmatz (1987).

A calculated volume of SR vesicles was centrifuged at 130 000 x g for 20 minutes in a Beckman airfuge. The pellet was then resuspended to a concentration of 3 mg/ml in 300 µl of a solution containing 20 mM Mops, pH 6.8, 100 mM KCl, 5 mM $^{45}CaCl_2$ (15 000 cpm/ n mol), and incubated overnight at 0°C. The SR incubate was divided into 2 X 150 µl aliquots. Ruthenium red (20 µM) was added to one of these aliquots, which were then incubated for 5 minutes at 25°C. For $^{45}Ca^{2+}$ efflux, aliquots (20 µl) were rapidly filtered through dry Millipore filters (type HA, 0.45 µ pore size), and washed for various time intervals up to 20 seconds with appropriate volumes of wash buffer (20 mM Mops, pH 6.5, 100 mM KCl). The washing rate was approximately 1 ml/second and zero time points were determined by washing with 5 ml of 5 mM $LaCl_3$. The filters were dried, placed in 5 ml of Instagel and finally assayed for radioactivity in a Beckman LS-233 liquid scintillation counter.

2.10 Fluorescence measurements

Fluorescence measurements of TNP-ATP were performed at 25°C in a model SPF 500 Aminco-Bowman spectrofluorimeter. The excitation and emission wavelengths were set at 418 and 530 nm respectively, at 10 nm bandpasses. The fluorescence reaction medium consisted of 50 mM Tris-maleate, pH 8.0, 5 mM $MgCl_2$, 50 µM $CaCl_2$, 0.1-0.2 mg/ml SR protein and 2.2 µM TNP-ATP. Further additions are stated in the legends to the figures.

2.11 Perchloric acid deproteinisation

Perchloric acid deproteinisation of the pyruvate kinase (PK) enzyme preparation was based on the method of Jaworek et al. (1974a). Ice-cold perchloric acid (0.20 ml of 40%, w/v) was added to 2.0 ml of pyruvate kinase (diluted to a concentration of 2 mg/ml with the coupled-assay buffer). The sample was then extracted with occasional mixing for 20 minutes at 0°C. The PK protein precipitate was removed by centrifugation at 4 000 rpm for 20 minutes, and the resulting supernatent adjusted to pH 6.5 with 5 M KOH. After incubation at 0°C for 1 hour, the $KClO_4$ precipitate was collected by centrifugation at 2 000 rpm for 5 minutes. The supernatent was then analysed for ADP content as described in 2.12.

2.12 Determination of ADP

ADP, at levels >5.0 x 10^{-8} M were measured spectrophotometrically be a coupled enzyme system (Jaworek et al., 1974b), using an HP 8450 diode array spectrophotometer. All readings were taken at room temperature by measuring the changes in optical density at 340 nm.

The reaction medium (2.0 ml) contained 20 mM histidine, pH 6.8, 100 mM KCl, 5 mM $MgCl_2$, 0.5 mM EGTA, deproteinised and neutralised PK sample, PEP (1 mM), NADH (0.0625 mM) and LDH (45 µg/ml).

The absorbance at 340 nm was monitored and after a constant value had been attained, PK (86 µg/ml) was added to the assay mixture. After completion of the reaction (approximately 5 minutes), a further PK aliquot (86 µg/ml) was added and the A_{340nm} followed until no further change occured (approximately 5 minutes). The absorbance values were corrected for changes produced by addition of enzyme alone. The ADP concentration of the sample was determined by using an $NADH_{340}$ millimolar extinction coefficient of 6.22. This coupled enzyme system was also used to determine steady-state free [ADP] (see section 3.4.4).

2.13 Chemical cross-linking with glutaraldehyde

SRV (0.2-1 mg/ml of protein) and PK (0.2-1 mg/ml of protein) were preincubated in buffer (40 mM Mops, pH 7.4, 1.5 mM $MgCl_2$, 50 µM $CaCl_2$, 30 mM KCl) for 15 minutes at room temperature. Chemical cross-linking was initiated by adding 2 mM or 5 mM glutaraldehyde, based on the method of McIntosh and Ross (1985). The reaction were carried out for the times specified in the figure legends, in the presence and absence of ADP (100 µM) and ATP (1 mM). Glutaraldehyde-induced cross-linking was stopped by mixing an aliquot of the reaction mixture with an equal volume of solubilisation medium (0.2 M Tris-HCl, pH 6.8, 2% SDS w/v, 8 M urea and 4% β-mercaptoethanol w/v). Aliquots containing 10-30 µg of protein were loaded onto gradient gels (4-15% acrylamide) and SDS-PAGE analysis of the cross-linked products was then performed according to Laemmli (1970).

2.14 Difference spectrophotometric titrations

Binding of TNP-ATP to SRV was measured by differential spectroscopy using an Aminco DW-2 dual wavelength spectrophotometer. Measurements were performed at room temperature in 2 cm pathlength cuvettes with an assay medium containing 0.2 mg/ml SR protein, 20 mM Tris-maleate, pH 7.4-8.0, 20% (v/v) glycerol, 5 mM $MgCl_2$, 50 μM $CaCl_2$, and the indicated concentrations of CP, CPK, KCl, ATP and TNP-ATP. Both the sample and reference cuvettes contained TNP-ATP and buffer, but SR protein was only present in the sample cuvette. Absorbance difference spectra were recorded by spectrophotometric wavelength scanning in the split beam mode in the range 400-550 nm.

2.15 Protein Ultrafiltration

Protein ultrafiltration was performed to produce protein-free solutions for analysis as in Section 3.4.4. Flux rates were initially determined at varying Ca^{2+}-ATPase and PK concentrations in the coupled enzyme assay (2.7a). Immediately after a measurable Ca^{2+}-activated reaction rate had been obtained, the coupled assay reaction mixture was filtered under pressure through an Aminco Diaflo ultrafiltration unit, fitted with a PM-10 filter. The PM-10 filter retains compounds with a molecular weight > 10 kD. The protein-free filtrate was then assayed for "free" ADP content by the NADH-linked spectrophotometric assay (see 2.12).

2.16 Calculation of binding parameters

Binding parameters were calculated according to an iterative non-linear least squares method (Wilkinson, 1961).

3.0 RESULTS

3.1 CHARACTERISATION OF ISOLATED SARCOPLASMIC RETICULUM MEMBRANE FRACTIONS

3.1.1 Morphological characterisation of isolated sarcoplasmic reticulum fractions shown by electron microscopy

Fractions of sarcoplasmic reticulum representing terminal cisternae (TC) and longitudinal tubules or light sarcoplasmic reticulum (LSR) were prepared by sucrose density gradient centrifugation, according to the method of Saito et al. (1984) (see "Experimental Procedures"). Pellets of TC and LSR were fixed in glutaraldehyde, embedded in resin and examined by transmission electron microscopy (Ryter and Kellenberger, 1958).

Representative electron micrographs of LSR and TC fractions are shown in Figs. 7 and 8 respectively. Vesicles derived from LSR (Fig. 7A and B) are fairly uniform and sealed. They contain little or no intravesicular electron dense material. There was minimum contamination with mitochondrial fragments. The TC fraction consists of sphere-like vesicles which are characterised by electron opaque intravesicular contents (Fig. 8A and B). This electron dense material either has a "ropelike" appearance or appears to be aggregated (Chu et al., 1986). In addition, at higher magnifications (Fig. 8B), regular dense particles are seen on the surface of vesicles.

These findings are similar to those described by Saito et al., 1984. The LSR fraction consists of vesicles containing predominantly the Ca^{2+}-ATPase containing membrane. The TC vesicular membrane surface consists of both junctional face membrane and Ca^{2+}-ATPase containing membrane (Chu et al., 1986). The intravesicular electron dense material characteristic of the TC vesicles has been correlated with Ca^{2+}-binding protein

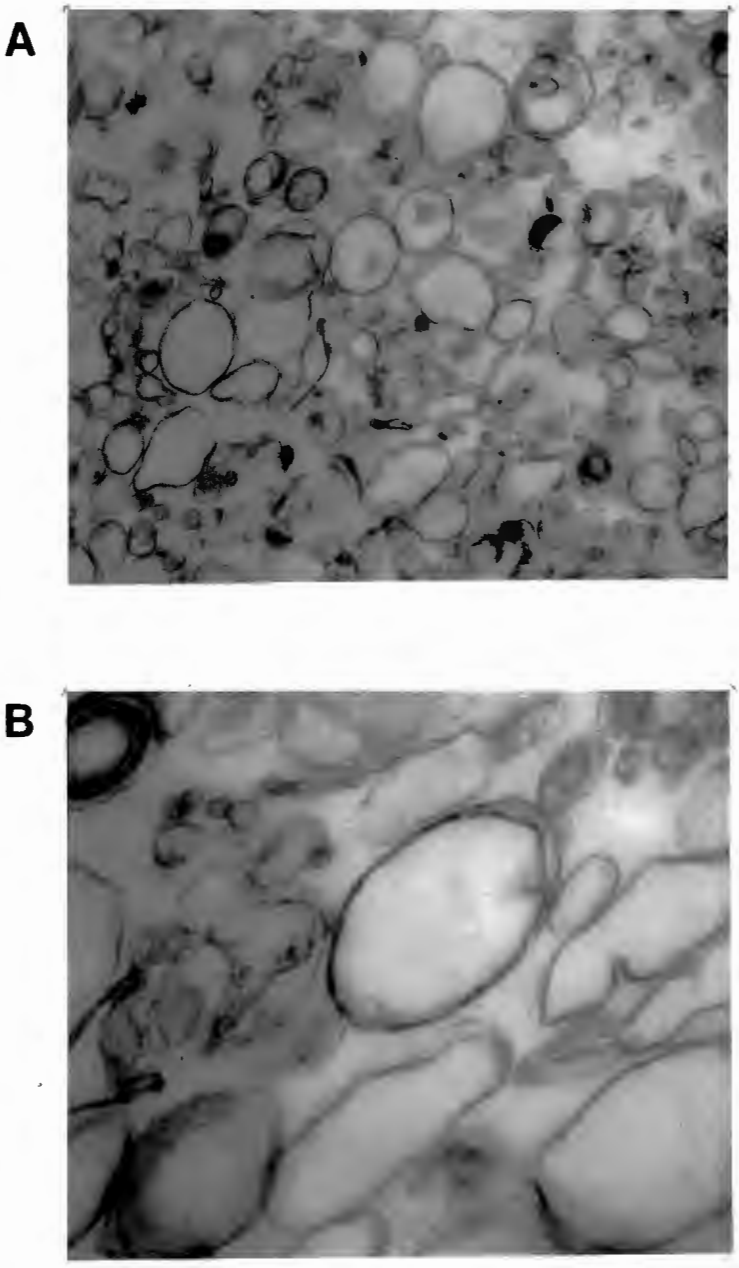

Figure 7: Thin-section electron microscopy of the isolated light sarcoplasmic reticulum region (LSR).

Sections were prepared as described under "Experimental Procedures". (A) x 90 000. (B) x 240 000. LSR vesicles are generally uniform and sealed, and intravesicular material is virtually absent.

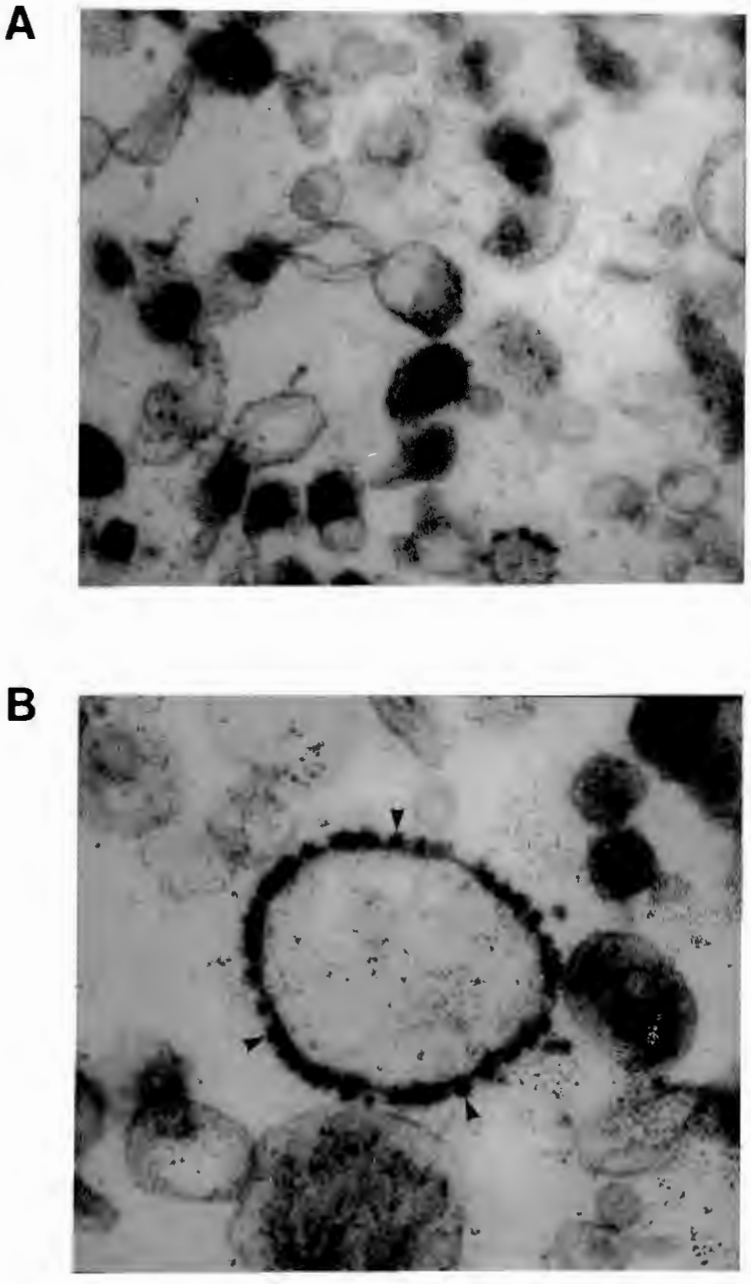

Figure 8: Thin-section electron microscopy of the isolated terminal cisternae region (TC).

Sections were prepared as described under "Experimental Procedures". (A) x 240 000, TC vesicles are sphere-like and contain electron-dense intravesicular material. (B) x 360 000, numerous "feet" structures (indicated by arrowheads) are visible as regular dense particles on the membrane surface. The intravesicular material has a filamentous appearance in this magnified vesicle.

(calsequestrin) that is confined to the lumen of TC vesicles. The electron dense surface particles of TC vesicles have been described as "feet" structures (Saito et al., 1984; Volpe et al., 1987). These are presumed to represent the link between TC and transverse tubules (see Introduction, Fig. 2) and can be observed as discrete units separated from one another.

It is concluded that the fractions isolated represent the defined sarcoplasmic reticulum fragments, TC and LSR, as previously described (Saito et al., 1984). These fractions were then used for further functional studies.

3.1.2 SDS-PAGE analysis of isolated membrane fractions

SDS-PAGE analysis (Laemmli, 1970) was carried out on the sarcoplasmic reticulum fractions isolated by sucrose gradient centrifugation (Fig. 9).

SDS-PAGE of two separate sucrose gradient preparations is shown in lanes 3 - 10 of Fig. 9. For both preparations, fractions F1 and F2 (obtained from the top end of the gradient) contain mainly ATPase (Mr = 110 k) and phosphorylase (Mr = 93k). These fractions also contain a range of soluble proteins of lower molecular weight. Fraction F3 consists predominantly of ATPase with a small proportion of calsequestrin (Mr = 63 k). F3 represents the LSR fraction described by Saito et al. (1984). Fraction F4 consists of ATPase and is enriched with calsequestrin as compared to fraction F3. F4 therefore corresponds to the terminal cisternae fraction that contains the electron-dense calcium binding protein, calsequestrin (Saito et al., 1984, Fleischer et al., 1979).

The protein composition of sarcoplasmic reticulum vesicles, prepared by the method of Eletr and Inesi (1972), is shown for comparative purposes in lanes 1 and 2 of Fig. 9. This preparation

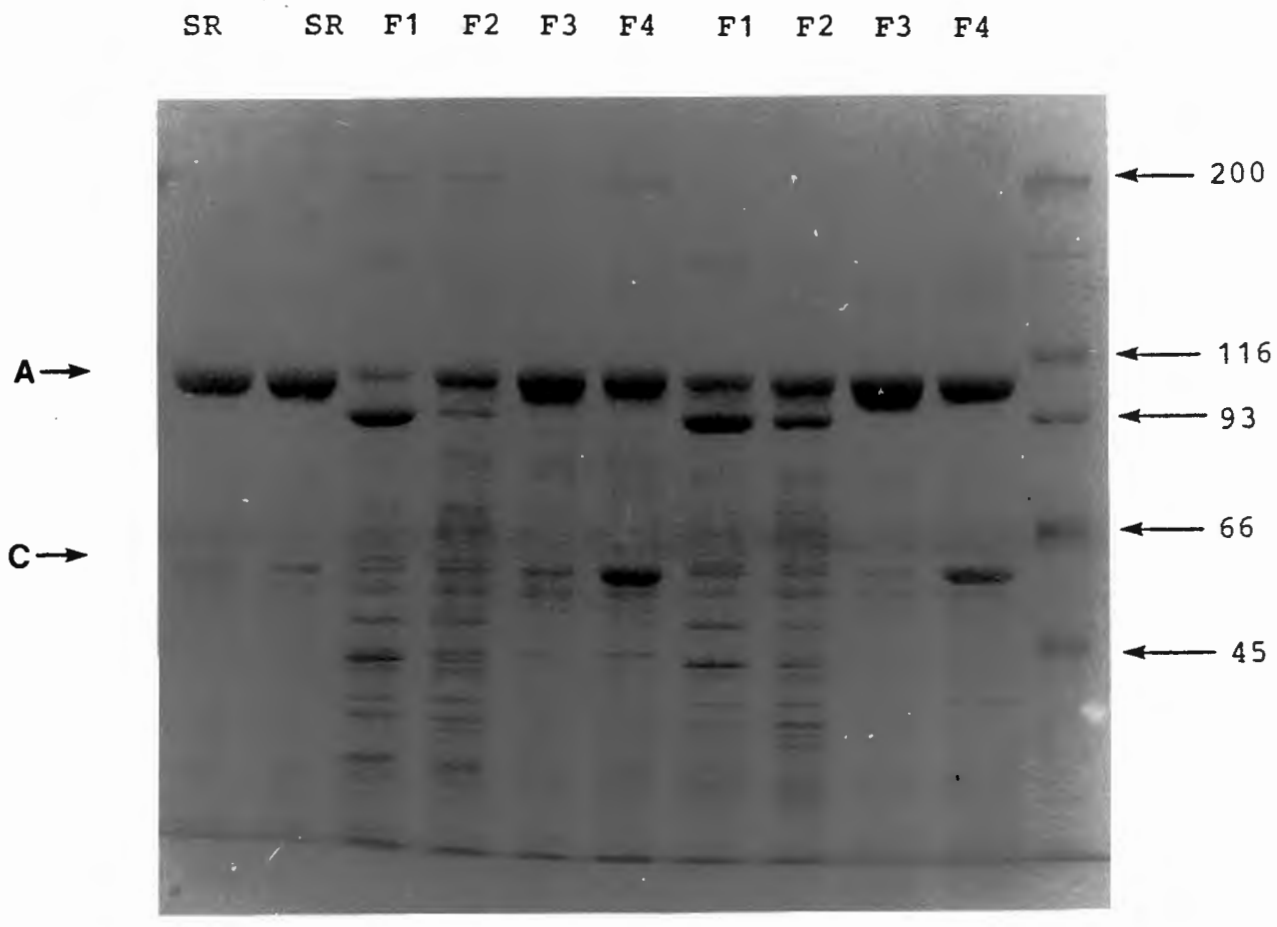

Figure 9: SDS-PAGE of sucrose gradient fractions.

SDS-PAGE (4-16% gradient gel) was performed according to Laemmli (1970), (see "Experimental Procedures"). Lanes 3-10 represent two separate sucrose gradient preparations, isolated according to the method of Saito et al. (1984). The LSR fraction (F3) consists mainly of Ca^{2+}-ATPase (A), whereas the TC fraction (F4) consists of Ca^{2+}-ATPase (A) but is enriched with calsequestrin (C). Lanes 1 and 2 represent the mixed SR preparation of Eletr and Inesi (1972), which is shown for comparitive purposes. The molecular weight standards (extreme light lane) were myosin (200 kD), β-galactoside (116 kD), phosphorylase (93 kD), bovine serum albumin (66 kD) and ovalbumin (45 kD).

does not attempt to separate light and heavy fractions of SR vesicles. SDS-PAGE electrophoresis shows it to contain more than 90% ATPase. Calsequestrin and M55 proteins are present at low concentrations. It should be noted that this mixed preparation is the one which has been most frequently used in functional studies and has been used in the experiments as described in sections 3.2, 3.3 and 3.4.

3.1.3 Ca^{2+}uptake in the presence and absence of ruthenium red

Ruthenium red (RR) is a pharmacological agent which has been reported to modulate Ca^{2+} release from isolated SR (Volpe et al., 1987). RR is a Ca^{2+} channel blocker which stimulates Ca^{2+} uptake and decreases Ca^{2+} efflux from heavy SR fractions derived from the TC region of SR (Seiler et al., 1984). Ca^{2+} uptake by LSR was approximately 4 fold higher than that of TC in the absence of RR (Table 1). RR caused a decrease (21%) in Ca^{2+} accumulation by LSR. However, RR stimulated Ca^{2+} uptake approximately 3 fold in the TC fraction. The Ca^{2+} transport values for the TC fraction thus approach those for the LSR fraction in the presence of RR. The Ca^{2+} transport for LSR was found to be 1005 nmol/mg/min. This value is lower than that obtained for non-fractionated SR (3000-4000 nmol/mg/min from preliminary experiments), and is presumably due to the fractionation procedure, which includes high speed centrifugation with sucrose gradients, that can cause inhibition of transport (Champeil et al., 1981). Chu et al. (1986) show a transport activity of approximately 1500 nmol/mg/min for LSR. The low Ca^{2+} transport in the absence of RR observed for TC as compared to LSR is consistent with the results of Chu et al. (1986). This difference in Ca^{2+} transport activity has been attributed to the existence of "open" Ca^{2+} release channels in the

TABLE 1: Ca^{2+} Transport of SR Fractions

SR Fraction	$^{45}Ca^{2+}$ Transport (nmol/mg/min)		Ratio (+RR/-RR)
	no RR	20 μM RR	
LSR	1005	798	0.79
TC	235	663	2.8

Ca^{2+} transport was measured by $^{45}Ca^{2+}$ using a Millipore filtration method in the presence and absence of 20 μM ruthenium red (RR). The reaction mixture contained 20 mM Mops (pH 6.8), 100 mM KCl, 5 mM $MgCl_2$, 5 mM K-oxalate, 0.5 mM EGTA, 0.5 mM $^{45}CaCl_2$ and 0.1 mg/ml SR protein, at 25°C. Numbers represent the average value of two separate preparations.

junctional face membrane of the TC (Morrii et al., 1985). These channels can be chemically gated by the addition of RR which then results in enhanced Ca^{2+} transport in TC, to give values approaching those of LSR.

3.1.4 Ca^{2+}-ATPase activities in the presence and absence of ruthenium red

ATPase activities of isolated TC and LSR fractions were measured spectrophotometrically by the NADH-coupled method as described by Horgan et al. (1972). The results are shown is Table 2.

The basal ATPase rate (in the absence of calcium) was 1.3 fold higher for LSR than for TC. Ca^{2+} stimulation of ATPase activity produced a 1.4 fold higher rate of hydrolysis for LSR as compared to TC.

The data differ somewhat to those of Chu et al. (1986), in that the Ca^{2+} ionophore A23187 (which abolishes the Ca^{2+} gradient across the membrane), increased ATPase activity 2.9 fold in LSR and 2.5 fold in TC, compared to 2.2 fold (LSR) and 1.1 fold (TC) from the data of Chu et al. The fact that the Ca^{2+} ionophore did stimulate ATPase activity in TC is probably due to contamination by LSR. RR had a negligible effect on the basal ATPase rate of TC and LSR. RR was found to have an inhibitory effect on the Ca^{2+}-ATPase activities of the isolated TC and LSR fractions. In the absence of ionophore, RR inhibited the Ca^{2+}-ATPase activities of TC and LSR by 20% and 19% respectively. A23187 enhanced the Ca^{2+}-ATPase activities of both TC and LSR in the presence of RR.

LSR showed a higher Ca^{2+}- ATPase activity than TC, reflecting the higher ATPase content of the LSR fraction.

TABLE 2: Ca^{2+}-ATPase Activities of SR Fractions

SR Fraction	RR Present	A23187	ATPase Activity nmol/min/mg		ATPase Activity nmol/min/mg	Ratio (+RR/-RR)
			Basal	Total	Total-Basal	
LSR	-	-	219	1051	832	0.81
	+	-	260	936	676	
	-	+	230	2620	2390	0.65
	+	+	230	1785	1555	
TC	-	-	172	767	595	0.81
	+	-	181	662	481	
	-	+	147	1640	1493	0.64
	+	+	166	1123	957	

ATPase activity was measured spectrophotometrically at pH 6.8 and 25°C by the NADH-coupled method as described under "Experimental Procedures". The assay was carried out in the presence and absence of both 4% (w/v) A23187 and 20 μM ruthenium red (RR). Basal activity was determined in the absence of Ca^{2+}. Numbers represent the average value of two separate preparations.

3.1.5 Ca^{2+} pumping efficiency

The Ca^{2+} pumping efficiency or coupling ratio is the ratio of Ca^{2+} transport activity to Ca^{2+}-ATPase activity (Ca^{2+}/ATP) determined under similar conditions (Meltzer and Berman, 1985; Chu *et al.*, 1986).

TC showed low Ca^{2+} transport activity, with a coupling ratio of 0.4. RR increased the Ca^{2+} transport activity and increased the coupling ratio more than 4 fold to 1.8. RR caused a slight decrease in the Ca^{2+} transport activity of LSR. The coupling ratio is not appreciably altered (Table 3).

The increase in Ca^{2+} transport activity induced by RR in the TC cannot be attributed to an increase in ATPase activity, as RR actually inhibits ATPase activity in both fractions. The enhanced Ca^{2+} transport and hence increased coupling ratio of TC observed in the presence of RR is presumably related to inhibition of Ca^{2+} release (Chu *et al.*, 1986).

Chu *et al.* (1986) found higher coupling ratios for LSR compared to TC in the presence of RR (1.69 versus 1.45), whereas values of 1.42 versus 1.78 respectively were determined in this study. This is probably due to experimental variation. This does not, however, materially affect the final conclusions with regard to the lower Ca^{2+}-ATPase content and presence of release channels in TC vesicles.

TABLE 3: Coupling Ratios of SR Fractions

SR Fraction	Coupling Ratio (Ca^{2+}/ATP)	
	No RR	20 μM RR
LSR	1.40	1.42
TC	0.40	1.78

$^{45}Ca^{2+}$ transport activity and Ca^{2+}-ATPase activity of the LSR and TC fractions was measured at 25°C as decribed in the legends to Tables I and II. Numbers represent the average value of two separate preparations, in the presence and absence of 20 μM ruthenium red (RR).

3.1.6 The effect of ruthenium red on Ca^{2+} efflux after passive loading

Ca^{2+} efflux from isolated TC and LSR vesicles was measured after passive $^{45}Ca^{2+}$ loading, based on the method of Shoshan- Barmatz (1987).

Passive Ca^{2+} efflux from TC and LSR vesicles is shown in Fig. 10. Ca^{2+} efflux from TC vesicles was rapid and approximately 70% of the Ca^{2+} content was released within 4 seconds. In contrast, Ca^{2+} efflux from LSR vesicles was slower and approximately 45% of trapped Ca^{2+} was released within the same time interval. RR slowed down and inhibited Ca^{2+} efflux from both TC and LSR fractions. The effects of RR are more marked in TC. The TC fraction has a 3 fold higher Ca^{2+} content compared to LSR at time zero (130 nmol/mg protein versus 44 nmol/mg protein). This phenomenon can be attributed to the high intravesicular content of the Ca^{2+}-binding protein in the terminal region (Saito et al., 1984). This is supported by the electron dense intravesicular material observed in the TC electron micrographs shown in 3.1.1. The fact that RR slightly inhibits Ca^{2+} efflux from loaded light SRV may be a consequence of the presence of some RR sensitive channels in this fraction.

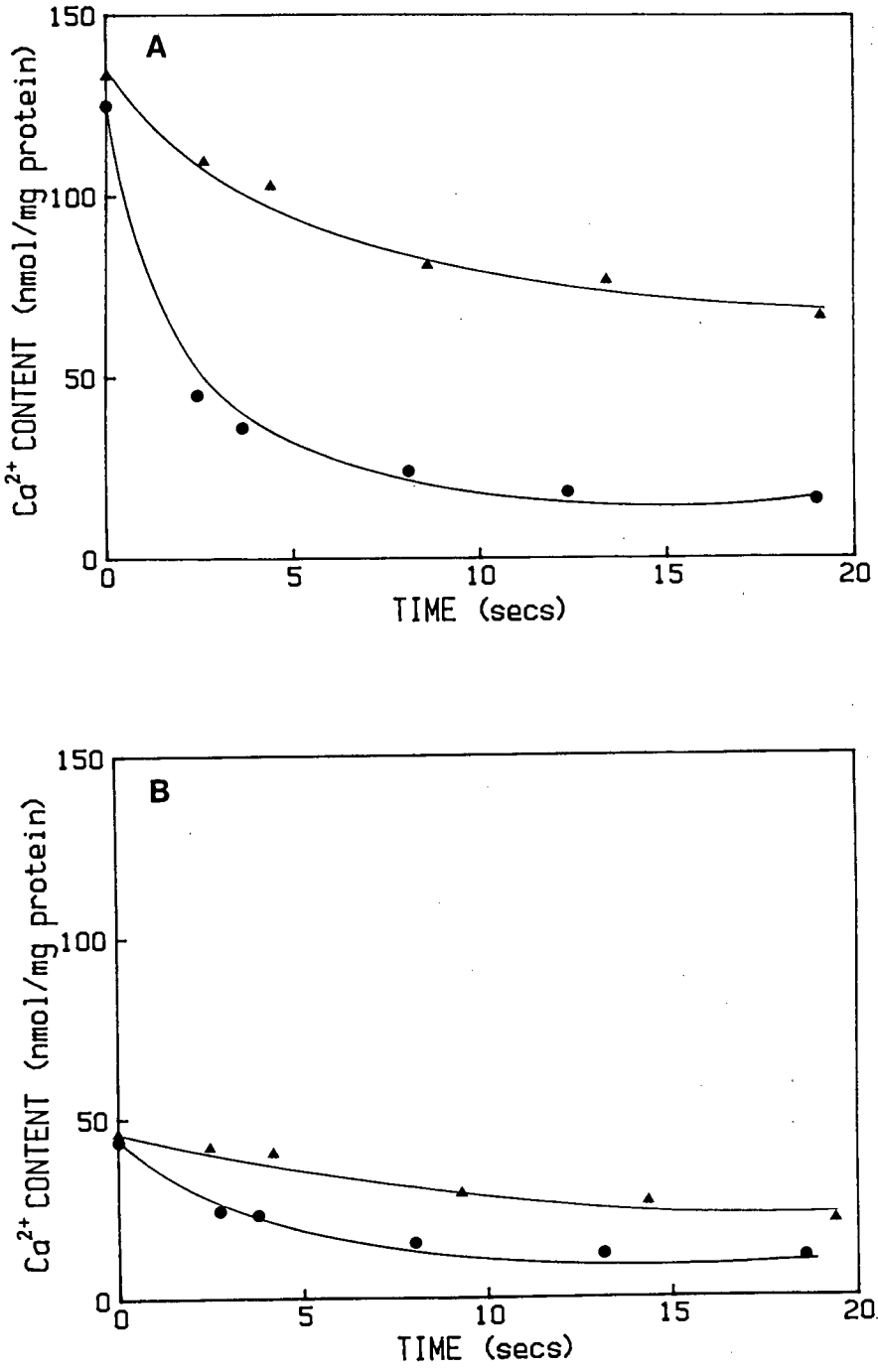

Figure 10: Ca^{2+} efflux from isolated terminal cisternae and light SR vesicles after passive loading.

SR vesicles (TC, figure A; LSR, figure B) were equilibrated with 5 mM $^{45}CaCl_2$ overnight at 4°C. Measurement of Ca^{2+} efflux was performed by a filtration assay, as described under "Experimental Procedures".

Key : ● no ruthenium red.
▲ 20 μM ruthenium red

3.1.7 Phosphoenzyme-dependent TNP-ATP fluorescence properties of isolated membrane fractions

The ATP analog TNP-ATP binds to the Ca^{2+}-ATPase of SR with high affinity (Watanabe and Inesi, 1982; Dupont et al., 1982). Binding of TNP-ATP has been determined by the increase in its fluorescence in the non-turning over enzyme (Davidson and Berman, 1987). TNP-ATP fluorescence is increased 10-fold upon induction of enzyme turnover with ATP and Ca^{2+}, and the increased fluorescence is related to ADP-insensitive E_2P levels (Dupont and Pougeois, 1983; Wakabayashi et al., 1986; Davidson and Berman, 1987).

The characteristics of isolated TC and LSR fractions with respect to ATP plus Ca^{2+} induced phosphoenzyme dependent TNP-ATP fluorescence are shown in Fig. 11. TNP-ATP fluorescence produced by the TC fraction was approximately 65% of that produced by the LSR fraction. This observation could be due to a decrease in TNP-ATP binding or modification of the nucleotide site.

The TC fraction appears to bind approximately 80% of the amount of TNP-ATP bound by the LSR fraction. This decreased binding of TNP-ATP by the TC fraction may be attributable to the decreased Ca^{2+}-ATPase specific activity of TC as compared to LSR (Saito et al., 1984). The difference in TNP-ATP binding may be reflected in the decreased fluorescence signal produced by TC upon addition of ATP.

Decreased fluorescence of TC might also be the result of a reduced nett Ca^{2+} uptake facility, due to the presence of open Ca^{2+} release channels. The presence of release channels in the TC produces greater "leakiness" of the membranes, and may result in a decrease in $E_2P.2Ca$ accumulation. ATP-dependent TNP-ATP fluorescence has been shown to be related to E_2P formation (Dupont and Pougeois, 1983; Wakabayashi et al., 1986; Davidson and Berman, 1987). Thus the low $E_2P.2Ca$ levels in TC may result in a decreased fluorescence

signal. Intravesicular Ca^{2+} concentration approaches the K_d for the low affinity, internally orientated Ca^{2+} binding sites (0.6 - 1 mM, Carvalho et al., 1976) in well-sealed LSR vesicles. Ca^{2+} accumulation inside the vesicles would be expected to inhibit breakdown of $E_2P.2Ca$ and to increase the fluorescence signal of LSR.

ATP hydrolysis of LSR and TC was measured under conditions of the fluorescence assay. ATP hydrolysis in LSR vesicles was slower than that in TC vesicles. LSR vesicles under the fluorescence conditions of pH 8.0 and 20% (v/v) glycerol are well sealed. High intravesicular Ca^{2+} concentration following turnover would be expected to inhibit E-P hydrolysis and steady- state turnover in LSR. Enhanced turnover of TC could be due to membrane "leakiness" caused by the presence of Ca^{2+} release channels. This "leakiness" relieves the constraints of high intravesicular Ca^{2+} concentration.

It was of interest therefore to study the effect of RR, which would block the Ca^{2+} release channels, on ATP-induced TNP-ATP fluorescence. However, RR caused a marked decrease in the ATP-dependent TNP-ATP fluorescence (Fig. 11) due to quenching by inner filter effects. This precluded further studies in this direction.

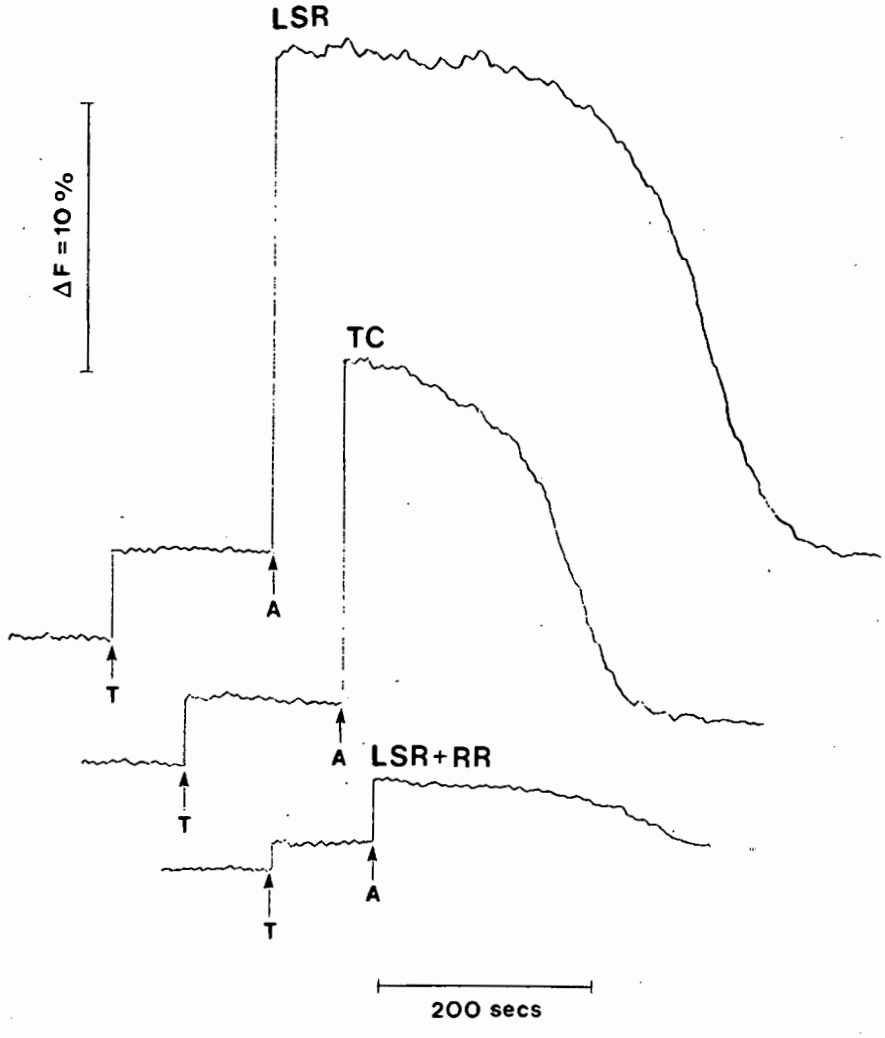

Figure 11: Fluorescence of bound TNP-ATP in isolated terminal cisternae and light SR vesicles.

TC and LSR vesicles (0.1 mg/ml), were incubated at 25°C in a medium containing 50 mM Tris-maleate, pH 8.0, 20% (v/v) glycerol, 5 mM $MgCl_2$ and 50 µM $CaCl_2$. The vesicles were then assayed for E-P dependent enhanced TNP-ATP fluorescence by the addition of 2 µM TNP-ATP (T) and 50 µM ATP (A). The addition of 20 µM ruthenium red (RR) appeared to markedly quench the fluorescence signal.

3.2 EFFECTS OF TNP-ATP ON CATALYSIS

3.2.1 The effect of the ionophore A23187 on calcium activated ATPase activity

Ca^{2+} ionophores have been shown to directly activate Ca^{2+}- ATPase activity (Neet and Green, 1977). The Ca^{2+} ionophore A23187 confers increased Ca^{2+} permeability to lipid bilayers of the sarcoplasmic reticulum by partitioning into the bilayer and forming Ca^{2+} ion conductance pathways (Berman, 1982) A23187 is thus very useful in experimental design to remove inhibition of activity caused by build-up of high intravesicular [Ca^{2+}] (Caswell and Pressman, 1972).

The effect of A23187 on Ca^{2+}-stimulated ATPase activity was measured using the NADH-coupled assay (Horgan et al., 1972) and the results are shown in Fig. 12. The concentration of ionophore is expressed relative to SR protein concentration (w/w). A23187 stimulated ATPase activity in the concentration range 0 - 10% A23187/SR protein (w/w) (Fig. 12), with an apparent half-maximal effect at 0.52% A23187/SR protein (w/w). The maximum stimulation was observed with approximately 4% A23187/SR protein (w/w), and this concentration of ionophore was used in all subsequent NADH-coupled assay experiments.

The enhanced ATPase activity observed in the presence of A23187 is associated with removal of any inhibition of catalysis caused by intravesicular Ca^{2+} accumulation. The ionophore dissipates the Ca^{2+} gradient formed and the vesicles are rendered "leaky" thereby allowing the release of Ca^{2+} from the lumen (Scarpa et al., 1972). 4% A23187/SR protein (w/w) has previously been reported as the concentration of ionophore required to render SR vesicles "completely leaky" (Champeil et al., 1986; Champeil and Gullain, 1986).

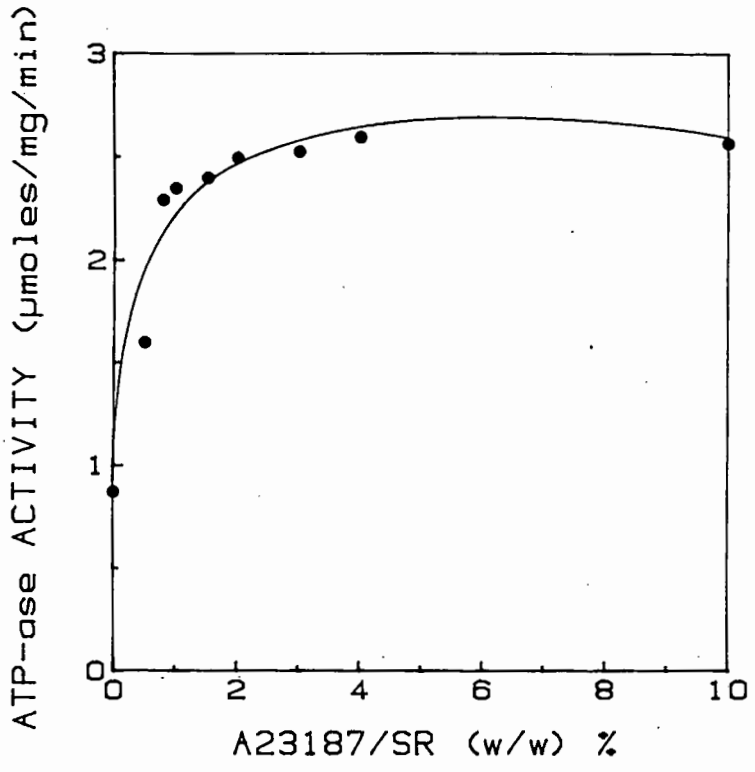

Figure 12: The effect of A23187 on Ca^{2+}-stimulated ATPase activity.

ATPase activity was measured spectrophotometrically at pH 6.8 and 25°C by the NADH-coupled method (see "Experimental Procedures"). The concentration of A23187 is expressed relataive to that of SR protein (w/w).

3.2.2. The effect of TNP-ATP on calcium activated ATPase activity as measured by the pH stat assay

The effect the nucleotide analog of TNP-ATP on calcium activated ATPase activity as measured by the pH stat assay (Davidson and Berman, 1985) is shown in Figs. 13 and 14. Protons released by ATP hydrolysis are neutralised by titration with standardised NaOH in the pH stat assay:

$$ATP \xrightarrow{ATPase} ADP + Pi + nH^{+}$$

TNP-ATP concentration was varied in the range 0-15 μM in the presence of 100 mM KCl, 300 μM Mg.ATP and 100 μM Ca^{2+} (Fig. 14). Ca^{2+}-ATPase activity in the absence of TNP-ATP was 0.77 μmol/min/mg. TNP-ATP stimulated the hydrolysis of Mg.ATP, with $K_{0.5}$ (apparent) = 0.80 μM. The maximum stimulation (49 ± 4%) was produced at approximately 5.0 μM TNP-ATP. Above 5.0 μM TNP- ATP the stimulation of ATPase activity decreased, and at 15.0 μM TNP-ATP stimulation was 21%. Higher concentrations of TNP-ATP, however, produced an inhibition of ATPase activity with the pH stat assay (data not shown). TNP-ATP stimulation of ATPase activity, as measured by the pH stat assay, was approximately 2.5 fold higher in the presence of 100 mM KCl than in the absence of KCl. The Ca^{2+}-stimulated ATPase activity was approximately 1.8 fold higher with 100 mM KCl present (data not shown). The stimulation of ATPase activity by TNP-ATP that was observed in the pH stat assay is consistent with the findings of Carvalho-Alves *et al.* (1985) and Dupont *et al.*, 1985. TNP-ATP binds with high affinity to the Ca^{2+}-ATPase of SR (Watanabe and Inesi, 1982; Dupont *et al.*, 1982). Dupont *et al.* (1985) propose that the activation of hydrolytic activity by TNP-ATP observed in the pH stat assay is due to TNP-ATP binding to the low affinity regulatory nucleotide site.

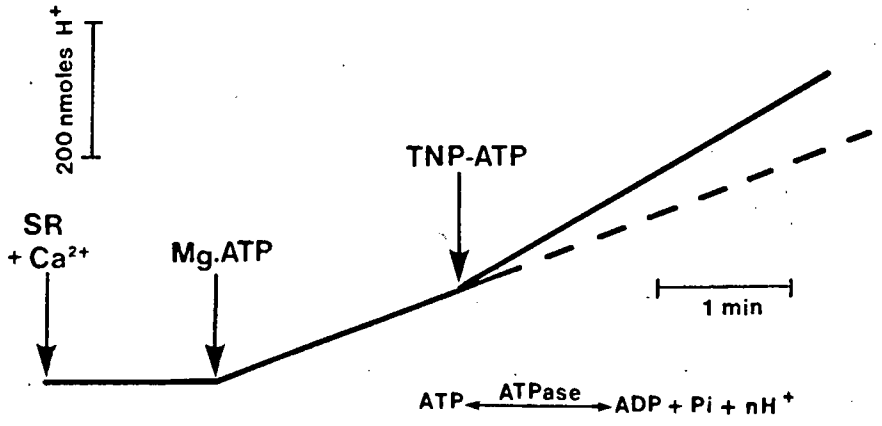

Figure 13: pH stat assay trace representing the effect of TNP-ATP on Ca^{2+}-ATPase activity.

The reaction medium contained 1 mM Mops (pH 7.4), 100 mM KCl, 5 mM $MgCl_2$, 100 µM $CaCl_2$, 30 µg/ml SR protein and 40 µM X-537A, at 25°C. ATPase activity was monitored after the addition of 300 µM ATP. Maximum stimulation of hydrolysis was observed in the presence of 5 µM TNP-ATP.

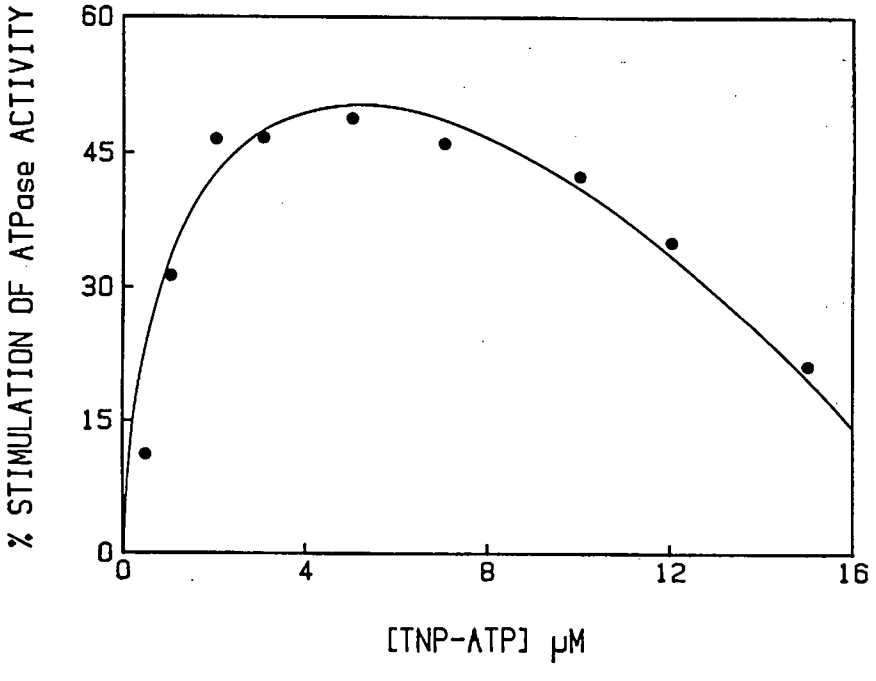

Figure 14: Concentration dependence of the TNP-ATP induced stimulation of Ca^{2+}-ATPase activity as measured by the pH stat assay.

Ca^{2+}-ATPase activity was measured at constant ATP concentrations (300 µM) by the pH stat method in a reaction medium as described in Fig. 13. The results are expressed as the percentage stimulation of Ca^{2+}-ATPase activity observed upon addition of TNP-ATP (0-15 µM) to the reaction mixture.

3.2.3 The effect of TNP-ATP on calcium activated ATPase activity as measured by the NADH-coupled enzymatic assay

The effect of the nucleotide analog TNP-ATP on calcium- activated ATPase activity as measured by the NADH-coupled assay (Horgan et al., 1972) is shown in Figs. 15 and 16. The interaction of the coupled enzyme system with the ATPase in the NADH-coupled assay is via the common metabolite, ADP:

$$ATP \xrightarrow{ATPase} ADP + Pi + nH^+$$

$$ADP + PEP \xrightarrow{PK} Pyruvate + ATP$$

$$Pyruvate + NADH \xrightarrow{LDH} Lactate + NAD^+$$

TNP-ATP concentration was varied in the range 0-120 μM in the presence of 100 mM KCl, 300 μM Mg.ATP and 20 μM Ca^{2+} (Fig. 16). Ca^{2+}-ATPase activity in the absence of TNP-ATP was 2.0 μmol/min/mg. TNP-ATP inhibited the hydrolysis of Mg.ATP, with $K_{0.5}$ (apparent) = 24 μM. In the presence of 5.0 μM TNP-ATP, which stimulated Ca^{2+}-ATPase activity 49% in the pH stat assay, Ca^{2+}-ATPase activity was decreased 25% (Fig. 15).

The inhibition of Ca^{2+}-ATPase activity by TNP-ATP in the NADH-coupled assay is consistent with previous reports (Berman, 1986). Significantly, no stimulation of ATPase activity in the range 0 - 5.0 μM TNP-ATP was observed in the NADH-coupled assay. This is in contrast to the stimulation produced by TNP-ATP in the pH stat assay (see Fig. 13).

TNP-ATP could either cause competitive inhibition of ATPase activity by competing with Mg.ATP at the catalytic nucleotide site, or could interact with pyruvate kinase and lactate dehydrogenase directly and so limit response of the NADH-coupled system. The effect of TNP-ATP on the NADH-coupled system alone was therefore investigated.

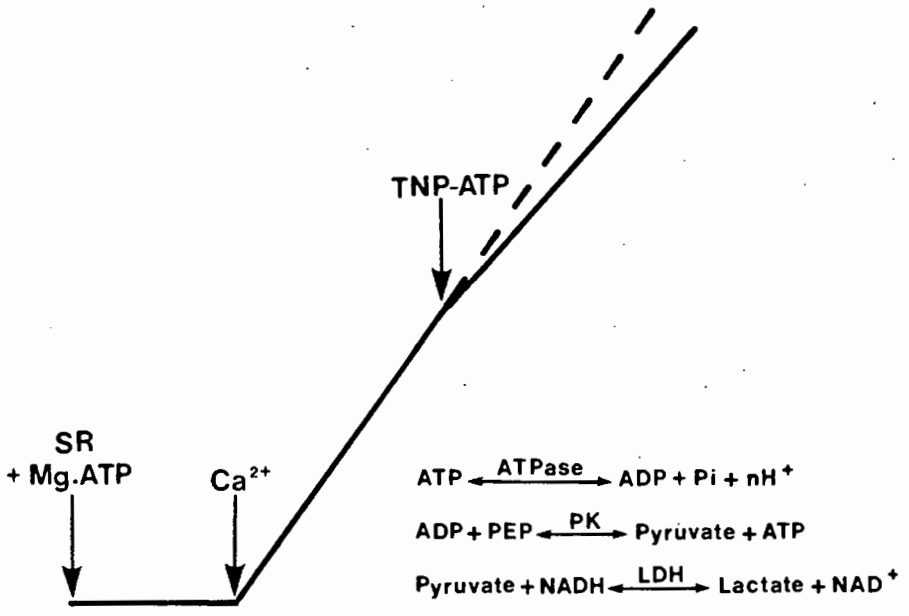

Figure 15: NADH-coupled assay trace corresponding to the effect of TNP-ATP on Ca^{2+}-ATPase activity.

Ca^{2+}-stimulated ATPase activity was measured spectrophotometrically by the NADH-coupled method (see "Experimental Procedures"), in the presence of 20 µM Ca^{2+}, 100 mM KCl and 300 µM ATP. Addition of 5.0 µM TNP-ATP caused an apparent 25% inhibition of Ca^{2+}-ATPase activity.

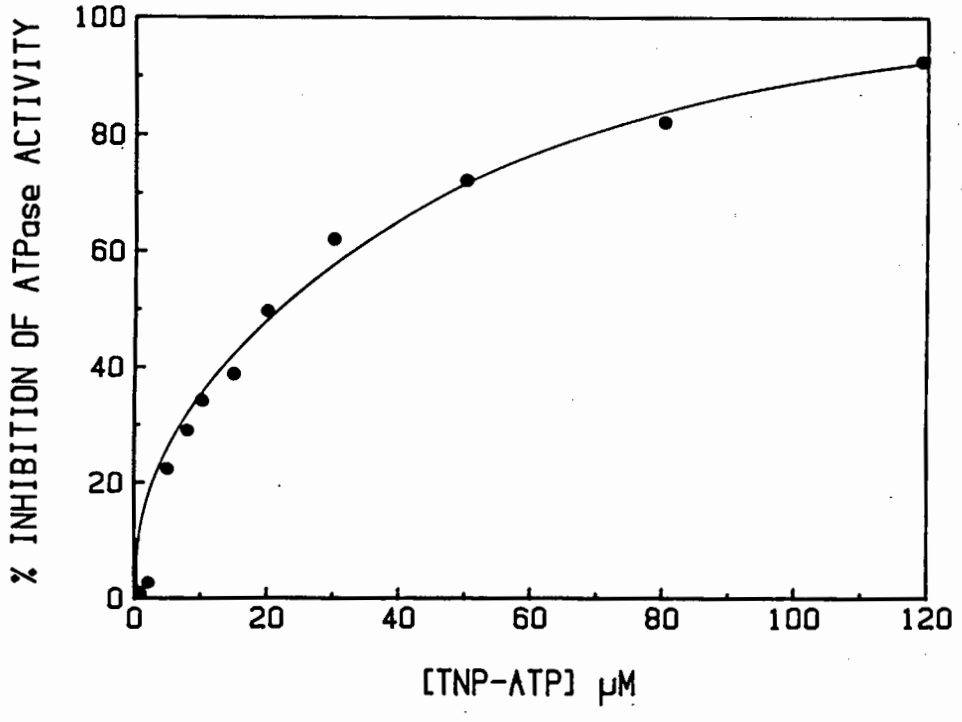

Figure 16: Concentration dependence of the TNP-ATP induced inhibition of Ca^{2+}-ATPase activity as measured by the NADH-coupled assay.

Ca^{2+}-ATPase activity was measured at constant ATP concentrations (300 µM) by the NADH-coupled method as described in Fig. 15. The results are expressed as the percentage inhibition of Ca^{2+}-ATPase activity observed in the presence of TNP-ATP (0-120 µM).

3.2.4 The effect of TNP-ATP on the coupled enzyme system - ADP infusion experiments

The inhibitory effect of TNP-ATP observed in Fig. 16 could have been due to inhibition by TNP-ATP of the coupling enzymes (pyruvate kinase, lactate dehydrogenase), and not a direct inhibitory effect on the Ca^{2+}-ATPase. This possibility was tested by constant rate infusion of ADP into the coupled assay reaction medium containing the same components as used in 3.2.3, with the exception that no SR protein was added. Any inhibition observed could thus be attributable to an effect of TNP-ATP on the coupling enzymes and not the SR protein. The concentration of ADP infused (2.0 mM) and rate of infusion (10 µl/min), was based on the calculated rate of ADP production that resulted in the same change in NADH absorbance per minute as 10 µg/ml SR protein.

TNP-ATP was shown to have a negligible inhibitory effect on the coupling enzymes in the concentration range 0-80 µM (Fig. 17). TNP-ATP, 5.0 µM, produced an inhibition of 4% on the coupling enzymes alone compared to an inhibition of 25% in the presence of SR protein. With 50.0 µM TNP- ATP an inhibition of 13% was observed with ADP infusion, compared to an inhibition of 72% with SR protein present.

It appears therefore that the inhibitory effect of TNP-ATP observed in the NADH-coupled assay is due to its direct effect on ATPase activity of SR vesicles rather than on the enzymatic coupling reactions. TNP-ATP appears to competitively inhibit Mg.ATP binding to the Ca^{2+}-ATPase as measured by the NADH-coupled assay.

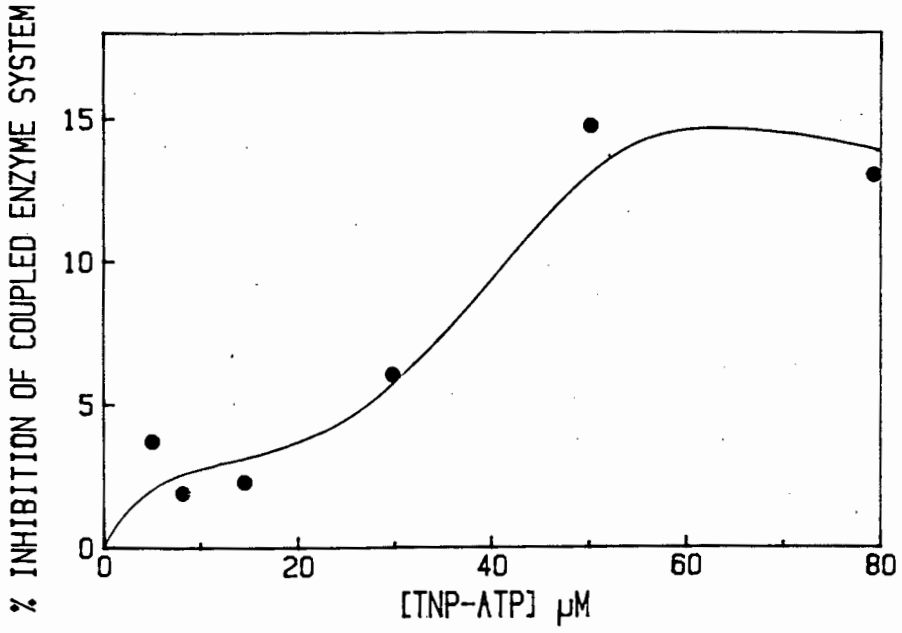

Figure 17: ADP infusion experiments showing the effect of TNP-ATP on the coupled enzyme system.

ADP (2.0 mM) was infused at a constant rate (10 μl/min) into the NADH-coupled assay reaction medium containing the same components as described in Fig. 15, except that SR protein was omitted. This produced a change in NADH absorbance per minute equivalent to that shown in the presence of 10 μg/ml SR protein. The effect of TNP-ATP (0-80 μM) the coupled enzymes is described in terms of the percentage inhibition of the NADH 340 nm absorbance signal.

3.2.5 The effect of TNP-8-azido nucleotides on Ca^{2+}-activated ATPase activity

The TNP-8-azido nucleotides are a series of photoaffinity probes which have been recently synthesised in our laboratory (Seebregts and McIntosh, 1988). Both the TNP nucleotides (Watanabe and Inesi, 1982), and the TNP-8-azido nucleotides have been shown to bind wiht high affinity to the regulatory site of the Ca^{2+}-ATPase. The effects of TNP-8-azido nucleotides on Ca^{2+}- activated ATPase activity were measured by the pH stat assay (Davidson and Berman, 1985). The results are summarised in Table 4.

Using 3.0 μM nucleotide, $8N_3$ TNP-ATP and $8N_3$ TNP-ADP produced 37% and 25% activation of ATPase activity respectively. $8N_3$ TNP-AMP produced slight inhibition (3%) of ATPase activity.

Dupont et al. (1985) described TNP-nucleotide dependence of ATPase activation. They reported that with 0.5 μM nucleotide, TNP-ATP produced a 70% activation. TNP-ADP and TNP-AMP produced 20% and 45% inhibition respectively.

Non-covalently bound N_3 derivatives of TNP nucleotides, with the apparent exception of $8N_3$ TNP-ADP, appear to have a similar effect as the underivatised TNP nucleotides.

TABLE 4: Effects of TNP-8-azido Nucleotides on Ca^{2+}-ATPase Activity as Measured by the pH stat Assay

(Numbers represent the activation factors (V1/V0) induced by 3.0 μM nucleotide at 70 μM ATP)

	$8N_3$ TNP-ATP	$8N_3$ TNP-ADP	$8N_3$ TNP-AMP
$\frac{V1}{V0}$	1.37	1.25	0.97

3.2.6 The effect of TNP-ATP on AcP dependent hydrolysis

Acetyl phosphate (AcP) is a synthetic organic compound which acts as an energy-rich phosphate donor. AcP has been used successfully as a pseudosubstrate in place of ATP for mechanistic studies of the Ca^{2+}-ATPase of SR (Pucell and Martonosi, 1971; Rossi et al., 1979; Liguri et al., 1980; Bodley and Jencks, 1987). It has been shown that both ATP and AcP hydrolysis are Mg^{2+} dependent and Ca^{2+}-activated and that AcP and ATP react through the same pathway for much of the reaction cycle.

Unlabeled AcP was synthesised according to the method of Kornberg et al., 1956. The effects of TNP-ATP on calcium- activated AcPase activity were measured by the pH stat assay (Davidson and Berman, 1985), (Fig. 18). TNP-ATP inhibited AcPase activity. Inhibition was approximately 90% in the presence of 4.0 μM TNP-ATP. Increasing Mg^{2+} concentration was shown to decrease the observed TNP-ATP inhibition. With 1 mM Mg^{2+} present, 1.0 μM TNP-ATP produced an 82% inhibition of AcPase activity, whereas in the presence of 25 mM Mg^{2+}, 1.0 μM TNP-ATP produced a 31% inhibition.

The inhibition of AcP hydrolysis by TNP-ATP can be explained in terms of direct competitive inhibition. AcP and TNP-ATP compete with each other for the high affinity catalytic nucleotide binding site of the enzyme. Mg.ATP is the true physiological substrate of the Ca^{2+}-ATPase (Weber et al., 1966; Kanazawa et al., 1971; Yamamoto et al., 1979; de Meis and Vianna, 1979; Makinose and Boll, 1979). In the experiments described above, Mg.AcP is functioning as a pseudosubstrate in place of Mg.ATP. Therefore an increase in substrate (Mg.AcP) concentration at constant inhibitor (TNP-ATP) concentration decreases the degree of inhibition, consistent with the model of competitive inhibition as described by Segal, 1976 (K_i = 0.2-0.4 μM).

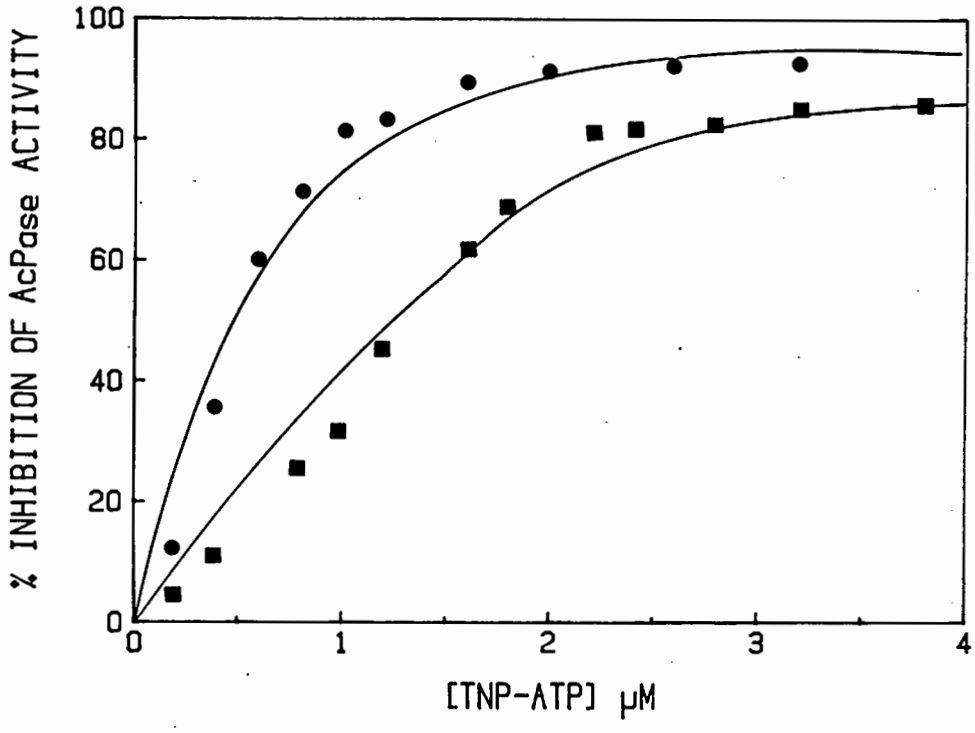

Figure 18: Concentration dependence of the TNP-ATP induced inhibition of Ca^{2+}-AcPase activity as measured by the pH stat assay.

The reaction medium contained 1 mM Mops (pH 7.4), 100 mM KCl, 100 μM $CaCl_2$, 0.2 mg/ml SR protein and 40 μM X537A at 25°C. Ca^{2+}-ATPase activity was measured on addition of 5 mM AcP, in the presence of 1 mM $MgCl_2$ (●) and 25 mM $MgCl_2$ (■). Data are expressed as the percentage inhibition of Ca^{2+}-AcPase activity observed in the presence of TNP-ATP (0-4.0 μM).

3.2.7 The effect of millimolar Mg.ATP on the calcium activated ATPase activity

The Ca^{2+}-ATPase activity of SR exhibits a complex dependence on ATP concentration. Previous studies have shown that the ATP stimulation occurs over two concentration ranges (Inesi et al., 1967; Kanazawa et al.,1971; Dupont, 1977; Verjovski-Almeida and Inesi, 1979; Moller et al., 1980; Coll and Murphy, 1985). Enzyme turnover is enhanced in a saturable manner with ATP in the micromolar range (Km = 2-20 μM) and turnover is further activated by millimolar ATP (K_d = 0.4-3 mM), (Bishop et al., 1987), which is reported to stimulate the rate limiting $E_2 \rightarrow E_1$ transition (de Meis and Boyer, 1978). ATP concentration dependence of enzyme catalysis has been explained in terms of two classes of ATP binding sites, a high affinity catalytic nucleotide site and a low affinity regulatory site (Dupont et al., 1985; Bishop et al., 1987).

A pH stat trace corresponding to the effects of millimolar Mg.ATP on the Ca^{2+}-activated ATPase activity are shown in Fig. 19. Following stimulation of ATPase activity by 1 mM Mg.ATP (in the presence of 100 μM Mg.ATP), addition of 5.0 μM TNP-ATP resulted in no further activation.

These results are consistent with previous findings (Taylor and Hatton, 1979; Dupont et al., 1985). The activation of hydrolysis by TNP-ATP and by millimolar Mg.ATP are complementary.

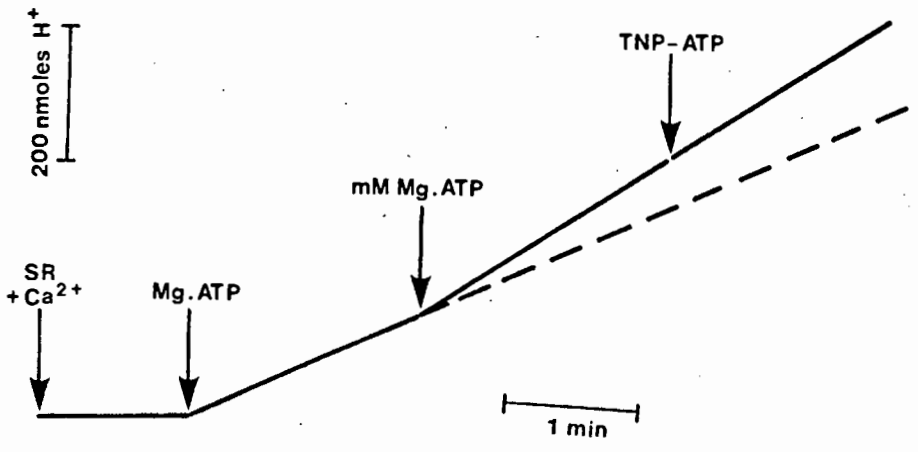

Figure 19: pH stat assay trace representing the effect of millimolar ATP on Ca^{2+}-ATPase activity.

The reaction medium (25°C) contained 1 mM Mops, pH 7.4, 100 mM KCl, 5 mM $MgCl_2$, 100 µM $CaCl_2$, 30 µg/ml SR protein, 40 µM X-537A and the indicated concentrations of TNP-ATP and ATP.

3.3 EFFECTS OF K^+ ON TNP-ATP BINDING TO THE Ca^{2+}-ATPase

3.3.1 Difference Spectra of TNP-ATP bound to non-phosphorylated and phosphorylated Ca^{2+}-ATPase

The ATP analog, TNP-ATP, is very useful for studying binding stoichiometry and conformational changes of the Ca^{2+}-ATPase of SR (Watanabe and Inesi, 1982; Berman, 1986). TNP-ATP undergoes readily monitored spectroscopic changes upon binding of the nucleotide to the Ca^{2+}-ATPase. Equilibrium binding of TNP-ATP to the Ca^{2+}-ATPase has been measured by differential spectrophotometry (Watanabe and Inesi, 1982). In addition, difference spectral shifts occur on enzyme phosphorylation (Berman, 1986). Difference spectra produced by TNP-ATP binding have also previously been reported for F_oF_1-ATPase (Grubmeyer and Penefsky, 1986).

The procedure used in this study involved spectrophotometric wavelength scanning in the split beam mode in the range 400-550 nm. Both sample and reference cuvettes contained TNP-ATP and buffer, but only the sample cuvette contained SR vesicles. Difference spectra of TNP-ATP bound to non-phosphorylated and phosphorylated Ca^{2+}-ATPase are shown in Fig. 20. The addition of TNP-ATP (2 μM) to SR protein (0.2 mg/ml) produced a characteristic difference spectrum, with respect to free TNP-ATP, in the visible region. The spectrum has a trough at 455 nm and a peak at 510 nm. Addition of ATP (100 μM) resulted in a decrease in the absorbance difference peak at 510 nm, and reduced the TNP-ATP difference spectrum to approximately one-half of its original intensity. Significantly, a new absorbance peak of lower absorbance with λmax at 493 nm was produced with ATP.

These results are consistent with previous findings (Watanabe and Inesi, 1982; Berman, 1986). The 493 nm species produced upon ATP-binding has been described as the spectrophotometric equivalent of the ATP plus Ca^{2+}-induced "superfluorescent" species by Berman (1986). When using differential spectrophotometry, therefore, TNP-ATP acts as a reporter of conformational changes occuring at the catalytic site of the Ca^{2+}-ATPase.

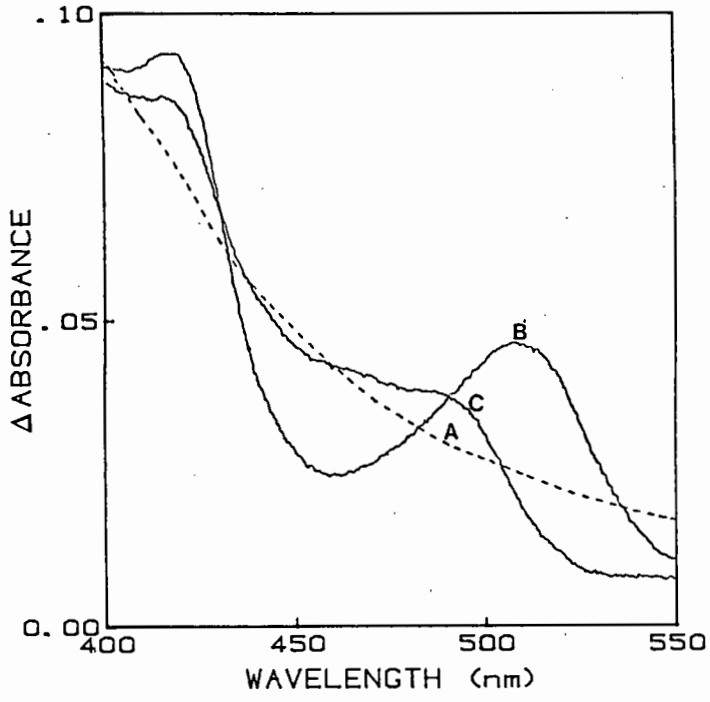

Figure 20: Difference spectra of TNP-ATP bound to non-phophorylated and phosphorylated Ca^{2+}-ATPase.

Difference spectra, between sample cuvette, containing 0.2 mg/ml SR protein, and buffer reference cuvette were obtained by split-beam differential spectrophotometry. The traces recorded represent no added TNP-ATP (A), addition of 2.0 μM TNP-ATP (B) and subsequent addition of 100 μM ATP (C). The assay medium contained 20 mM Tris-maleate, pH 8.0, 20% (v/v) glycerol, 5 mM $MgCl_2$ and 50 μM $CaCl_2$.

3.3.2 The effect of K^+ on the difference binding spectrum of TNP-ATP

Mechanisms of interaction of K^+ with the Ca^{2+}-ATPase of SR have previously been reported. K^+ binding to the monovalent cation binding site of the Ca^{2+}-ATPase stimulates E-P hydrolysis with a $K_{0.5}$ of 51 mM (Shigekawa and Dougherty, 1978). Phosphoenzyme dependent TNP-ATP fluorescence is sensitive to K^+, and decreases in a manner which is consistent with binding of K^+ to the monovalent cation site (Davidson and Berman, 1985). K^+ binding, as measured by inhibition of TNP-ATP fluorescence, has a $K_{0.5}$ (apparent) of 49 mM (Davidson and Berman, 1985).

There are two possible mechanisms for the observed TNP-ATP fluorescence decrease in the presence of K^+:

a)K^+ stimulates E-P hydrolysis and therefore decreases relative levels of E_2P, the enzyme species reported to be responsible for enhanced TNP-ATP fluorescence (Davidson and Berman, 1987), or

b)K^+ decreases the affinity of the nucleotide binding site for TNP-ATP, as proposed by Bishop et al., 1986. However, an increase in ATPase activity upon addition of TNP-ATP was observed with the pH stat assay, in the presence of 100 mM KCl (see Fig. 14). The stimulation of ATP hydrolysis produced by TNP-ATP means that there must be some TNP-ATP binding to cause this effect.

The effect of K^+ on the spectrophotometric difference spectrum of bound TNP-ATP is shown in Fig. 21. ATP (100 µM) produced the characteristic spectrum described in 3.3.1, with an absorbance peak of λmax 493 nm. The addition of 100 mM KCl to the turning-over enzyme decreased the magnitude of the difference spectrum, but the 493 nm peak was still distinguishable. Additional scans were taken at 5 minute intervals up to 20 minutes, as the ATP was hydrolysed.

These scans show the disappearance of the 493 nm peak and the reappearance of the 510 nm peak characteristic of TNP-ATP binding to the Ca^{2+}-ATPase. The absorbance difference peak at 510 nm seen after 20 minutes was, however, decreased in intensity as compared to the original spectrum. This decreased 510 nm peak could be attributable to:

a)K^+ induced changes in the affinity of TNP-ATP bound.

b)ADP competing with TNP-ATP for the nucleotide binding site.

The reappearance of the 510 nm peak, following hydrolysis of added ATP, shows that TNP-ATP is binding to the Ca^{2+}-ATPase in the presence of K^+, and probably corresponds to the E_1TNP species. Difference binding spectra of TNP-ATP were also used to estimate the apparent affinity of K^+ for the turning-over enzyme. An ATP regenerating system (creatine phosphate, creatine phosphokinase) was used, which, from preliminary experiments, was shown not to affect the difference binding spectrum of TNP-ATP. KCl, in the concentration range 0-150 mM was added to both cuvettes. An estimation of the apparent affinity of the turning-over enzyme for K^+ was obtained by measurement of $A_{530-493nm}$ (Figs. 22 and 23). The $K_{0.5}$ (apparent) for K^+ binding was 42 mM.

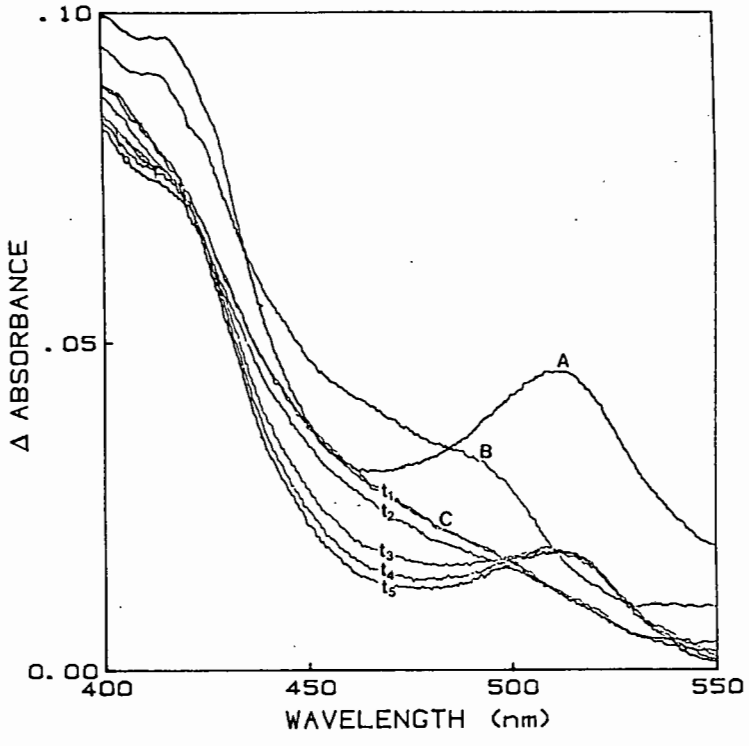

Figure 21: The effect of K^+ on the difference binding spectrum of TNP-ATP.

Differential spectra were recorded in an assay medium as described in Fig. 20. Additions were : (A), 2 μM TNP-ATP; (B), 100 μM ATP; (C), 100 mM KCl. Additional spectra were recorded at 0, 5, 10, 15 and 20 minutes after the addition of KCl (traces t_1-t_5 respectively).

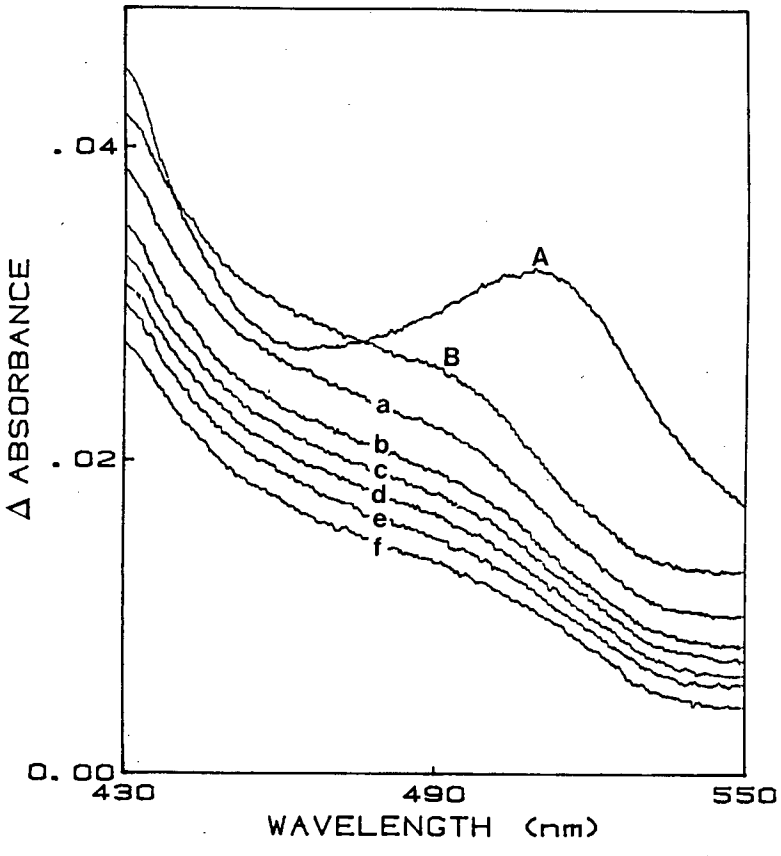

Figure 22: K^+ titration of the turnover dependent TNP-ATP difference binding spectrum.

Difference spectra were recorded in an assay medium as described in Fig. 20, with the inclusion an ATP-regenerating system (5 mM creatine phosphate and 0.04 mg/ml creatine phosphokinase). Additions were : (A), 2 μM TNP-ATP; (B), 100 μM ATP. Sequential additions of KCl gave cumulative concentrations of 20, 40, 60, 80, 100 and 150 mM, represented by traces a-f respectively.

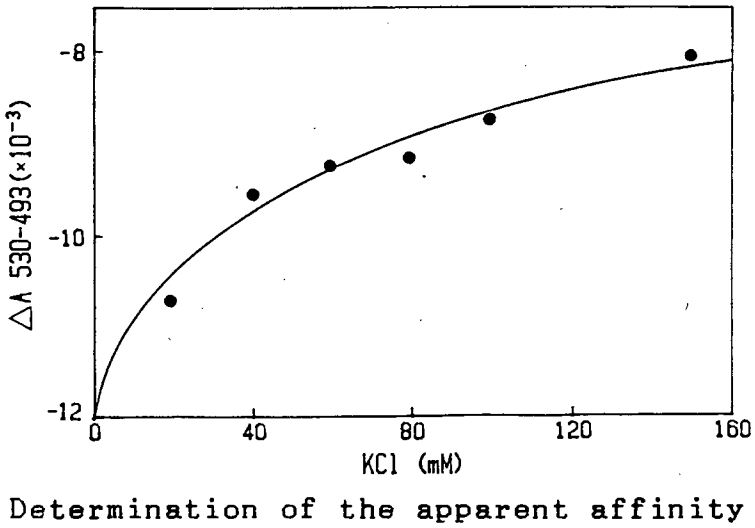

Figure 23: Determination of the apparent affinity of K^+ for the turning-over enzyme.

An estimation of the apparent affinity of the turning-over Ca^{2+}-ATPase for K^+ was determined from the absorbance difference pair 530-493 obtained from the difference spectra as described in Fig. 22.

3.3.3 Determination of the apparent affinity of TNP-ATP binding to the turning-over enzyme in the presence and absence of K^+

Binding of TNP-ATP to the Ca^{2+}-ATPase under non-turnover conditions has been measured by difference spectrophotometric titration (Watanabe and Inesi, 1982; Davidson and Berman, 1985; Berman, 1986). These TNP-ATP binding studies involved spectrophotometric wavelength scanning in the split beam mode in the range 450-520 nm, subsequent to the addition of aliquots of TNP-ATP to both sample (with SR) and reference (without SR) cuvettes. The difference in absorbance between the observed peak at 510 nm and trough at 460 nm was calculated and plotted against the concentration of TNP-ATP added. Stoichiometry of TNP-ATP binding was calculated from extrapolated linear portions of the titration curve. Values of TNP-ATP binding to the non-turning- over enzyme range from 5-8 nmol/mg SR protein (Watanabe and Inesi, 1982; Davidson and Berman, 1985; Berman, 1986). KCl does not appear to have an effect on the level of TNP-ATP bound to the Ca^{2+}-ATPase under non-turnover conditions (Davidson and Berman, 1985).

Effects of KCl on TNP-ATP binding to the turning-over enzyme were investigated. These experiments involved the addition of increasing amounts of TNP-ATP in steps of 0.2 μM (in the concentration range 0-2.0 μM) to the turning-over enzyme, in the presence and absence of 100 mM KCl. The difference absorption spectrum of TNP-ATP bound to the turning-over enzyme with respect to free TNP-ATP was characterised by a peak at 493 nm and a trough at 438 nm (Fig. 24).

Binding capacities of TNP-ATP were calculated from the extrapolation of estimated linear portions of plots of the absorbance difference pair, 493-438 nm, against the amount of TNP-ATP added. TNP-ATP binding to the turning-over enzyme was measured to be 5.5 nmol/mg SR protein and 1.9 nmol/mg SR protein in the absence and presence of 100 mM KCl respectively (Fig. 25).

The observed decrease in TNP-ATP binding to the turning-over enzyme in the presence of K^+ supports the proposal of Bishop et al. (1986). KCl has been shown to decrease the levels of phosphoenzyme dependent TNP-ATP fluorescence (Bishop et al., 1984; Davidson and Berman, 1985). Bishop et al. (1986) propose that this decreased fluorescence can be attributed to K^+ induced changes in the affinity of the nucleotide binding site for TNP- ATP.

The affinity of TNP-ATP for the Ca^{2+}-ATPase is very high. Under the conditions of this experiment, most of the TNP- ATP added is bound to the enzyme until the high affinity site is titrated. The affinity cannot be assessed by the steepness of the initial slope in Fig. 25 A and B. K^+ does, however, appear to decrease the amount of TNP-ATP that is bound. The decreased binding could therefore be either due to K^+ inhibiting TNP-ATP binding, or a shift in the phosphoenzyme species equilibrium.

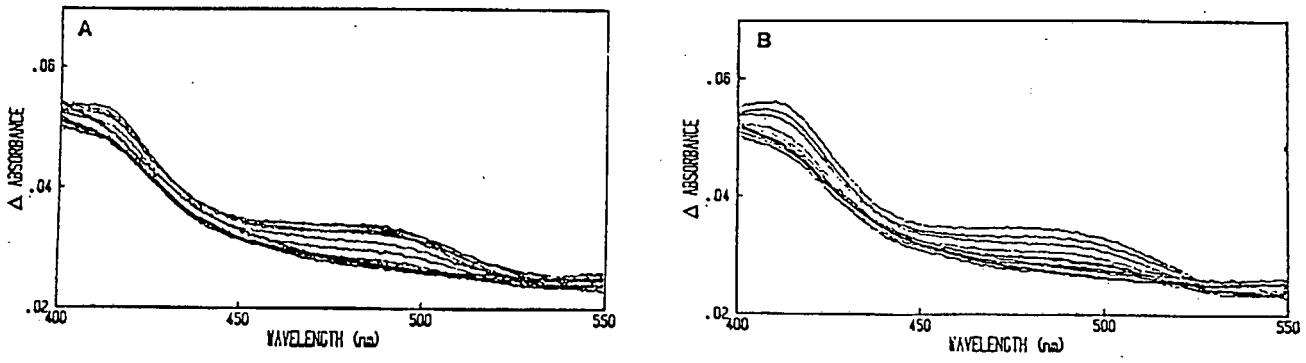

Figure 24: Difference spectrophotometric titration of TNP-ATP binding to the turning-over enzyme.

Difference spectra were recorded as described in Fig. 20, in an assay medium containing 20 mM Tris-Maleate, pH 8.0, 20% (v/v) glycerol, 5 mM $MgCl_2$, 50 µM $CaCl_2$, 5 mM creatine phosphate, 0.04 mg/ml creatine phosphokinase and 100 µM ATP. Increasing amounts of TNP-ATP, in steps of 0.2 µM, were added to both cuvettes. (A), in the absence of KCl; (B), in the presence of 100 mM KCl.

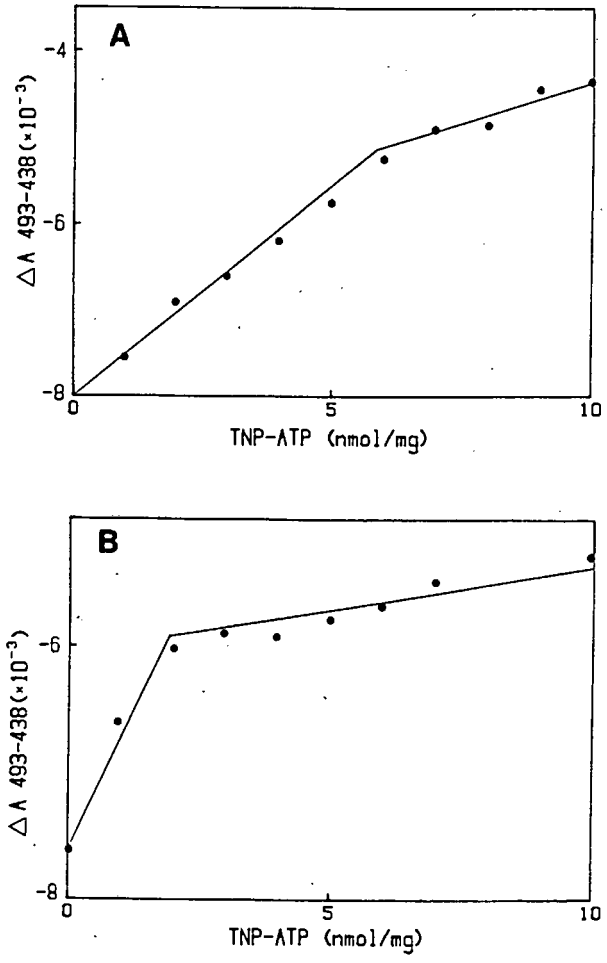

Figure 25: Determination of TNP-ATP binding to the turning-over enzyme.
The absorbance difference pair, 493-438 obtained from difference spectra as described in Fig. 24, was plotted against the concentration of TNP-ATP added : (A), in the absence of KCl; (B) in the presence of 100 mM KCl.

3.4 INTERACTION OF PYRUVATE KINASE WITH THE Ca^{2+}-ATPase

3.4.1 The effect of pyruvate kinase on the Ca^{2+}-activated ATPase activity

The ATP analog TNP-ATP accelerates hydrolysis of ATP as measured by the pH stat assay, during which ADP accumulates in the medium (See Fig. 14). However, TNP-ATP did not stimulate enzyme turnover when measured by the coupled pyruvate kinase/lactate dehydrogenase (PK/LDH) reaction system (See Fig. 16). The lack of stimulation of Ca^{2+}-ATPase activity produced by TNP-ATP in the coupled assay could be attributable to the excess concentration of coupling enzymes present in the reaction mixture which may be binding TNP-ATP. Thus the free TNP-ATP does not reach appreciable concentrations in the aqueous medium. In order to test for this possibility, the effects of LDH and PK on the pH stat assay were investigated.

LDH in the concentration range 20.6 µg/ml - 103 µg/ml was added to the pH stat assay reaction medium. The [LDH] used in the NADH coupled assay was 20.6 µg/ml. LDH had no effect on ATPase activity over the measured concentration range. The addition of TNP-ATP (5.0 µM) produced a 45 $\pm$ 4% activation of ATPase activity in the presence of LDH. LDH thus appears to have no effect on the TNP-ATP induced activation of ATPase activity observed in the pH stat assay.

PK in the concentration range 42 µg/ml - 210 µg/ml was added to the reaction medium of the pH stat assay. The [PK] previously used in the NADH-coupled assay was 42 mg/ml. Significantly, PK stimulated Ca^{2+}-ATPase activity (Figs. 26 and 27), with $K_{0.5}$ (apparent) = 47 µg/ml. The maximum stimulation (45 $\pm$ 3%) was observed in the presence of 210 µg/ml PK. TNP-ATP (5.0 µM) produced a 46 $\pm$ 2% activation of Ca^{2+}-ATPase activity over and above the PK induced stimulation.

Control experiments relative to the PK effect were carried out. A heat denatured enzyme sample was prepared by placing 200 µl of PK suspension in a boiling tube and heating at 100°C for 5 minutes in a water bath. The heat denatured PK had no effect on Ca^{2+}-ATPase activity as measured by the pH stat assay. The PK stimulation of ATPase activity as shown in Fig. 26 could also be attributable to the presence of a non-protein component of the enzyme preparation. To test for this possibility, PK stock solution was dialysed for 18 hours against several changes of the pH stat assay buffer. The concentration of dialysed PK was then determined by its absorbance at A_{280} relative to that of non-dialysed PK. The effect of dialysed PK on the Ca^{2+}-ATPase activity was then measured by the pH stat assay. Dialysed PK stimulated Ca^{2+}-ATPase activity and produced a concentration dependence of stimulation similar to the non-dialysed PK. The maximum stimulation observed at 210 µg/ml dialysed PK was 43%.

Stimulatory effects of PK produced a $K_{0.5}$ (apparent) of 47 µg/ml which corresponds to a mole ratio of approximately 1:1 of PK to Ca^{2+}-ATPase. Total Ca^{2+}-ATPase activity was approximately 0.80 µmol/min/mg. Ca^{2+}-independent ATPase activity was less than 0.05 µmol/min/mg. PK (120 µg/ml) did not cause any detectable stimulation of the Ca^{2+}-independent ATPase activity.

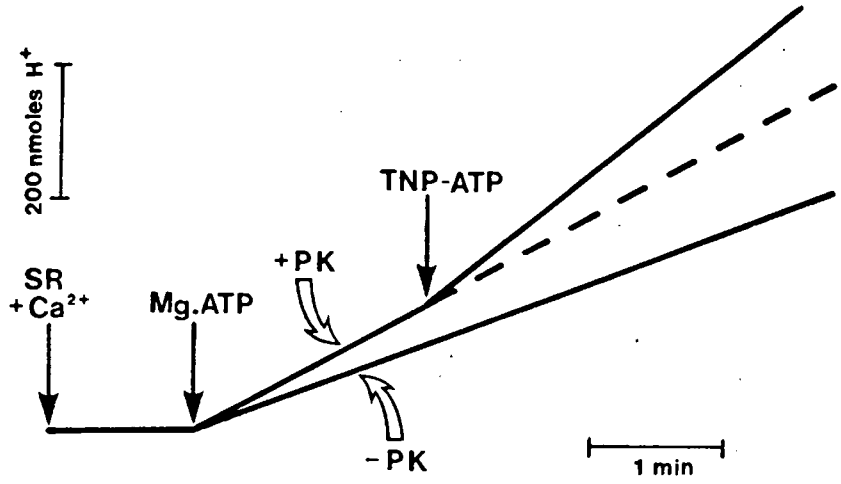

Figure 26: pH stat assay trace representing the effects of PK and TNP-ATP on Ca^{2+}-ATPase activity.

The reaction medium contained 1 mM Mops, pH 7.4, 100 mM KCl, 5 mM $MgCl_2$, 100 µM $CaCl_2$, 30 µg/ml SR protein and 40 µM X-537A, at 25°C. ATPase activity was monitored after the addition of 300 µM ATP. Maximum stimulation of hydrolysis was observed in the presence of 210 µg/ml PK. Activation of Ca^{2+}-ATPase by 5.0 µM TNP-ATP is observable over and above the PK effect.

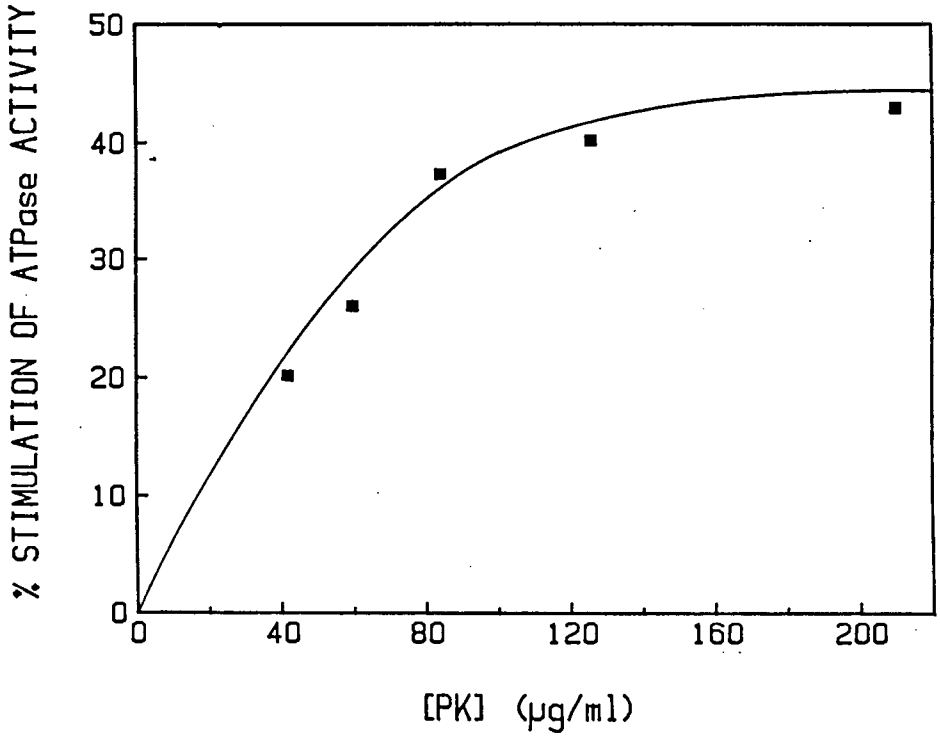

Figure 27: Concentration dependence of the PK-induced stimulation of Ca^{2+}-ATPase activity as measured by the pH stat assay.

Ca^{2+}-ATPase activity was measured at constant ATP concentrations (300 µM) by the pH stat assay in a reaction medium as described in Fig. 26. Results are expressed in terms of the percentage activation of Ca^{2+}-ATPase activity observed in the presence of PK (0-210 µg/ml).

3.4.2 The effect of pyruvate kinase on ADP quenching of AcP-induced TNP-ATP fluorescence

The PK stimulation of ATPase activity described in 3.4.1 may be a consequence of facilitation of ADP transfer in the presence of PK. In order to investigate this possibility, the effect of PK on ADP quenching of AcP-induced TNP-ATP fluorescence was determined. AcP has been used successfully as an ATP pseudosubstrate for mechanistic studies (Pucell and Martonosi, 1971; Rossi et al., 1979; Liguri et al., 1980; Bodley and Jencks, 1987). Binding of TNP-ATP to the non-phosphorylated Ca^{2+}-ATPase produces enhanced fluorescence (Berman, 1986; Davidson and Berman, 1987). Phosphorylation of the enzyme with ATP and Ca^{2+} results in a several-fold increase in fluorescence (Watanabe and Inesi, 1982; Dupont and Pougeois, 1983), and this enhanced fluorescence is associated with formation of the E_2P phosphoenzyme intermediate (Dupont and Pougeois, 1983; Wakabayashi et al., 1986; Davidson and Berman, 1987). Enhanced TNP-ATP fluorescence is also observed upon enzyme phosphorylation with the pseudosubstrate AcP. AcP-induced TNP-ATP fluorescence is slower than the fluorescence produced with ATP (data not shown). ADP quenches AcP-induced TNP-ATP fluorescence by forming ATP, which results in a decrease of E_1P and consequently of E_2P levels:

$$E_1P + ADP \longrightarrow E_1 + ATP$$

Inhibition of fluorescence by ADP may be caused by ADP binding to $E_1.2Ca$ and E_2 intermediates at the active site, and shifting the equilibrium. This does not, however, affect the overall conclusion.

The effect of PK on ADP quenching of AcP-induced TNP-ATP fluorescence was examined. Preliminary experiments were conducted to determine the ADP content of the PK enzyme preparation. An aliquot of PK was deproteinised by treatment with perchloric acid

(See "Experimental Procedures"). The resulting extract was analysed for ADP by an NADH-linked absorbance assay (Jaworek et al., 1974b). The ADP content of a PK extract corresponding to an original enzyme concentration of 300 µg/ml was calculated to be < 1 µM (Fig. 28). A control experiment was also performed to determine if the PK enzyme preparation itself had any marked quenching effect on AcP-induced TNP-ATP fluorescence. Titration of PK in the concentration range 0-200 µg/ml had a negligible effect on the level of AcP-induced TNP-ATP fluorescence.

The ADP-sensitivity of inhibition of AcP-induced TNP-ATP fluorescence was determined by ADP titration in the presence and absence of 100 µg/ml PK (Fig. 29). ADP quenching of AcP-induced TNP-ATP fluorescence was shown to be enhanced in the presence of PK. The apparent affinity of Ca^{2+}-ATPase for ADP was increased by PK and the $K_{0.5}$ (apparent) was diminished from 36 µM to 9 µM (Fig. 30). In a separate series of experiments, the PK concentration dependence of enhanced ADP quenching of AcP-induced TNP-ATP fluorescence was investigated. The quenching effect produced by 10 µM ADP was measured at PK concentrations in the range 0-200 µg/ml. Increasing [PK] enhanced the ADP quenching effect with $K_{0.5}$ (apparent) = 40 µg/ml (Fig. 31). The curves are hand-drawn.

The possibility that PK binds a portion of the TNP-ATP, thereby allowing ADP to bind to the ATPase more readily appears unlikely considering the total amount of PK added is equivalent to 0.42 µM, compared to a TNP-ATP concentration of 2 µM. In addition, pH stat results show that TNP-ATP stimulation is not affected by the presence of PK (Fig. 26).

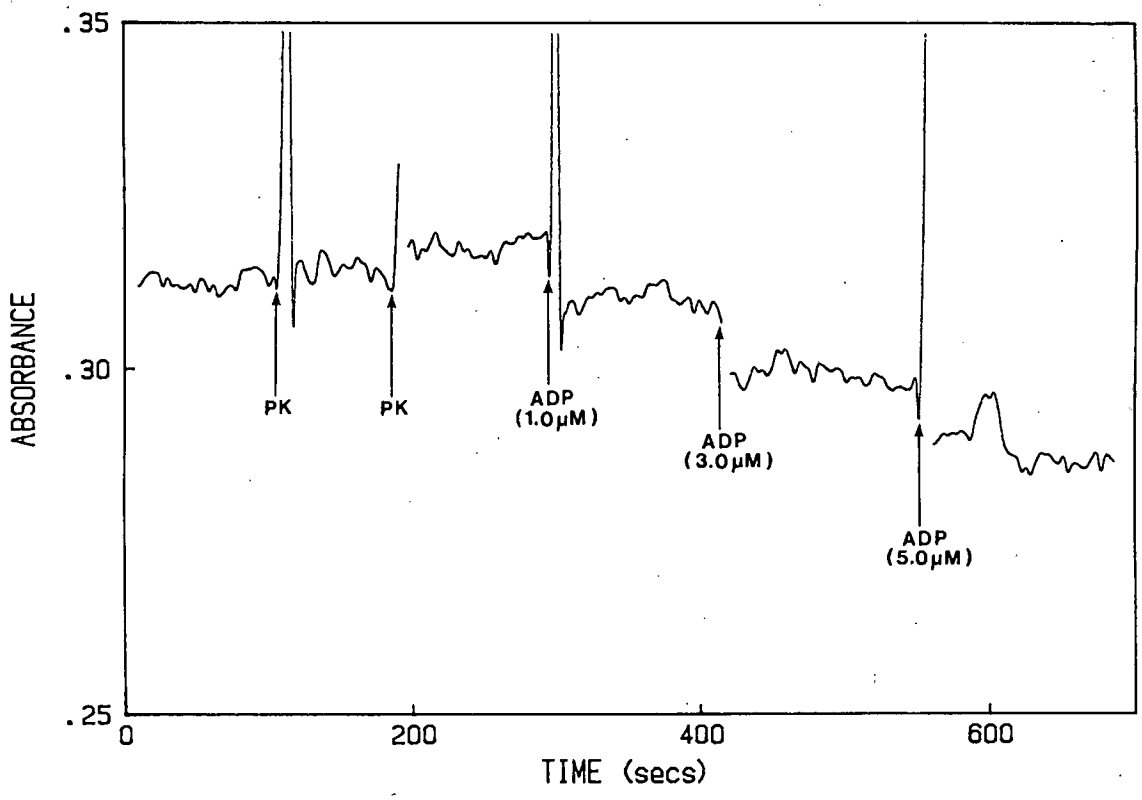

Figure 28: Determination of the ADP content of a perchloric acid treated PK sample.

The ADP content of a deproteinised PK extract, corresponding to an original enzyme concentration of 300 μg/ml, was analysed by an NADH-linked absorbance assay as described under "Experimental Procedures". PK additions illustrated correspond to concentrations of 86 μg/ml.

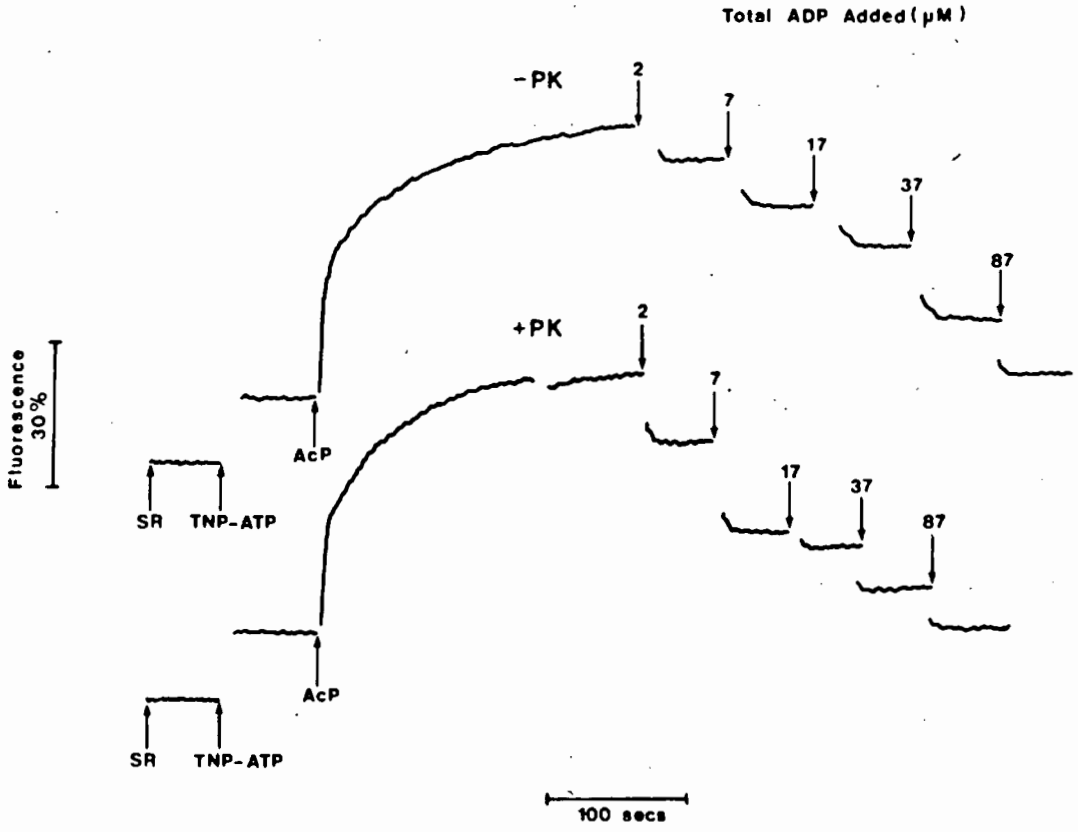

Figure 28: Fluorescence traces showing the effect of PK on ADP quenching of acetyl phosphate induced TNP-ATP fluorescence.

SR vesicles (0.2 mg/ml) were incubated at 25°C in a medium containing 50 mM Tris-maleate, pH 8.0, 20% (v/v) glycerol, 5 mM $MgCl_2$ and 50 μM $CaCl_2$. The vesicles were then assayed for E-P dependent enhanced TNP-ATP fluorescence by the addition of 2 μM TNP-ATP and 1 mM AcP. Sequential additions of ADP gave cummulative concentrations as indicated. ADP quenching effects were determined in the presence and absence of 100 μg/ml PK.

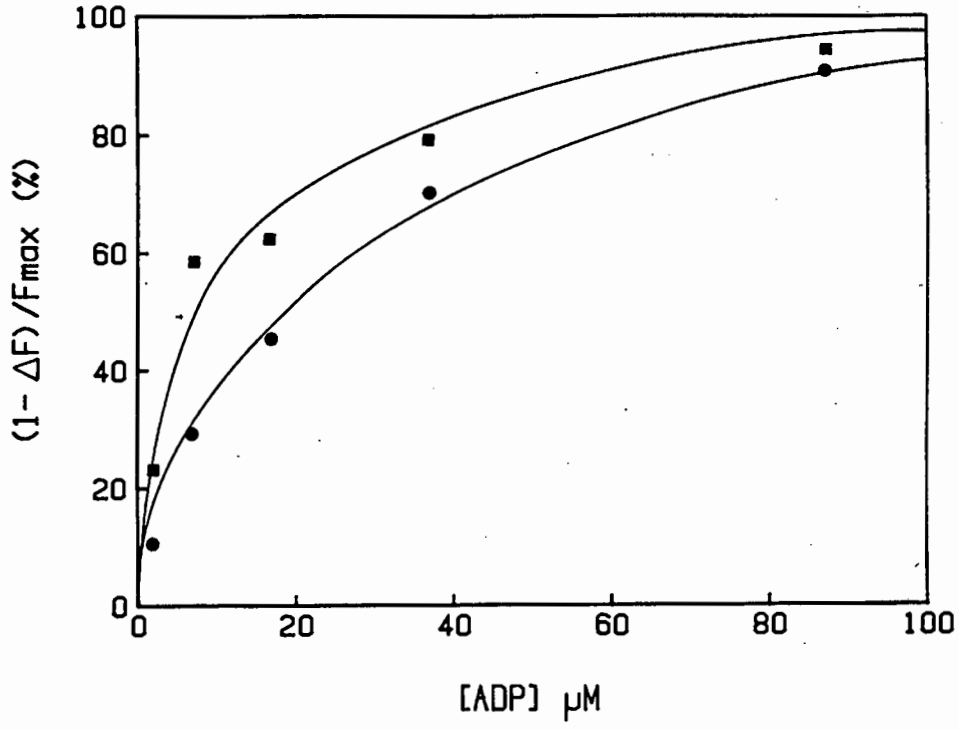

Figure 30: Determination of the apparent affinity of Ca^{2+}-ATPase for ADP in the presence and absence of PK.

ADP quenching of AcP-induced TNP-ATP fluorescence was measured from the traces described in Fig. 29.
Key : ● no PK
■ 100 μg/ml PK

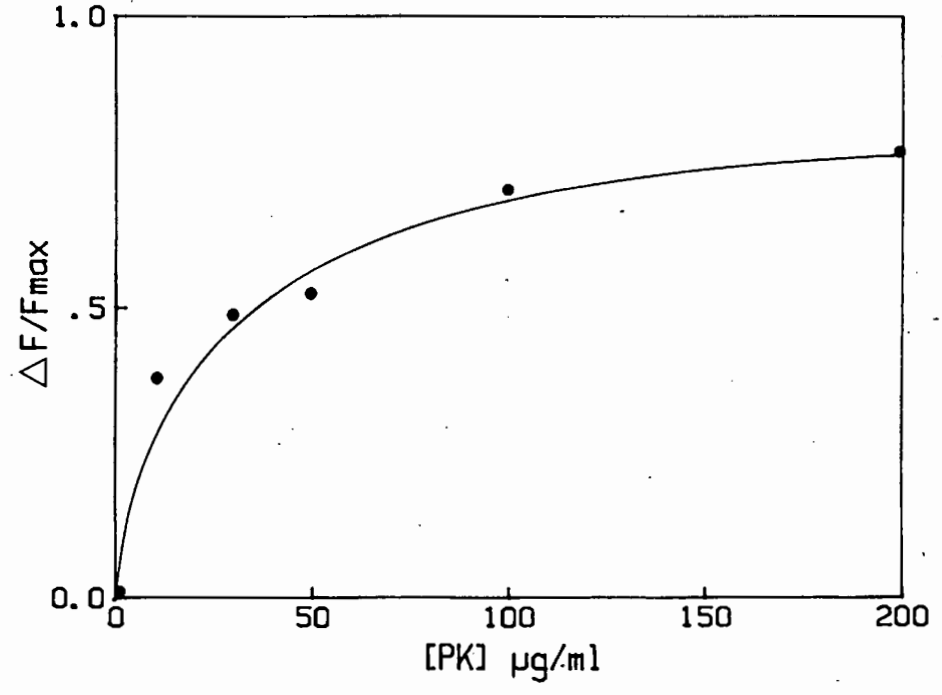

Figure 31: PK concentration dependence of enhanced ADP quenching of AcP-induced TNP-ATP fluorescence.

SR vesicles (0.2 mg/ml) were assayed for E-P dependent enhanced TNP-ATP fluorescence as described in Fig. 29. The quenching of fluorescence produced by 10 μM ADP was determined at PK concentrations in the range 0-200 μg/ml.

3.4.3 Pyruvate kinase reaction velocity measurements

Reaction velocity measurements involving PK were made to determine the apparent Michaelis constants for ADP binding to the enzyme. PK activity measurements were based on the coupled enzyme assay (Horgan et al., 1972). NADH oxidation by LDH in the presence of pyruvate formed by PK was monitored by the decrease in absorbance at 340 nm:

$$\text{PEP} + \text{ADP} \xrightarrow{\text{PK}} \text{Pyruvate} + \text{ATP}$$

$$\text{Pyruvate} + \text{NADH} + \text{H}^+ \xrightarrow{\text{LDH}} \text{Lactate} + \text{NAD}^+$$

Aliquots of ADP in the concentration range 0-700 μM were added to the coupled enzyme system described above. PK concentration was varied from 0.1 mg/ml - 0.5 mg/ml. The reaction velocities were determined by measuring the rate of decrease in absorbance at 340 nm, and PK activity was expressed as μmol/mg/min. The results are shown in Fig. 32. ADP binding to PK was shown to be non co-operative (n_H = 0.89) with K_m = 195 μM and V_{max} = 253 μmol/mg/min. This is consistent with a previously reported K_m value for ADP of 210 μM (Reynard et al., 1961).

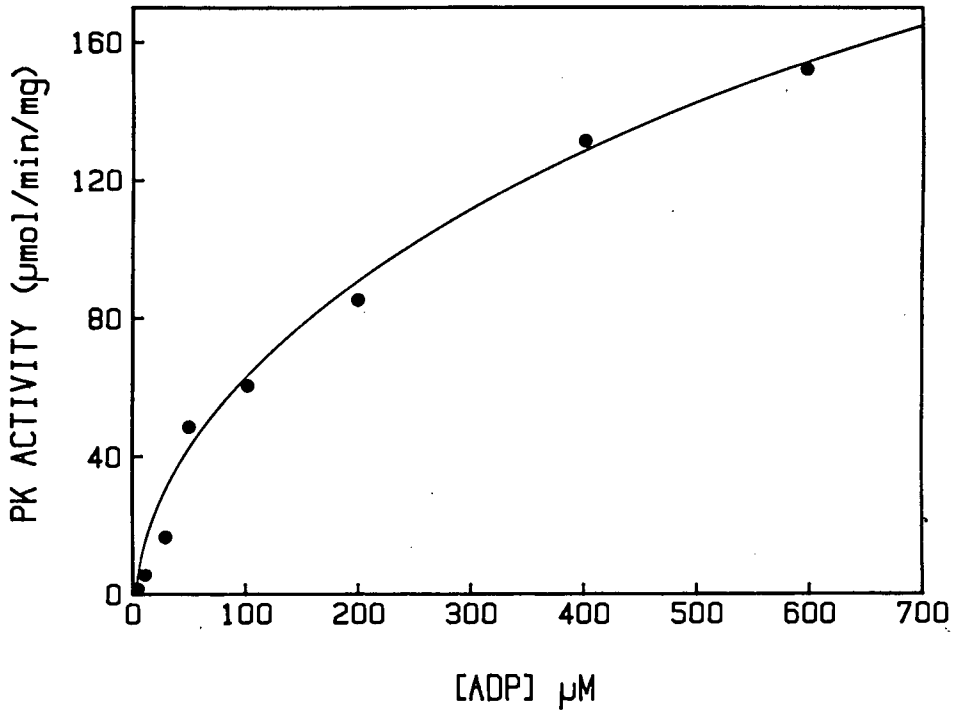

Figure 32: Determination of the apparent Michaelis constants for ADP binding to PK.

PK reaction velocity measurements were performed in a medium containing 20 mM Histidine, pH 6.8, 100 mM KCl, 5 mM $MgCl_2$, 2.5 mM PEP, 0.1 mM NADH and 8 units/ml LDH at 25°C. PK concentration was varied from 0.1 mg/ml - 0.5 mg/ml. Aliquots of ADP (0-700 µM) were added to the reaction mixture and the reaction velocities determined from the rate of decrease in NADH absorbance at 340 nm. ADP binding parameters were calculated by an iterative non-linear least square procedure according to Wilkinson (1961).

3.4.4 Protein ultrafiltration studies showing the effect of pyruvate kinase on the steady-state free ADP concentration

PK has a direct effect on ATPase turnover as measured by the pH stat assay (Fig. 27), during which ADP is released into the reaction medium. PK also enhances ADP quenching of AcP-induced TNP-ATP fluorescence of the Ca^{2+}-ATPase (Fig. 29). These observations suggest that the effects of PK on the Ca^{2+}-ATPase are via interaction with the common metabolite, ADP. ADP transfer from the catalytic site of the Ca^{2+}-ATPase may be facilitated by ternary complexation with PK. Srivastava and Bernhard (1986a, 1987) propose that due to the high concentration of many enzymes in the cell, direct transfer of metabolites from one enzyme site to the next occurs via enzyme-enzyme complex formation. This "direct transfer mechanism" differs from the usually assumed "random diffusion pathway" whereby metabolite dissociates from one enzyme site into the aqueous environment before forming a complex with the next enzyme site. In order to test for the possible existence of a "direct transfer mechanism" in the interaction of PK and the Ca^{2+}-ATPase, the effect of PK on the steady-state [ADP] at varying flux rates in the coupled enzyme assay was determined. Flux rates were varied by the addition of different Ca^{2+}-ATPase and PK concentrations.

Immediately after a measurable Ca^{2+}-activated reaction rate had been obtained in the coupled assay, the reaction mixture was filtered according to the protein ultrafiltration method as described under "Experimental Procedures".

The rate of ATPase activity produced in the coupled enzyme assay at steady state is equivalent to the rate of ADP formation. The predicted [ADP]free was calculated from the measured reaction rate using K_m = 195 μM, V_{max} = 253 μmol/mg/min for PK (See 3.4.3). The

predicted PK reaction velocity was also calculated from the observed [ADP]free. The results are summarised in Table 5. [ADP]free observed is lower than predicted, assuming free ADP is the only kinetically competent substrate for PK. The reaction velocities were greater than those calculated on the basis of [ADP]free. The maximum discrepancy was observed at [ATPase] = 0.145 µM and [PK] = 0.084 µM, where the observed reaction velocity was 4 fold higher than that predicted according to the random diffusion mechanism.

The values shown in Table 5 represent 3 separate experimental values for $[ADP]_{free}$ under the defined conditions. Although the results are interpreted in terms of possible direct metabolite transfer as postulated by Srivastava and Bernhard (1986a), further experimentation, involving nucleotide concentration measurements, is probably required to elucidate the precise reaction mechanism. There are several possible reasons for the discrepancy between observed and predicted values, including: a) ATPase separated from PK on filter; b) Recoveries low; c) Predicted values incorrect. Srivastava and Bernhard (1986a) have shown that for the NAD-dependent dehydrogenases, experimental results and calculated prediction agree fairly precisely, but in some cases experimental velocities are greater than those predicted. In contrast, Ehrlich (1987) reports that no evidence was found for direct transfer of NADPH between two NAD-dependent dehydrogenases, isocitrate dehydrogenase and glutamate dehydrogenase. Ehrlich (1987) acknowledges, however, the importance of studies such as those of Srivastava and Bernhard, in that direct transfer may indicate adaptation of enzymes for specific metabolic roles.

TABLE 5: Effect of PK on the Steady-State [ADP] at Varying Flux Rates in the Coupled Assay

ATPase (μM)	PK (μM)	[ADP]free (μM)		Rate (μmol/min/mg)	
		Observed	Predicted	Observed	Predicted
0.029	0.084	0.29	0.34	0.44	0.38
0.145	0.84	0.09	0.12	0.15	0.12
0.145	0.084	0.32	1.25	1.61	0.41

Flux rates were determined at the different Ca^{2+}-ATPase and PK concentrations described using the NADH-coupled assay (see "Experimental Procedures"). Immediately after a measurable reaction rate had been obtained, the reaction mixture was filtered under pressure through a PM 10 filter in an Aminco Diaflo ultrafiltration unit. The filtered protein-free solution was assayed for ADP content by an NADH-linked absorbance assay (see "Experimental Procedures").
For individual enzyme catalysed reactions, the dependence of the reaction velocity (v) on metabolite (M) concentration is described by the Michaelis-Menten equation:

$$E + M \underset{Km}{\rightleftharpoons} E\text{-}M \xrightarrow{kcat} E + P$$

$$v = \frac{kcat \times [E]t}{1 + (Km/[M])} = \frac{Vmax}{1 + (Km/[M])} \quad \ldots\ldots (1)$$

where E = enzyme, M = metabolite, P = product, Km = affinity of the enzyme for the metabolite, kcat = first order rate constant for the conversion of the E-M complex to E and P, Vmax = limiting maximal velocity observed when all of the enzyme is present as E-M. (Srivastava and Bernhard, 1986a).

Predicted [ADP]free and PK reaction rates were calculated from appropriate substitution of the observed [ADP]free, and reaction rates, into equation (1), using Km = 195 μM, Vmax = 253 μmol/mg/min.

3.4.5 Intermolecular cross-linking studies of the Ca^{2+}-ATPase and pyruvate kinase

Chemical cross-linking with glutaraldehyde has proved successful in assessing protein quaternary structure (Hermann et al., 1981), and has been used to determine interactions and oligomer distribution of the (Na^+, K^+)-ATPase in detergent (Craig, 1982). Cross-linking studies have been performed both on the membrane bound Ca^{2+}-ATPase and on the enzyme dispersed in detergent (Louis and Shooter, 1972; Murphy, 1976; Chyn and Martonosi, 1977; Louis et al., 1977; Hebdon et al., 1979; Bailin, 1980; Cheisi, 1984; McIntosh and Ross, 1985). These studies sought to assess ATPase-ATPase interactions and to possibly demonstrate a preferred oligomeric state of the Ca^{2+}-ATPase. The results of these studies have, however, been inconclusive, mainly due to the high density of Ca^{2+}-ATPase molecules in the membrane, which produces random non-specific polypeptide interactions. Ross and McIntosh (1987) have identified a glutaraldehyde cross-linked ATPase monomer species with altered hydrodynamic properties on SDS-gel electrophoresis. This cross-linked ATPase migrates with an apparent molecular weight of 125 000 (E(125)), and is proposed to form as a result of intramolecular cross-linking at the active site.

Glutaraldehyde cross-linking involving PK and the Ca^{2+}-ATPase was performed in an attempt to detect possible PK-ATPase protein interaction. The assay involved reacting SR vesicles and PK with glutaraldehyde under conditions which favour interpolypeptide cross-linking. Aliquots of the protein mixture containing the cross-linked products were analysed by SDS-PAGE according to the method of Laemmli (1970). Molecular weights were assigned by comparison with the mobility of known standard marker proteins (Fig. 33).

Control experiments showing the cross-linking products formed by PK and SRV alone were initially performed. The cross-linking patterns observed from these control experiments showed the relative positions of, and the concentration and time-dependent increase in the glutaraldehyde cross-linked enzyme species. The time dependence for the reaction of SR vesicles and PK with 2 mM and 5 mM glutaraldehyde is shown in Fig. 34. Lane 1 shows the protein bands produced in the absence of glutaraldehyde. An ATPase polypeptide band is apparent at 110 kD, consistent with the calculated molecular mass of 109 771 daltons, based on the primary amino acid sequence (Brandt et al.,1986). The Ca^{2+}-ATPase constitutes approximately 80% of the SR protein content of the vesicle preparation, although myosin (Mr = 200 kD), phosphorylase (Mr = 93 kD), calsequestrin (Mr = 63 kD) and M-55 Ca^{2+}-binding protein are also present. The PK molecule has a molecular mass of 237 kD and consists of 4 sub-units each with Mr = 57.2 kD (Morawiecki, 1960; Steinmetz and Deal, 1966). A relatively broad protein band at Mr = 58 kD is observed upon SDS-PAGE, which corresponds to the monomeric PK species. Treatment of SR vesicles and PK with glutaraldehyde resulted in a concentration and time-dependent increase in cross-linked products of the individual enzyme species. PK cross-linked mainly to a dimer (Mr = 144 kD). PK trimers and tetramers and SR dimers were observed in the region 185 kD to 240 kD. Bands corresponding to tetrameric SR and larger PK aggregates were distinguishable above 300 kD. At longer reaction times, large aggregates of polypeptides covalently joined by glutaraldehyde were formed which did not enter the running or stacking gels. Cross-linking of the PK and Ca^{2+}-ATPase monomeric polypeptides would be expected to produce a new protein band with a molecular weight of approximately 170-180 kD.

Significantly, no new glutaraldehyde cross-linked polypeptide species was observed in this molecular weight region. The ATPase E(125) species formed from intramolecular cross-linking is distinguishable at 125 kD. Cross-linking of SR vesicles and PK was next carried out in the presence of the common metabolite, ADP. ADP (100 μM) was added to the reaction medium and the protein mixture was cross-linked under the same conditions as previously used (Fig. 35). The distribution of cross-linked products formed by interaction with glutaraldehyde was similar to that observed in the absence of ADP. Therefore the presence of ADP, under cross-linking conditions, does not appear to result in an observable PK : ATPase cross-linked species. Another question addressed was whether any new cross-linked species or any change in the observed distribution of the oligomeric species occurs upon ATP-induced Ca^{2+}-ATPase turnover. SR vesicles and PK were cross-linked with 2 mM glutaraldehyde for 5 minutes under the conditions as described in Fig. 36. No noticeable changes in the relative proportions of the various PK and SR cross-linked oligomers were observed in the presence of Ca^{2+} plus ATP. Neither increasing the [PK] relative to the [SR] or increasing both the [PK] and [SR] appears to effect the cross-linked aggregation pattern. The presence of PK, in the presence or absence of ADP and ATP, also had no effect on E(125) formation.

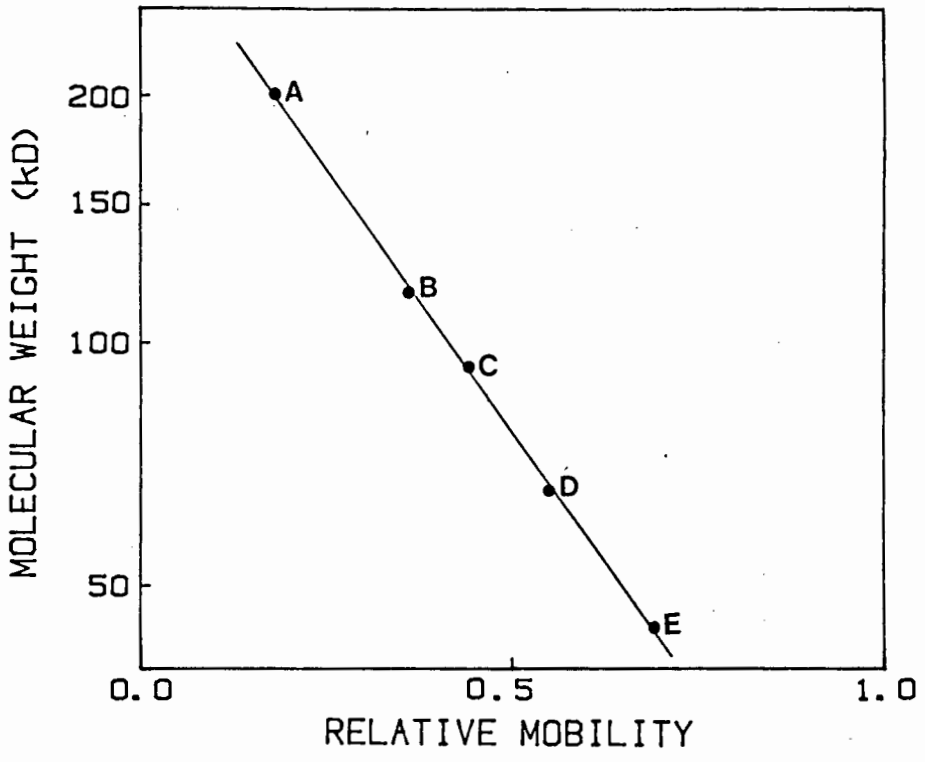

Figure 33: Standard curve of molecular weight vs relative mobility for SDS-PAGE.

Protein standards indicated are : (A), myosin (200 kD); (B), β-galactosidase (116 kD); (C), phosphorylase (93 kD); (D), bovine serum albumin (66 kD); (E), ovalbumin (45 kD).

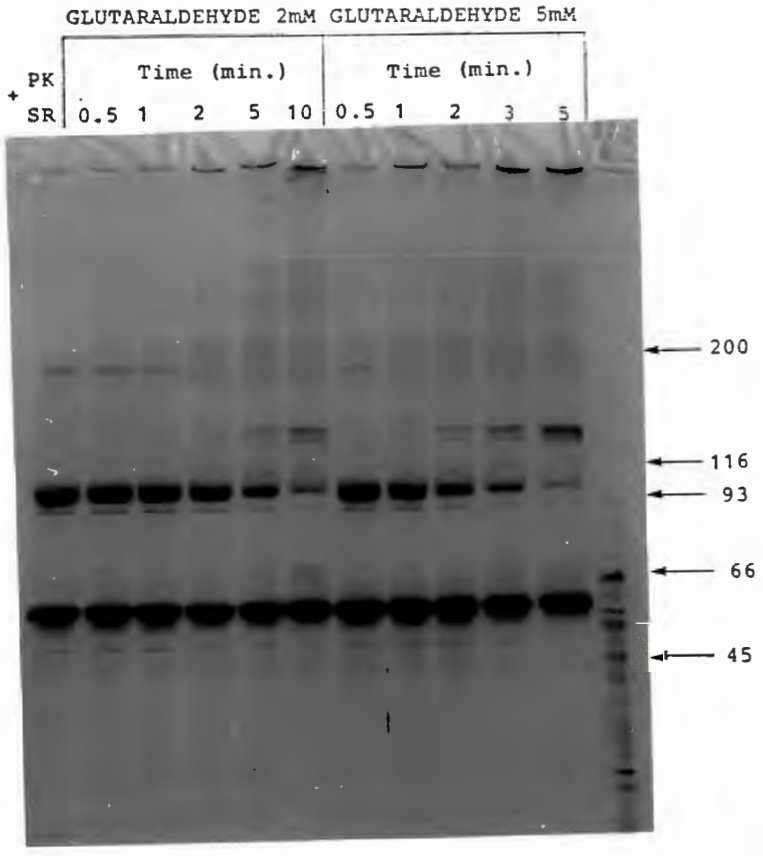

Figure 34: Reaction of glutaraldehyde with SR proteins and PK as shown by their banding pattern on SDS-PAGE.

SR vesicles (0.2 mg/ml) and PK (0.2 mg/ml) were preincubated in buffer containing 40 mM Mops, pH 7.4, 1.5 mM $MgCl_2$, 50 µM $CaCl_2$ and 30 mM KCl, for 15 minutes at room temperature. Cross-linking was initiated by the addition of 2 mM and 5 mM glutaraldehyde, and the reactions carried out for the indicated time intervals. The molecular weight standards (extreme right lane) were myosin (200 kD). β-galactosidase (116 kD), phosphorylase (93 kD), bovine serum albumin (66 kD) and ovalbumin (45 kD).

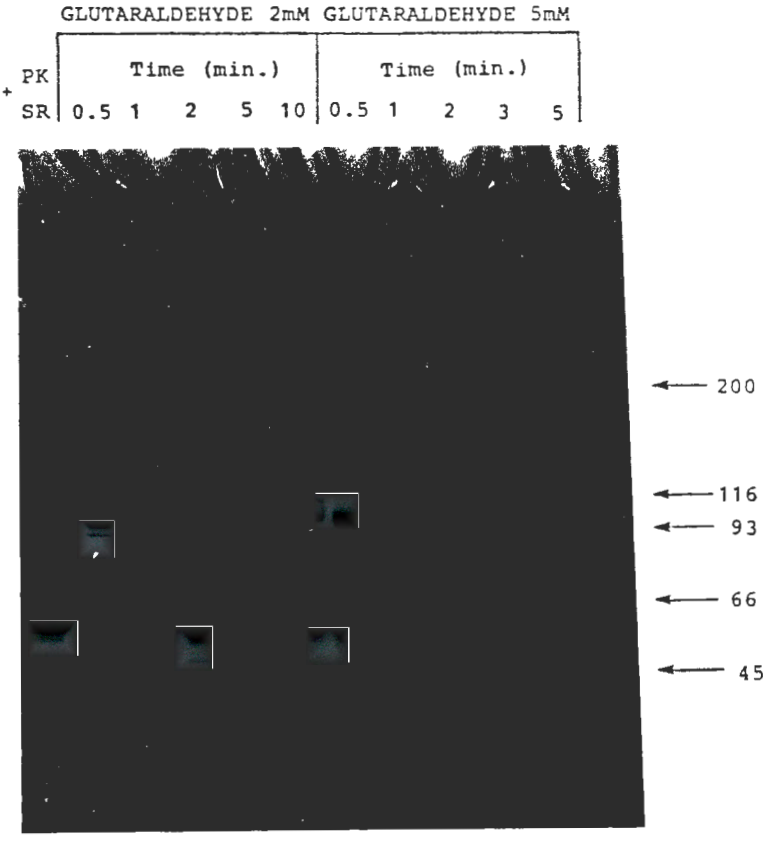

Figure 35: Effect of ADP on cross-linking of SR and PK with glutaraldehyde.

Reaction conditions and times were identical to those described in Fig. 34, except for the addition of 100 μM ADP to the incubation buffer.

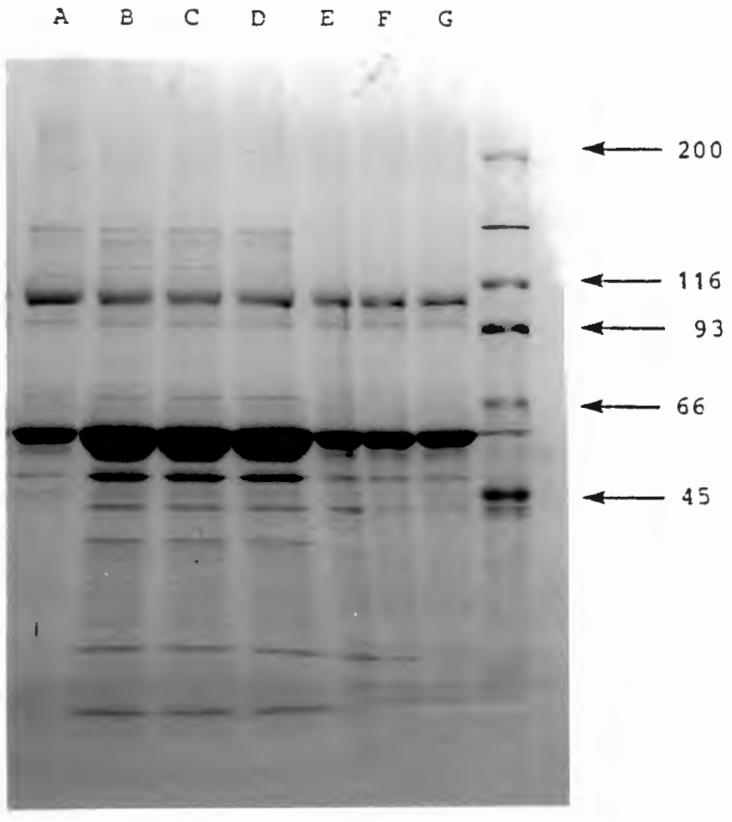

Figure 38: Effect of ATP and protein concentration on cross-linking of SR and PK with glutaraldehyde.

SR vesicles and PK were preincubated in buffer containing 50 mM Mops, pH 7.4, 1.5 mM $MgCl_2$, 50uM $CaCl_2$ and 30 mM KCl, for 15 minutes at room temperature. Cross-linking with 2 mM glutaraldehyde was carried out for 5 minutes for the following reaction conditions:
(A), PK (0.2 mg/ml) + SR (0.2 mg/ml) in the presence of 1 mM ATP;
(B), PK (1 mg/ml) + SR (0.2 mg/ml);
(C), PK (1 mg/ml) + SR (0.2 mg/ml) in the presence on 100 µM ADP;
(D), PK (1 mg/ml) + SR (0.2 mg/ml) in the presence of 1 mM ATP;
(E), PK (1 mg/ml) + SR (1 mg/ml);
(F), PK (1 mg/ml) + SR (1 mg/ml) in the presence of 100 µM ADP;
(G), PK (1 mg/ml) + SR (1 mg/ml) in the presence of 1 mM ATP.
Molecular weight markers (extreme right lane) are as described in Fig. 34.

4.0 DISCUSSION

4.1 ISOLATION AND PROPERTIES OF SARCOPLASMIC RETICULUM MEMBRANE FRACTIONS

SR vesicles may be conveniently divided into defined fractions corresponding to the in vivo longitudinal tubules (LSR), which surround the muscle myofibrils, and the terminal cisternae (TC), which are associated with the transverse tubules via bridging "feet" structures at the triads (Saito et al., 1984). This triadic junction is of particular interest, as the signal that induces Ca^{2+} release is thought to be transmitted in this region (Lai et al., 1988).

In this study, defined fractions of the sarcotubular system were isolated by sucrose density gradient centrifugation (Saito et al., 1984). Electron microscopy of the LSR fraction showed the presence of closed membranous vesicles without intra-vesicular electron dense material, which is consistent with the fact that the LSR vesicular membrane consists mainly of Ca^{2+}-ATPase (Saito et al., 1984). The TC fraction consisted predominantly of intact sphere-like vesicles which contained significant amounts of intravesicular electron opaque material. The intravesicular material is reported to represent Ca^{2+}-binding protein (calsequestrin)(Meissner, 1975). The TC consists of both Ca^{2+}-ATPase containing membrane and junctional face membrane (Saito et al., 1984). The TC junctional face membrane contained visible electron dense surface structures ("feet") (see Fig. 8) which reportedly span the approximately 120 Å gap between the TC and the tranverse tubule (Franzini-Armstrong, 1970). Functional studies were performed on the isolated LSR and TC fractions to provide evidence for the biochemical subspecialisation of these two SR regions. From these studies, several lines of

evidence emerge which confirm the localisation of a Ca^{2+} release system in the TC, in contrast with the LSR region:

a) LSR showed a higher Ca^{2+}-ATPase activity than TC in the presence and absence of the ionophore A23187. This higher LSR ATPase activity is a direct reflection of the greater ATPase content of LSR vesicular membranes. Costello et al., (1986) report that the Ca^{2+}-ATPase constitutes 35% and 90% of the protein of TC and LSR respectively. RR had an inhibitory effect on the Ca^{2+}-ATPase activities of both TC and LSR. Therefore, the increased Ca^{2+} uptake of TC in the presence of RR cannot be explained in terms of enhanced turnover of the Ca^{2+}-ATPase, but rather is evidence for Ca^{2+} efflux channels.

b) TC vesicles had a lower Ca^{2+} uptake capacity than LSR (235 versus 1005 nmol/mg/min). The addition of RR stimulated Ca^{2+} uptake in TC, but rather unexpectedly decreased Ca^{2+} uptake of LSR, with the result that similar Ca^{2+} transport values were obtained for the 2 fractions, in the presence of RR. These values therefore do not appear to reflect the different ATPase contents of the TC and LSR fractions as reported by Costello et al. (1986).

c) The Ca^{2+}-pumping efficiency of TC was increased from 0.40 to 1.78 in the presence of RR, whereas with LSR no appreciable change in the Ca^{2+}-pumping efficiency was observed with RR. The RR-induced increase in the TC Ca^{2+}-pumping efficiency is related to the RR enhancement of Ca^{2+} transport activity, by blocking Ca^{2+} efflux.

d) Passively loaded TC vesicles exhibited rapid Ca^{2+} efflux as compared to LSR. RR slowed down and inhibited Ca^{2+} efflux in both fractions, although the effect was more pronounced with TC. In addition, a higher intravesicular Ca^{2+} content was observed

These findings are consistent with the results of Chu et al., 1986. TC vesicles have a higher permeability to Ca^{2+} as compared to LSR vesicles, which is a direct reflection of the proposed presence of Ca^{2+} release channels involved in muscle excitation-contration coupling (Ikemoto et al., 1985; Morii et al., 1985; Meissner et al., 1986). Recent studies on Ca^{2+} release have focused on the neutral plant alkaloid ryanodine, which reacts specifically with the SR Ca^{2+} release channel (Pessah et al., 1986). The ryanodine receptor from skeletal muscle SR has been isolated and shown to have an apparent molecular mass of 360-400 kD (Inui et al., 1987; Lai et al., 1988). This isolated receptor displays a Ca^{2+} conductance equivalent to that of the native Ca^{2+} release channel when incorporated into lipid bilayers. Of interest is the morphological identity of the receptor with the "feet" structures (observable in Fig. 8). This finding has important physiological implications in the mechanism of muscle excitation-contraction coupling, as it indicates there is a direct interaction between the SR Ca^{2+} release channels and the transverse tubule.

The ATP analog, TNP-ATP, binds with high affinity to the SR Ca^{2+}-ATPase (Watanabe and Inesi, 1982; Dupont et al., 1982) and provides an effective probe for monitoring catalytic events associated with energy transduction. A unique feature of bound TNP-ATP is that its fluorescence is greatly enhanced upon induction of enzyme turnover (Watanabe and Inesi, 1982; Dupont and Pougeois, 1983). Exclusion of water molecules from the active site during turnover produces a more hydrophobic environment in the vicinity of the probe, which readily explains the enhanced TNP-ATP fluorescence (Dupont, 1983). Fluorescence enhancement of bound TNP-ATP in the TC fraction was diminished as compared to LSR. This decreased TC fluorescence signal could be attributable to either decreased TNP-ATP binding or

altered properties of the nucleotide binding site. TNP-ATP binding, as monitored by the fluorescence increase observed in the non-turning-over enzyme, was approximately 20% lower in TC than in LSR. This observation may be a direct reflection of the lower Ca^{2+}-ATPase content of the isolated TC fraction (Saito et al., 1984). The diminished TC fluorescence signal observed upon subsequent induction of enzyme turnover with ATP may therefore result from decreased TC Ca^{2+}-ATPase specific activity.

The presence of open Ca^{2+} release channels in the TC region may also contribute to the lower fluorescence. These Ca^{2+} release channels enhance the Ca^{2+} permeability of the TC vesicles which results in low net energised Ca^{2+} transport (Chu et al., 1986). Diminished $E_2P.2Ca$ levels may result from a decreased $[Ca^{2+}]_{in}$. This would affect the turnover-dependent TNP-ATP fluorescence enhancement which is closely related to E_2P levels (Dupont and Pougeois, 1983; Wakabayashi et al., 1986; Davidson and Berman, 1987). With LSR, the absence of Ca^{2+} release channels produces relatively well-sealed vesicles and allows accumulation of intravesicular Ca^{2+}. The intravesicular $[Ca^{2+}]$ of LSR would approach the K_d for the low affinity internally orientated Ca^{2+} binding sites (0.6-1 mM, Carvalho et al., 1976), which restrains $E_2P.2Ca$ breakdown and subsequently enhances fluorescence. Another feature of the TNP-ATP fluorescence data is the faster rate of ATP hydrolysis observed with the TC as compared to LSR (see Fig. 11). This again appears to be a reflection of the presence of open Ca^{2+} release channels in the terminal region which enhance vesicle permeability and relieve the constraints of high $[Ca^{2+}]_{in}$ on the catalytic cycle. With LSR, build-up of intravesicular Ca^{2+} appears to inhibit steady-state turnover of the ATPase.

The morphological subspecialisation of the TC and LSR regions of the SR membrane appears therefore to be reflected in the observed differences in turnover-dependent TNP-ATP fluorescence.

It is of interest to compare the TNP-ATP fluorescence properties of the "naturally uncoupled" TC preparation with those of a "chemically uncoupled" SR preparation. Conditions such as mild acid (Berman et al., 1977) and EGTA, at neutral pH (McIntosh and Berman, 1978), appear to dissociate calcium transport from ATP hydrolysis. Preincubation of a 'mixed' SR vesicle preparation (Eletr and Inesi, 1972) with EGTA produces "chemically uncoupled" vesicles with diminished Ca^{2+} transport activity (Berman, 1986). The TC preparation can be regarded as being "naturally uncoupled" because it shows a reduced nett Ca^{2+} uptake capacity attributable to the presence of open Ca^{2+} release channels (Chu et al., 1986).

Turnover-dependent TNP-ATP fluorescence enhancement is diminished between 60-70% in the EGTA-induced uncoupled state as compared to the fluorescence of native coupled vesicles (Berman, 1986). Slight increases in passive permeability following EGTA treatment cannot account for the observed near total inhibition of Ca^{2+} transport. The decrease in TNP-ATP fluorescence has been attributed to a functional defect in energy coupling in EGTA-treated vesicles, which is manifested in modification of the environment of the regulatory nucleotide binding site. This provides support for the proposal that EGTA-induced uncoupling is an "intramolecular" process involving a ligand binding site of the Ca^{2+}-ATPase. The observed phenomenon could not be due to increased membrane permeability, since TNP-ATP fluorescence was also decreased in solubilised EGTA-treated SR as compared to normal SR (Berman, 1986).

Similarly, turnover-induced TNP-ATP fluorescence of the "naturally uncoupled" TC preparation was decreased by 35-40% as compared to that of LSR. This decreased fluorescence signal obtained for the TC fraction may, however, be attributable to enhanced passive Ca^{2+} efflux through the Ca^{2+} release channels. Therefore this form of uncoupling can be regarded as "extramolecular" as it may be related to molecules other than the Ca^{2+}-ATPase (i.e. the Ca^{2+} release channels).

4.2 EFFECTS OF TNP-ATP ON CATALYSIS

TNP-ATP is a high affinity marker for binding to the Ca^{2+}-ATPase and has proved successful because of its ATP-like characteristics and microenvironmental sensitivity (Watanabe and Inesi, 1982; Dupont et al., 1982). TNP-ATP is reported to be very slowly hydrolysed by the Ca^{2+}-ATPase (Watanabe and Inesi, 1982; Dupont et al., 1982), although Dupont et al., (1985) conclude that any TNP-ATPase activity observed is "parasitic", being attributable to basal Mg-ATPase activity.

Dupont et al. (1985) first reported that Ca^{2+}-activated ATPase hydrolysis is stimulated by TNP-ATP binding to the phosphorylated enzyme, as measured by the pH stat assay. In the present studies, TNP-ATP stimulated Mg.ATP hydrolysis as measured by the pH stat assay with $K_{0.5}$ (apparent) = 0.80 μM (Fig. 14). Maximum stimulation of ATP hydrolysis occured at 5.0 μM TNP-ATP. Higher concentrations of TNP-ATP resulted in less stimulation. Millimolar Mg.ATP was also shown to stimulate ATPase activity following induction of enzyme turnover. The stimulatory effects of TNP-ATP and millimolar Mg.ATP were complementary, i.e. following stimulation of ATPase activity by TNP-ATP, the addition of millimolar Mg.ATP produced no further activation. The ATP modulation of catalysis is relatively complex and has been explained in terms of two classes of nucleotide binding sites, a high affinity catalytic site and a low affinity regulatory site (Dupont et al., 1985; Bishop et al., 1987). The regulatory nucleotide site has previously been characterised in terms of the secondary activation of enzyme turnover induced by ATP in the millimolar range (Inesi et al., 1967; de Meis and Fialho de Mello, 1973; Dupont, 1977; Dean and Tanford, 1978; de Meis and Vianna, 1979). These effects are proved to be non-hydrolytic (regulatory) as evidenced by the fact that non-hydrolysable analogs

(e.g. AMP-PCP and AMP-CPP) are able to stimulate ATPase activity (Dupont, 1977; Taylor and Hatton, 1979; Cable et al., 1985). The complementary activation of hydrolysis by TNP-ATP and by millimolar Mg.ATP, as shown by the pH stat results, suggest that the binding of the nucleotide analog is as effective as binding of millimolar Mg.ATP in producing the secondary activation of ATPase activity. This can be attributable to the higer affinity of Ca^{2+}-ATPase for TNP-ATP as compared to ATP (Dupont et al., 1982). Therefore the stimulation of ATPase activity by TNP-ATP as observed in the pH stat assay appears to be due to TNP-ATP binding to the regulatory nucleotide site (Dupont et al., 1985).

Various models have been proposed for the location of the regulatory nucleotide binding site on the Ca^{2+}-ATPase (Dupont, 1977; Verjovski-Almeida and Inesi, 1979; Moller et al., 1980; Anderson et al., 1982; Pick and Karlish, 1982; Silva and Verjovski-Almeida, 1983; McIntosh and Boyer, 1983; Dupont et al., 1985). Through kinetic and stoichiometric measurements involving TNP-AMP, Bishop et al., (1987) have recently concluded that the regulatory site only exists in the phosphorylated conformation of the enzyme. Thus the regulatory site is not separate from the catalytic site, but is equivalent to the modified catalytic site following phosphorylation. This supports the model proposed by McIntosh and Boyer (1983) whereby the enzyme only possesses a single nucleotide binding site, but a second molecule of ATP can bind to the phosphorylated site, with a decreased affinity, upon liberation of ADP.

K^+ alters the relative levels of phosphoenzyme intermediates in the Ca^{2+}-ATPase catalytic cycle. Although phosphoenzyme species are shifted in favour of E_1P in the presence of K^+ (Shigekawa and Pearl, 1976; Yamada and Ikemoto, 1980; Wakabayashi et al., 1986),

K^+ accelerates phosphoenzyme decomposition and has the nett effect of accelerating enzyme turnover 1.8 to 2 fold (Shigekawa and Pearl, 1976). A similar K^+ acceleration effect (1.8 fold) was observed in this study with the pH stat assay. There is a build-up of E_2P in the absence of K^+, whereas the nett acceleration of turnover by K^+ decreases accumulation of E_2P. The 2.5 fold higher TNP-ATP stimulation observed in the presence of K^+ may be attributable to an acceleration of E_1P to E_2P conversion which is not inhibited by high levels of E_2P build-up. TNP-ATP may therefore activate this rate-limiting intermediary reaction which reflects a major enzyme conformational change linked to the vectorial transfer of Ca^{2+}.

Of significance is the fact that no stimulation of turnover in the range 0-5.0 μM TNP-ATP was observed in the coupled assay, which is in direct contrast with the results obtained for the pH stat assay. TNP-ATP was found to inhibit hydrolysis of Mg.ATP as measured by the coupled enzymatic assay, with $K_{0.5}$ (apparent) = 24 μM (Fig. 16). This inhibitory effect of TNP-ATP could have been attributable to inhibition of the coupling enzymes (PK and LDH), but this possibility was excluded following the results of ADP infusion experiments. TNP-ATP was shown to have a negligible inhibitory effect on the coupling system, and therefore the observed inhibition appears to result from a direct effect on ATPase activity.

TNP-ATP appears to competitively inhibit binding of Mg.ATP to the catalytic nucleotide site in the coupled enzyme assay. pH stat studies using the pseudosubstrate AcP also demonstrated direct competitive inhibition between TNP-ATP and Mg.AcP for the catalytic nucleotide binding site (Fig. 18). In previous studies, TNP-ATP has been shown to inhibit heavy meromysin (Hiratsuka and Uchida, 1973), mitochondrial F_oF_1-ATPase (Grubmeyer and Penefsky, 1981) and the

(Na^+, K^+)-ATPase (Moczydlowski and Fortes, 1981b), by competing for the catalytic site.

The results from the pH stat assay and coupled enzyme assay appear to demonstrate two different effects of TNP-ATP on ATPase activity. TNP-ATP stimulation as measured by the pH stat assay has been attributed to secondary activation of turnover induced by TNP-ATP binding to the regulatory nucleotide site (Dupont et al., 1985). However, TNP-ATP inhibition as measured by the coupled enzyme assay is consistent with competition between TNP-ATP and ATP for the catalytic nucleotide site. ADP liberated during steady-state hydrolysis serves as substrate for the accepting enzyme PK in the coupled enzyme assay. Further experiments were performed to investigate this discrepancy and are discussed in section 4.4. It should be noted that TNP-ATP, in the μM range, and in the presence of 300 μM Mg.ATP, stimulated enzyme turnover in the presence of 100 mM KCl as measured by the pH stat assay. Bishop et al. (1986) have suggested that K^+ inhibits binding of TNP-ATP, which explains the decrease in turnover dependent TNP-ATP fluorescence by KCl. Binding of TNP-ATP and the effects of turnover and of KCl were studied by absorbance difference spectroscopy, and are considered below.

4.3 EFFECTS OF K^+ ON TNP-ATP BINDING TO THE Ca^{2+}-ATPase

Absorbance difference spectra of TNP-ATP bound to the Ca^{2+}-ATPase have proved to be a useful spectroscopic property for providing functional information on enzyme conformational changes (Watanabe and Inesi, 1982; Berman, 1986). The high affinity binding properties of TNP-ATP are reflected in the composite difference absorption spectrum, with respect to free TNP-ATP, produced by the addition of TNP-ATP (2 μM) to SR protein (Fig. 20). The spectrum of TNP-ATP bound to the non-phosphorylated enzyme had a trough at 455 nm and a peak at 510 nm. Phosphorylation with ATP (100 μM) decreased the magnitude of the difference spectrum and produced a new absorbance peak with max at 493 nm. This 493 nm species has been defined as the spectrophotometric equivalent of the ATP plus Ca^{2+}-induced "superfluorescent" species, as the kinetics of its appearance and decay resemble those of ATP plus Ca^{2+}-induced fluorescence (Berman, 1986).

The observed shift in the absorbance difference spectrum following phosphorylation therefore reflects a conformational change occuring at the nucleotide binding site of the Ca^{2+}-ATPase. This change may be linked to conversion of the high energy E_1P conformation to the E_2P conformation which is associated with Ca^{2+} transfer. The appearance of the 493 nm absorbance species appears to be equivalent to the "superfluorescent" form, E_2P, the phosphoenzyme species reported to be responsible for enhanced TNP-ATP fluorescence (Davidson and Berman, 1987).

K^+ has been shown to moderate various intermediary reactions of the catalytic cycle of the Ca^{2+}-ATPase (see section 1.2.1). Addition of KCl (100 mM) decreased the magnitude of the ATP-induced TNP-ATP difference spectrum (Fig. 21), and there was a significant decrease in the 493 nm species. This could reflect K^+-induced

stimulation of hydrolysis of the ADP-sensitive phosphoenzyme, E_2P (Shigekawa and Akowitz, 1979). Scans recorded up to 20 minutes after the addition of KCl showed the disappearance of the 493 nm species and the reappearance of the 510 nm peak. The 510 nm peak, characteristic of TNP-ATP bound to the Ca^{2+}-ATPase, is diminished in intensity as compared to the 510 nm peak observed with the non-phosphorylated enzyme. This 510 nm peak probably corresponds to E_1TNP species and thus provides evidence for TNP-ATP binding to the high energy E_1P conformation in the presence of K^+. The difference in magnitude of the new 510 nm peak, as compared to that observed with the non-phosphorylated enzyme, may reflect changes in the affinity of TNP-ATP bound in the presence of K^+, or competition between liberated ADP and TNP-ATP for the nucleotide binding site.

TNP-ATP fluorescence is sensitive to K^+, and decreases in a manner consistent with K^+ binding to the monovalent cation site (Davidson and Berman, 1985). Therefore the K^+-induced decrease in the 493 nm peak, equivalent to the "superfluorescence" species (Berman, 1986), could be attributable to binding of the cation. The apparent $K_{0.5}$ (42 mM) for K^+ binding as measured by $A_{530-493nm}$ (Fig. 23), is comparable to the $K_{0.5}$ (49 mM) for K^+ binding as measured by inhibition of TNP-ATP fluorescence (Davidson and Berman, 1985), and the $K_{0.5}$ (51 mM) for K^+ induced stimulation of E-P hydrolysis (Shigekawa and Dougherty, 1978).

Absorbance difference spectra were also used to estimate the affinity of TNP-ATP binding to the turning-over enzyme. Extrapolated linear portions of plots of A 493-438 nm indicated decreased TNP-ATP binding in the presence of K^+. This observation supports the proposal of Bishop *et al*. (1986) that K^+ decreases the affinity of TNP-ATP for the nucleotide binding site. Moczydlowski and Fortes (1981a) have reported that K^+ also decreased the

affinity of the (Na^+, K^+)-ATPase for TNP-ATP. However, it should be noted that:

a) The data show that K^+ abolishes the 493 nm species, but the reappearance of the 510 nm difference absorbance peak, following hydrolysis of added ATP, shows that the enzyme is still able to bind some TNP-ATP in the presence of K^+. This 510 nm peak is smaller in magnitude than the initial 510 nm peak and probably corresponds to the E_1TNP species.

b) An increase in ATPase activity upon addition of TNP-ATP is observed with the pH stat assay in the presence of 100 mM KCl. This means that there must be some TNP-ATP binding to cause the effect.

In summary, therefore, although K^+ diminishes TNP-ATP binding, there is an additional effect that diminishes the amount of an intermediate catalytic species, probably $E_2P.2Ca$.

4.4 INTERACTION OF PYRUVATE KINASE WITH THE Ca^{2+}-ATPase

Several mechanisms could explain the apparent discrepancy between TNP-ATP effects as measured by the pH stat and coupled enzymatic assays (see 4.2). The coupling enzymes present in the NADH-coupled assay may have been binding TNP-ATP and thus preventing the nucleotide analog from reaching significant concentrations. Appropriate concentrations of the coupling enzymes (PK and LDH) were therefore included in the pH stat reaction medium in order to ascertain whether there was any change in the TNP-ATP stimulation previously observed. LDH appeared to have no effect on the TNP-ATP induced stimulation of Ca^{2+}-ATPase activity. Similarly, TNP-ATP induced activation of hydrolysis was unaffected by the presence of PK. An unexpected finding was that PK appeared to have a direct effect on Ca^{2+}-ATPase turnover in the absence of PEP, as measured by the pH stat assay (Fig. 27). This protocol would not be expected to decrease [ADP] in the medium. Therefore accumulation of ADP in the pH stat assay does not appear to be responsible for the observed differences. PK stimulated ATPase activity with $K_{0.5}$ (apparent) of 47 μg/ml, corresponding to a mole ratio of approximately 1:1 of PK to Ca^{2+}-ATPase. At this level, the [PK] is 0.20 μM. This will not significantly affect the [ADP] since the $K_{0.5}$ (ADP) for the Ca^{2+}-ATPase is approximately 12 μM (Arav *et al.*, 1983).

Previously observed stimulatory effects of TNP-ATP were measurable over and above the PK-induced activation, showing these two effects to be additive. This indicates that the mechanisms of activation induced by TNP-ATP and PK may involve different loci on the Ca^{2+}-ATPase. TNP-ATP stimulation, as measured by the pH stat assay, has been attributed to binding of the high affinity analog to the

regulatory nucleotide site of the Ca^{2+}-ATPase (Dupont et al., 1985). The possibility that PK may facilitate ADP release from the catalytic site of the Ca^{2+}-ATPase by a direct transfer mechanism (Srivastava and Bernhard, 1986a), and thus promote turnover, was therefore considered.

The effect of PK on ADP-quenching of AcP-induced TNP-ATP fluorescence provides support for the concept of facilitated binding of ADP. Inhibition of AcP-induced TNP-ATP fluorescence upon addition of ADP is a consequence of ATP formation from the E_1P enzyme intermediate. This subsequently causes a depletion in E_2P, the enzyme species associated with increased TNP-ATP fluorescence (Davidson and Berman, 1987). PK enhanced the observed ADP quenching effect and decreased the $K_{0.5}$ (apparent) from 36 μM to 9 μM. This indicates that the presence of PK increases the apparent affinity of the Ca^{2+}-ATPase for ADP. A postulated PK : ADP ligand may therefore function as a more favourable substrate for the Ca^{2+}-ATPase than ADP alone, which provides further evidence for possible PK interaction with the catalytic site of the Ca^{2+}-ATPase.

The direct transfer mechanism (see Introduction section 1.3) implies that the concentrations of free common metabolite during steady state turnover would be less than that predicted by Michaelis-Menten type behaviour. The effect of PK on the steady state concentration of the metabolite ADP was determined at different flux rates in the NADH-coupled assay, in order to monitor the possible existence of a direct transfer mechanism in the observed interaction of PK and the Ca^{2+}-ATPase. A velocity profile of ADP binding to PK was initially generated using the NADH-coupled assay, from which was calculated the apparent Michaelis constants (Fig. 32). The observed PK reaction velocities were greater than those predicted on the basis of free ADP constituting the only

kinetically competent substrate for PK. These findings suggest that the ATPase : ADP complex may function as a competent substrate for the PK catalysed reaction.

The experimental results are interpreted in terms of metabolite transfer via an intermediate enzyme-enzyme complex (Fig. 37). Transfer of ADP from the Ca^{2+}-ATPase to PK may occur via a pathway not involving dissociation and diffusion of ADP (random diffusion pathway). PK may facilitate rate-limiting release of ADP by a mechanism involving a kinetically competent ternary complex, PK : ADP : ATPase (direct transfer pathway)(Srivastava and Bernhard, 1986a).

Several lines of evidence provide support for the possible existence of direct enzyme-enzyme interaction between PK and the Ca^{2+}-ATPase. The concentrations of glycolytic enzymes are high in the muscle sarcoplasmic fluid (Ottaway and Mowbray, 1977). PK is reported to have a concentration of 173 μM in the muscle sarcoplasm (Srivastava and Bernhard, 1986a). Glycolytic enzymes have also been shown to be both adsorbed on actinic muscle filaments and bound to erythrocyte membranes (Kaprelyants, 1988). Cytosolic proteins have been reported to interact with membrane-bound proteins whose sites of interaction extend into the cytosol (Srere, 1985; Srivastava and Bernhard, 1986b). PK stimulation of Ca^{2+}-ATPase activity as measured by the pH stat assay is readily explained by a direct transfer mechanism which catalyses the off rate of ADP from the catalytic site of the Ca^{2+}-ATPase. In addition to this effect, enhanced ADP quenching of AcP-induced TNP-ATP fluorescence in the presence of PK indicates that possible enzyme-enzyme interaction facilitates the transfer of the common metabolite, ADP, in both directions. Srivastava and Bernhard (1987) postulate that the PK

structure is more thermodynamically stable in the reactant-ADP complex than in the product-ATP complex.

ADP is generally considered to dissociate rapidly from the phosphorylated species (Pickard and Jencks, 1984; Froehlich and Heller, 1985; Fernandez-Bella and Inesi, 1986) and not contribute to rate limitation. Therefore rate enhancement by PK may not arise by facilitation of ADP release. An alternative explanation is that PK is stimulating a slower step in the reaction cycle such as $E_1\text{-}P \longrightarrow E_2\text{-}P$, in the presence of KCl.

Evidence of direct interaction between the Ca^{2+}-ATPase and PK was sought by cross-linking studies. The postulate was that the two enzymes would become covalently linked in the presence of glutaraldehyde (see section 3.4.5). Intermolecular cross-linking produced a concentration and time-dependent formation of cross-linked oligomers of the individual enzyme species. No interpolypeptide interaction between the Ca^{2+}-ATPase and PK was observed, however, under the described conditions. The cross-linked aggregation pattern appeared to be unaffected by the presence of ADP or ATP.

The apparent absence of interaction could be due to a number of possible reasons. Intermolecular cross-linking between the enzyme species may not be favourable under the experimental conditions. For example, enzyme-enzyme interaction between PK and Ca^{2+}-ATPase may be transient, and therefore not able to be detected by glutaraldehyde cross-linking and subsequent SDS-PAGE analysis. Srivastava and Bernhard (1987) in fact report that enzyme-enzyme complexes are transient and their formation is concentration dependent. A further possibility is that a specific PK : ATPase oligomer cannot be cross-linked by glutaraldehyde beause of inappropriately positioned reactive residues. The interaction of

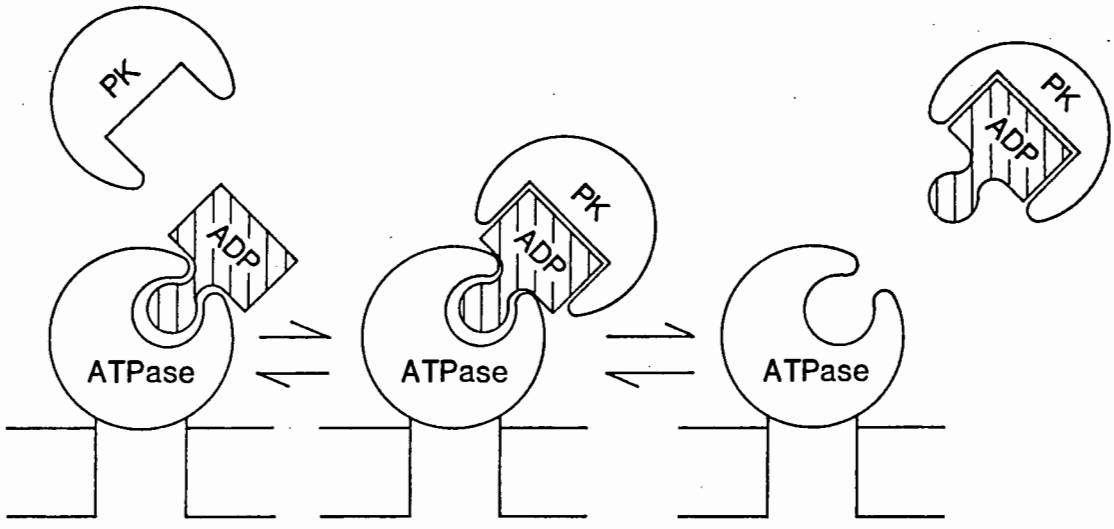

Figure 37: Schematic representation of the proposed mechanism for direct transfer of ADP between PK and the Ca^{2+}-ATPase (based on the model of Srivastava and Bernhard, 1986a).

5.0 CONCLUSION

This study was originally aimed at characterisation of the properties of the ATP analog, TNP-ATP, which binds with high affinity to the catalytic site on the non-phosphorylated Ca^{2+}-ATPase of sarcoplasmic reticulum (Watanabe and Inesi, 1982; Dupont et al., 1982). Evidence suggests that the enhanced fluorescence of TNP-ATP, observed upon enzyme turnover, can be attributed to binding of the nucleotide analog to the regulatory site (Dupont et al., 1985; Bishop et al., 1987).

The characteristics of isolated terminal cisternae (TC) and light SR (LSR) fractions with respect to turnover-dependent TNP-ATP fluorescence were investigated. TNP-ATP fluorescence enhancement was diminished in TC as compared to LSR. This decreased fluorescence signal could be a function of the lower Ca^{2+}-ATPase content of the terminal SR region. Alternatively, this phenomenon could be attributable to the presence of open Ca^{2+}-release channels. Functional characterisation of the SR fractions provided support for the localisation of the release channels in TC, which results in low nett energised Ca^{2+} transport and subsequent decreased levels of E_2P, the phosphoenzyme species responsible for enhanced TNP-ATP fluorescence (Davidson and Berman, 1987).

The TNP-ATP absorption spectrum undergoes a significant change following binding to the Ca^{2+}-ATPase, and this spectroscopic property has proved to be useful in monitoring conformational changes occurring during enzyme catalysis. The effect of K^+ on TNP-ATP binding to the Ca^{2+}-ATPase was determined from TNP-ATP absorbance difference spectra. The results of these studies suggested that the enzyme has a decreased affinity for TNP-ATP in the presence of K^+. TNP-ATP was still bound, however, as shown by

the appearance of a postulated E_1TNP species following ATP hydrolysis. The precise mechanism of these K^+-induced effects remains to be elucidated, but decreased TNP-ATP binding appears to be related to catalytic conformational changes consistent with K^+ binding to the monovalent cation site.

TNP-ATP was shown to stimulate Ca^{2+}-ATPase activity as measured by the pH stat assay, despite the inclusion of K^+ in the reaction medium. This provides additional evidence for TNP-ATP binding to the Ca^{2+}-ATPase in the presence of K^+. The stimulatory effects of TNP-ATP and millimolar Mg.ATP were complementary, and are described in terms of secondary activation of enzyme turnover induced by binding to the regulatory nucleotide site. However, TNP-ATP appeared to competitively inhibit binding of Mg.ATP to the catalytic site as measured by the NADH-coupled enzyme assay. The direct inhibition of the catalytic site by TNP-ATP appears to overcome possible stimulation of turnover.

Investigation into the apparent discrepancy between those observed TNP-ATP effects lead to the discovery that one of the coupling enzymes, namely pyruvate kinase (PK), directly stimulated ATPase activity as measured by the pH stat assay. This observation could account for the fact that numerous workers have found consistently higher ATPase activity in the coupled enzyme assay as compared to direct enzyme assays, e.g. pH stat or P_i release (Hasselbach, personal communication). The previously observed TNP-ATP stimulatory effects on enzyme turnover were measurable over and above PK-induced activation, indicating that the mechanisms of these effects involve different loci on the enzyme. Further studies revealed that PK enhanced ADP quenching of AcP-induced TNP-ATP fluorescence of the Ca^{2+}-ATPase, suggesting possible enzyme-enzyme interaction via the common metabolite, ADP.

Using experimentally determined kinetic parameters for ADP binding to PK, predicted reaction velocities were lower than those observed at different flux rates measured by the NADH-coupled assay, assuming free ADP constitutes the only kinetically competent substrate. The experimental findings are interpreted in terms of direct transfer of metabolite ADP between PK and the Ca^{2+}-ATPase (Srivastava and Bernhard, 1986a). PK may facilitate rate limiting ADP release from the Ca^{2+}-ATPase via the formation of a kinetically competent ternary complex, PK : ADP : ATPase. Further studies involving the effect of PK on the partial reactions of the Ca^{2+}-ATPase catalytic cycle may lead to the elucidation of the proposed interaction mechanism.

The postulated PK : Ca^{2+}-ATPase interaction may have physiological significance, in that the glycolytic enzymes are reported to exist at high concentrations in the muscle sarcoplasmic fluid (Ottaway and Mowbray, 1977). Srivastava and Bernhard (1986a, 1987) predict that, due to the high intracellular concentrations of many enzymes, transfer of metabolites via direct enzyme-enzyme interaction may be functionally relevant. Owing to the notable catalytic efficiency of enzymes, enzymological studies are usually performed with dilute solutions which are far from physiological. However, the potential existence of enzyme-enzyme interactions in the concentrated cellular fluid may significantly alter the spatial organisation of enzymes, and have important implications with respect to the measured energetics and kinetics of metabolic processes.

The Ca^{2+}-ATPase of sarcoplasmic reticulum has been extensively investigated, and represents one of the most well-characterised examples of the process of active transport. The catalytic mechanism of the enzyme is modulated in a relatively complex manner by substrate and ligand binding, as is evidenced in this review.

For these reasons, the effect of different probes such as TNP-ATP are useful in providing insight into the catalytic and transport activity of the Ca^{2+}-ATPase. Similarly, the effect of PK on ADP binding and release in this study reveals the possibility for more intense study of PK : ATPase association, and protein-protein interactions in general.

6.0 REFERENCES

Anderson, J.P., Lassen, K. and Moller, J.V. (1985) J. Biol. Chem. 260, 371-380

Anderson, J.P., Moller, J.V. and Jorgenson, P.L. (1982) J. Biol. Chem. 257, 8300-8307

Arav, R., Aderem, A.A. and Berman, M.C. (1983) J. Biol. Chem. 258, 10433-10438

Bailin, G. (1980) Biochem. Biophys. Acta. 624, 511-521

Barlogie, B., Hasselbach, W. and Makinose, M. (1971) Fed, European Biochem. Soc. Letters 12, 267-268

Bastide, F., Meissner, G., Fleischer, S. and Post R.L. (1973) J. Biol. Chem. 248, 8385-8391

Bennet, H.S. and Porter, K.R. (1953) Am. J. Anat. 93, 61-105

Berman, M., McIntosh, D. and Kench, J. (1977) J. Biol. Chem. 252, 994-1001

Berman, M.C. (1986) J. Biol. Chem. 261, 16494-16501

Berman, M.C. (1987) Biochim. Biophys. Acta. 694, 95-121

Bishop, J.E. and Al-Shawi, M.K. (1988) J. Biol. Chem. 263, 1886-1892

Bishop, J.E., Johnson, J.D. and Berman, M.C. (1984) J. Biol. Chem. 259, 15163-15171

Bishop, J.E., Nakamoto, R.K. and Inesi, G. (1986) Biochemistry 25, 696-703

Bodley, A.L. and Jencks, W.P. (1987) J. Biol. Chem. 262, 13997-14004

Brandt, C.J., de Leon, S., Martin, D.R. and Maclennan, D.H. (1987) J. Biol. Chem. 262, 3768-3774i

Brandt, C.J., Green, N.M., Korczak B. and Maclennan, D.H. (1986) Cell. 44, 597-607

Broglie, K.E. and Takahishi, M. (1983) J. Biol. Chem. 258, 12940-12946

Cable, M.B., Feher, J.J. and Briggs, F.N. (1985) Biochemistry 24, 5612-5619

Campbell, K.P. and Maclennan, D.H. (1981) J. Biol. Chem. 256, 4626-4632

Campbell, K.P. and Maclennan, D.H. (1983) J. Biol. Chem. 258, 1391-1394

Carvalho, M.G.C., De Souza, D.G. and de Meis, L. (1976) J. Biol. Chem. 251, 3629-3636

Carvalho-Alves, P.C., Oliviera, C.R.G. and Verjovski-Almeida, S. (1985) J. Biol. Chem. 260, 4282-4287

Caswell, A.H. and Pressman, B.C. (1972) Biochem. Biophys. Res. Comm. 49, 292-298

Chaloub, R.M. and de Meis, L. (1980) J. Biol. Chem. 255, 6168-6172

Champeil, P., Buschlem, S. and Gullain, F. (1981) Biochemistry 20, 1520-1524

Champeil, P., Gingold, M.P., Gullain, F. and Inesi, G. (1983) J. Biol. Chem. 258, 4453-4458

Champeil, P., Gullain, F. (1986) Biochemistry 25, 7623-7633

Champeil, P., Le Maire, M., Anderson, J.P., Gullain, F., Gingold, M., Lund, S., Moller, J.V. (1986) J. Biol. Chem. 261, 16372-16384

Chevallier, J. and Butow, R. (1971) Biochemistry 10, 2733-2737

Chiesi, M. (1984) Biochemistry 23, 3899-3907

Chiesi, M. and Carafoli, E. (1982) J. Biol. Chem. 257, 584-591

Chu, A., Volpo, P., Costello, B. and Fleischer, S. (1986) Biochemistry 25, 8315-8324

Chyn, T. and Martonosi, A. (1977) Biochim. Biophys. Acta 468, 114-126

Coan, C. and Inesi, G. (1977) J. Biol. Chem. 252, 3044-3049

Coll, R.J. and Murphy, A.J. (1985) FEBS Letts. 187, 131-134

Costello, B., Chadwick, C., Saito, A., Maurer, A., Chu, A. and Fleischer, S. (1986) J. Cell Biol. 103, 741-754

Craig, W.S. (1982) Biochemistry 21, 2667-2674

Csermely, P., Katopis, C., Wallace, B.A., Martonosi, A. (1987) Biochem. J. 241, 663-669

Davidson, G. and Berman, M. (1987) J. Biol. Chem. 262, 7041-7046

Davidson, G.A. and Berman, M.C. (1985) J. Biol. Chem. 260, 7325-7329

Dean, W.L. and Tanford, C. (1987) Biochemistry 17, 1683-1690

Degani, C. and Boyer, P.D. (1973) J. Biol. Chem. 248, 8222-8226

de Meis, L. (1971) J. Biol. Chem. 246, 4764-4773

de Meis, L. (1976) J. Biol. Chem. 251, 2055-2062

de Meis, L. (1981) The Sarcoplasmic Reticulum-Transport and Energy Transduction, Bittar, E.E. ed., John Wiley and Sons, New York

de Meis, L. and Boyer, P.D. (1978) J. Biol. Chem. 253, 1556-1559

de Meis, L. and Fialho de Mello, M.C. (1973) J. Biol. Chem. 248, 3691-3701

de Meis, L. and Sorenson, M.M. (1975) Biochem. 14, 2739-2744

de Meis, L. and Tume, R. (1977) Biochemistry 16, 4455-4463

de Meis, L. and Vianna, A.L. (1979) Ann. Rev. Biochem. 48, 275-292

Duggan, P.F. (1977) J. Biol. Chem. 252, 1620-1627

Dupont, Y. (1977) Eur. J. Biochem. 72, 185-190

Dupont, Y. (1980) Eur. J. Biochem. 109, 231-238

Dupont, Y. (1982) Biochim. Biophys. Acta 688, 75-87

Dupont, Y. (1983) FEBS Lett. 161, 14-20

Dupont, Y. (1984) FEBS Lett. 156, 93-98

Dupont, Y. and Leigh, J.B. (1978) Nature, 273, 396-398

Dupont, Y., Chapran, Y. and Pougeois, R. (1982) Biochem. Biophys. Res. Comm. 10, 1272-1279

Dupont, Y., Pougeois, R., Ronjat, M. and Verjovski-Almeida, S. (1985) J. Biol. Chem. 260, 7241-7249

Dux, L. and Martonosi, A. (1983a) J. Biol. Chem. 258, 2599-2603

Dux, L. and Martonosi, A. (1983b) J. Biol. Chem. 258, 11896-11902

Ebashi, S. and Lipmann, F. (1962) J. Cell. Biol. 14, 389-400

Ehrlich, S. (1987) Biochem. J. 248, 269-271

Eisenberg, B.R. and Eisenberg, R.S. (1982) J. Gen. Physiol. 79, 1-19

Eletr, S. and Inesi, G. (1972) Biochim. Biophys. Acta 282, 174-179

Endo, M. (1977) Physiol. Rev. 57, 71-108

Fagan, M.H. and Dewey, T.G. (1986) J. Biol. Chem. 261, 3654-3660

Fernandez-Belda, F. and Inesi, G. (1986) Biochemistry 25, 8083-8089

Fernandez-Belda, F., Kurzmack, M. and Inesi, G. (1984) J. Biol. Chem. 259, 9687-9698

Foster, J.F. and Sterman, M.D. (1956) J. Am. Chem. Soc. 78, 3656-3660

Franzini-Armstrong, C. (1970) J. Cell. Biol. 47, 488-499

Franzini-Armstrong, C. (1980) Fed. Proc. 39, 2403-2409

Franzini-Armstrong, C., Landmeser, L. and Pilar, G. (1975) J. Cell. Biol. 64, 493-497

Franzini-Armstrong, C., Porter, K.R. (1964) J. Cell. Biol. 22, 675-696

Froehlich, J.P. and Heller, P.F. (1985) Biochemistry 24, 126-136

Froehlich, J.P. and Taylor, E.W. (1975) J. Biol. Chem. 250, 2013-2021

Garrahan, P.J., Rega, A.F. and Alonso, G.L. (1976) Biochim. Biophys. Acta. 448, 121-132

Green, N.M., Allen, G. and Hebdon, G.M. (1980) Ann. NY Acad. Sci. 358, 149-158

Grubmeyer, C. and Penefsky, H.S. (1981) J. Biol. Chem. 256, 3718-3727

Gullain, F., Champeill, P. and Boyer, P.D. (1984) Biochemistry 23, 4754-4761

Gullain, F., Champeill, P., Lacapere, J. and Gingold, M.P. (1981) J. Biol. Chem. 256, 6140-6147

Hasselbach, W. (1964) Prog. Biophys. Mol. Biol. 14, 167-222

Hasselbach, W. (1978) Biochim. Biophys. Acta 515, 23-53

Hasselbach, W. and Makinose, M. (1961) Biochem. Z. 333, 518-528

Hebdon, G.M., Cunningham, L.W. and Green, N.M. (1979) Biochem. J. 179, 135-139

Hermann, R., Jaenicki, R. and Rudolph, R. (1981) Biochemistry 20, 5195-5201

Hermann, T.R., Gangola, P. and Shamoo, A.E. (1986) Eur. J. Biochem. 158, 555-560

Highsmith, S. and Cohen, J.A. (1987) Biochemistry 26, 154-161

Hill, T. and Inesi, G. (1982) Proc. Natl. Acad. Sci. USA 79, 3978-3982

Hiratsuka, T. (1976) Biochim. Biophys. Acta 453, 293-297

Hiratsuka, T. (1982) Biochim. Biophys. Acta 719, 509-517

Hiratsuka, T. and Uchida, K. (1973) Biochim. Biophys. Acta 330, 635-647

Horgan, D.J., Tume, R.K. and Newbold, R.P. (1972) Analytical Biochemistry 48, 147-152

Howell, J.N. (1982) Membr. Biochem. 4, 235-245

Huskins, K.R., Bernhard, S.A. and Dahlquist, F.W. (1982) Biochemistry 21, 4180-4188

Huxley, H.E. (1964) Nature 202, 1067-1071

Hymel, L., Maurer, A., Berenski, C., Junng, C.Y. and Fleischer, S. (1984) J. Biol. Chem. 259, 4890-4895

Ikemoto, N. (1974) J. Biol. Chem. 249, 649-651

Ikemoto, N. (1975) J. Biol. Chem. 250, 7219-7224

Ikemoto, N., Antoniu, B. and Meszaros, L. (1985) J. Biol. Chem. 260, 14096-14100

Ikemoto, N., Bhatnager, G.M., Nagy, B. and Gergely, J. (1972) J. Biol. Chem. 247, 7835-7837

Ikemoto, N., Miyao, A. and Kurobe, Y. (1981) J. Biol. Chem. 256, 10809-10814

Ikemoto, N., Morgan, J.F. and Yamada, S. (1978) J. Biol. Chem. 253, 8027-8033

Inesi, G. (1971) Science 171, 901-903

Inesi, G. (1972) Ann. Rev. Biophys. Bioenerg. 1, 191-210

Inesi, G. (1987) J. Biol. Chem. 262, 16338-16342

Inesi, G., Goodman, J.J. and Watanabe, S. (1967) J. Biol. Chem. 242, 4637-4643

Inesi, G., Kursmack, M., Coan, C. and Lewis, D.E. (1980) J. Biol. Chem. 255, 3025-3031

Inesi, G., Maring, E., Murphy, A.J. and Mcfarland, B.H. (1970) Arch. Biochim. Biophys. 138, 285-294

Inui, M., Saito, A. and Fleischer, S. (1987) J. Biol. Chem. 262, 1740-1747

Jaworek, D., Gruber, W. and Bergmeyer, H.U. (1974a) in Methods of Enzymatic Analysis Vol. 4, Academic Press, New York, 2099

Jaworek, D., Gruber, W. and Bergmeyer, H.U. (1974b) in Methods of Enzymatic Analysis Vol. 4, Academic Press, New York, 2128-2131

Jencks, W.P. (1980) Adv. Enzymol. 51, 75-106

Jencks, W.P. (1983) Curr. Top. Membr. transp. 19, 1-19

Jilka, R.L., Martonosi, A.M. and Tillack,, T.W. (1975) J. Biol. Chem. 250, 7511-7524

Kanazawa, T., Yamada, S., Yamamoto, T. and Tonomura, Y. (1971) J. Biochem. (Tokyo) 70, 95-123

Kaprelyants, A.S. (1988) TIBS 13, 43-46

Katz, A.M., Repke,D.I., Dunnett, J. and Hasselbach, W. (1977) J. Biol. Chem. 252, 1950-1956

Kawakita, M., Yasuka, K. and Kasiro, Y. (1980) J. Biochem. 87, 609-617

Khananshvili, D. and Jencks, W.P. (1988) Biochemistry 27, 2943-2952

Kim, D.H., Ohnishi, S.T. and Ikemoto, N. (1983) J. Biol. Chem. 258, 9662-9668

Knowles, A. and Racker, E. (1975) J. Biol. Chem. 250, 1949-1951

Knowles, J.R. (1980) Ann. Rev. Biochem. 49, 877-919

Kolthoff, J.M., Shore, W.S., Tan, B.H. and Matsuka, M. (1965) Anal. Biochem. 12, 497-508

Kornberg, A., Kornberg, S.R. and Simms, E.S. (1956) Biochim. Biophys. Acta 20, 215-227

Kosk-Kosicka, D., Kurzmack, M. and Inesi, G. (1983) Biochemistry 22, 2559-2567

Laemmli, U. (1970) Nature 227, 680-685

Lai, F.A., Erickson, H.P., Rousseau, E., Liu, Q. and Meissner, G. (1988) Nature 331, 315-319

Lehninger, A.L. (1975) Biochemistry, New York, Worth 2nd edition.

Leonardo, K.S. and Kutchai, H. (1985) Biochemistry 24, 4876-4884

Liguri, G., Stefani, M., Berti, A., Nassi, P. and Ramponi, G. (1980) Arch. Biochem. Biophys. 200, 357-363

Louis, C. and Shooter, E.M. (1972) Arch. Biochem. Biophys. 153, 641-655

Louis, C.F., Saunders, M.J. and Holroyd, J.A. (1977) Biochim. Biophys. Acta 493, 78-92

Lowry, O.H., Rosebrough, N.J., Farr, A.L. and Randall, R.J. (1951) J. Biol. Chem. 193, 265-275

Maclennan, D.H. and Holland, P.C. (1975) Ann. Rev. Biophys. Bioeng. 4, 377-404

Maclennan, D.H. and Reithmeier, R.A.F. (1982) in Membranes and Transport, Vol. 1, Martonosi, A. ed., Plenum, New York, 567-571

Maclennan, D.H. and Reithmeier, R.A.F. (1985) in Structure and Function of Sarcoplasmic Reticulum, Fleischer, S. and Tonomura, Y. eds., Academic Press, New York, 91-100

Maclennan, D.H. and Wong, P.T.S. (1971) Proc. Natl. Acad. Sci. USA 68, 1231-1235

Maclennan, D.H., Brandl, C.J., Korczak, B. and Green, N.M. (1985) Nature 316, 696-700

Makinose, M. (1971) FEBS Letts. 12, 269

Makinose, M. (1972) Fed. European Biochem. Soc. Letters 25, 113-115

Makinose, M. and Boll, W. (1979) in Cation Fluxes Across Biomembranes Mukohata, Y. and Packer, L. eds., Academic Press, New York, 89-100

Makinose, M. and Hasselbach, W. (1971) FEBS Lett. 12, 271-272

Makinose, M. and The, R. (1965) Biochem. Z. 343, 383-393

Marai, L. and Kuksis, A. (1973) Canad. J. Biochem. 51, 1248-1252

Martonosi, A. (1967) Biochem. Biophys. Res. Commun. 26, 753-757

Martonosi, A. and Ferretos, R. (1964) J. Biol. Chem. 239, 659-668

Martonosi, A., Dux, L., Taylor, K.A., Csermely, P., Mullner, N., Pikula, S., Papp, S., Varga, S., Jona, I. and Keresztes, T. (1987) Acta Biochim. Biophys. Hung. 22, 263-276

Mastro, A.M. and Keith, A.D. (1984) J. Cell. Biol. 99, 180-187

Masuda, H. and de Meis, L. (1973) Biochemistry 12, 4581-4585

Maurer, A., Tanaka, M., Ozawa, T. and Fleisher, S. (1985) Proc. Natl. Acad. Sci. USA 82, 4036-4040

McIntosh, D. and Berman, M.C. (1978) J. Biol. Chem. 253, 5140-5146

McIntosh, D.B. (1984) Curr. Top. Cell. Regul. 24, 471-483

McIntosh, D.B. and Boyer, P.D. (1983) Biochemistry 22, 2867-2875

McIntosh, D.B. and Ross, D.C. (1985) Biochemistry 24, 1244-1251

Means, G.E. and Feeney, R.E. (1971) Chemical Modification of Proteins, Holden-Day, Inc., San Francisco

Meissner, G. (1973) Biochim. Biophys. Acta 298, 906-926

Meissner, G. (1975) Biochim. Biophys. Acta 389, 51-68

Meissner, G. and Fleisher, S. (1971) Biochim. Biophys. Acta 241, 356-378

Meissner, G., Conner, G.E. and Fleischer, S. (1973) Biochim. Biophys. Acta 298, 246-269

Meissner, G., Darling, E. and Eveleth, J. (1986) Biochemistry 25, 236-244

Meltzer, S. and Berman, M.C. (1985) J. Biol. Chem. 258, 4244-4253

Mitchinson, C., Wilderspin, A.F., Trumanian, B.J. and Green N.M. (1982) FEBS Lett. 146, 87-92

Moczydlowski, E.G. and Fortes, F.A.G. (1981a) J. Biol. Chem. 256, 2346-2356

Moczydlowski, E.G. and Fortes, F.A.G. (1981b) J. Biol. Chem. 256, 2357-2366

Moller, J.V., Lind, K.E. and Anderson, J.P. (1980) J. Biol. Chem. 255, 1912-1920

Morawiecki, A. (1960) Biochim. Biophys. Acta 44, 602-604

Morrii, H., Takisawa, H. and Yamamoto, T. (1985) J. Biol. Chem. 260, 11536-11541

Murphy, A.J. (1976) Biochem. Biophys. Res. Commun. 70, 160-166

Murphy, A.J. (1976) Biochemistry 15, 4492-4496

Murphy, A.J. (1977) Arch. Biochem. Biophys. 180, 114-120

Nagai, T., Makinose, M. and Hasselbach, W. (1960) Biochim. Biophys. Acta 43, 223-238

Nakamoto, R. and Inesi, G. (1984) J. Biol. Chem. 259, 2961-2970

Neet, K.E. and Green, N.M. (1977) Arch. Biochem. Biophys. 178, 588-597

Ostwald, T.J. and Maclennan, D.H. (1974) J. Biol. Chem. 249, 974-979

Ostwald, T.J., Maclennan, D.H. and Dorrinton, K.J. (1974) J. Biol. Chem. 249, 5867-5871

Ottaway, J.H. and Mowbray, J. (1977) Curr. Top. Cell. Regul. 12, 107-208

Owens, K., Ruth, R.C. and Weglicki, W.B. (1972) Biochim. Biophys. Acta 288, 479-481

Peachey, L.D. (1965) J. Cell. Biol. 25, 209-231

Pessah, I.N., Francini, A., Scales, D., Waterhouse, A. and Casida, J. (1986) J. Biol. Chem. 261, 8643-8648

Pick, U. (1981) Eur. J. Biochem. 121, 187-195

Pick, U. and Karlish, S.J.D. (1980) Biochim. Biophys. Acta, 626, 255-261

Pick, U. and Karlish, S.J.D. (1982) J. Biol. Chem. 257, 6120-6126

Pick, U. and Racker, E. (1979) Biochemistry 18, 108-113

Pickart, C.M. and Jencks, W.P. (1984) J. Biol. Chem. 259, 1629-1643

Porter, K.R. and Palade, G.E. (1957) J. Biophys. Biochem. Cytol. 3, 269-299

Pucell, A. and Martonosi, A. (1971) J. Biol. Chem. 249, 3389-3397

Racker, E. (1972) J. Biol. Chem. 247, 8198-8200

Racker, E. and Eytan, E. (1975) J. Biol. Chem. 250, 7533-7534

Reynard, A.M., Hass, L.F., Jacobsen, D.D. and Boyer, P.D. (1961) J. Biol. Chem. 236, 2277-2282

Ross, D.C. and McIntosh D.B. (1987) J. Biol. Chem. 262, 2042-2049

Rossi, B., Leone, F., Gache, C. and Lazdunski, M. (1979) J. Biol. Chem. 254, 2302-2307

Rubin, B.B. and Katz, A.M. (1967) Science 158, 1189-1190

Ryter, A. and Kellenberg, E. (1958) Z. Naturf. 13, 597

Saito, A., Seiler, S., Chu, A. and Fleisher, S. (1984) J. Cell. Biol. 99, 875-885

Saito, K., Imamura, Y. and Kawakita, M. (1984) J. Biochem. (Tokyo) 95, 1297-1304

Scarpa, A., Beldassere, J. and Inesi, G. (1972) Gen. Physiol. 60, 35-739

Schwartzenbach, G. (1957) Complexometric Titration (translated by Inving, H.M.) Methuen, London

Scofano, H., Vierya, A. and de Meis, L. (1979) J. Biol. Chem. 254, 10227-10231

Scott, T.L. (1985) J. Biol. Chem. 260, 14421-14423

Seebregts, C.J. and McIntosh D.B. (1988) Labelling of Catalytic and Regulatory Nucleotide Binding Sites of Sarcoplasmic Reticulum Ca^{2+}-ATPase With New Photoaffinity Probes. 9th Congress of SA Biochemical Society, Wilderness

Segal, I.H. (1976) Biochemical Calculations, 2nd ed., John Wiley and Sons, New York, 246-252

Seiler, S., Wegener, A.D, Whang, D.D., Hathaway, D.R. and Jones, L.R. (1984) J. Biol. chem. 259, 8550-8557

Shamoo, A.E., Ryan, T.E., Stewart, P.S. and Maclennan, D.H. (1976) J. Biol. Chem. 251, 712-719

Shigekawa, M. and Akowitz, A.A. (1979) J. Biol. Chem. 254, 4726-4730

Shigekawa, M. and Dougherty, J.P. (1978) J. Biol. Chem. 253,1458-1464

Shigekawa, M. and Kanazawa, T. (1982) J. Biol. Chem. 257, 7657-7665

Shigekawa, M. and Pearl, L.J. (1976) J. Biol. Chem. 251, 6947-6952

Shigekawa, M., Doughertry, J.P. and Katz, A.M. (1978) J. Biol. Chem. 253, 1442-1450

Shigekawa, M., Wakabayashi,S. and Nakamura, N. (1983) J. Biol. Chem. 258, 8698-8707

Shosan, V., Maclennan, D.H. and Wood, D. (1981) Proc. Natl. Acad. Sci. USA 78, 451-462

Shoshan-Barmatz, V. (1987) Biochem. J. 243, 165-173

Silva, J.L. and Verjovski-Almeida, S. (1983) Biochemistry 22, 707-716

Somlyo, A.V. (1979) J. Cell. Biol. 80, 743-750

Somlyo, A.V., Gonzalez-Serratos, H., Shuman, H., McClellan, G. and Somlyo, A.P. (1981) J. Cell. Biol. 90, 577-594

Souza, D.O. and de Meis, L. (1976) J. Biol. Chem. 251, 6355-6359

Squier, T.C., Bigelow, D.J., Garcia de Ancos, J. and Inesi, G. (1987) J. Biol. Chem. 262, 4748-4754

Srere, P.A. (1985) in Organised Multienzyme Systems, Welch, G.R. ed., Orlando, Fla: Academic, 1-61

Srivastava, D.K. and Bernhard, S.A. (1986a) Science 234, 1081-1086

Srivastava, D.K. and Bernhard, S.A. (1986b) Curr. Top. Cell Regul. 28, 1-68

Srivastava, D.K. and Bernhard, S.A. (1987) Ann. Rev. Biophys. Biophys. Chem. 16, 175-204

Stahl, N. and Jencks, W.P. (1987) Biochemistry 26, 7654-7667

Steinmetz, M.A. and Deal, W.C. Jr. (1966) Biochemistry 5,1399-1405

Stewart, P.S. and Maclennan, D.H. (1974) J. Biol. Chem. 249, 985-993

Sumida, M. and Tonomura, Y. (1974) J. Biochem. (Tokyo) 75, 283-297

Tada, M., Yamamoto, T. and Tonomura, Y. (1978) Physiol. Rev. 58, 1-79

Takisawa, H. and Makinose, M. (1981) Nature (London) 298, 271-273

Takisawa, H. and Makinose, M. (1983) J. Biol. Chem. 258, 2986-2992

Tanford, C., Reynolds, J.A. and Johnson, E.A. (1987) Proc. Natl. Acad. Sci. USA 84, 7094-7098

Taylor, E.W. (1979) CRC Crit. Rev. Biochem. 103-164

Taylor, J.S. and Hattan, D. (1979) J. Biol. Chem. 254, 4402-4407

Taylor, K.A., Dux, L. and Martonosi, A. (1986) J. Mol. Biol. 187, 417-427

Thorley-Lawson, D.A. and Green, N.M. (1973) Eur. J. Biochem. 40, 403-413

Thorley-Lawson, D.A. and Green, N.M. (1977) Biochem. J. 167, 739-748

Vanderkooi, J.M., Ierokomos, A., Nakamura, H. and Martonosi, A. (1977) Biochemistry 16, 1262-1267

Varga, S., Csermely, P., Mullner, N., Dux, L. and Martonosi, A. (1987) Biochim. Biophys. Acta 896, 187-195

Veech, R.L., Lawson,J.W.R., Cornell, N.W. and Krebs, H.A. (1979) J. Biol. Chem. 254, 6538-6547

Verjovski-Almeida, S. and de Meis, L. (1977) Biochemistry 16, 329-334

Verjovski-Almeida, S. and Inesi, G. (1979) J. Biol. Chem. 254, 4402-4407

Vianna, A.L. (1975) Biochim. Biophys. Acta 410, 389-406

Volpe, P., Zorzato, F., Pozzan, T., Salviati, G. and Di Virgilo, F. (1987) Methods in Enzymology, 141, 3-53

Wakabayashi, S. and Shigekawa, M. (1987) J. Biol. Chem. 262, 11524-11531

Wakabayashi, S., Oqurusu, T. and Shigekawa, M. (1986) J. Biol. Chem. 261, 9762-9769

Wakil, S.J., Stoops, J.K. and Joshi, V.C. (1983) Ann. Rev. Biochem. 52, 537-579

Watanabe, T. and Inesi, G. (1982) J. Biol. Chem. 257, 11510-11514

Watanabe, T., Lewis, D., Nakamoto, R., Kurzmack, M., Fronticelli, C. and Inesi, G. (1981) Biochemistry 20, 6617-6625

Weber, A., Herz, R. and Reiss, I. (1966) Biochem. Z. 345, 329-369

Weber, J.P. and Bernhard, S.A. (1982) Biochemistry 21, 4189-4194

Welch, G.R. (1977) Prog. Biophys. Molec. Biol. 32, 103-191

Wilkinson, G.N. (1961) Biochem. J. 80, 324-332

Winegrad, S. (1970) J. Gen. Physiol. 55, 77-88

Winegrad, S. (1982) Ann. Rev. Physiol. 44, 451-462

Yamada, S. and Ikemoto, N. (1978) J. Biol. Chem. 253, 6801-6807

Yamada, S. and Ikemoto, N. (1980) J. Biol. Chem. 255, 3108-3119

Yamada, S. and Tonomura, Y. (1972) J. Biochem. 71, 1101-1104

Yamada, S., Sumida, M. and Tonomura, Y. (1972) J. Biochem. (Tokyo) 72, 1537-1548

Yamamoto, F., Takisawa, H. and Tonomura, Y. (1979) Curr. Top. Bioenerg. 9, 179-236

Yamamoto, H., Yagaya, M., Fukui, T. and Kawakita, M. (1988) J. Biochem. 103, 452-457

Yamamoto, T. and Tonomura, Y. (1967) J. Biochem. (Tokyo) 62, 558-575

Yamamoto, T. and Tonomura, Y. (1982) J. Biochem. 91, 477-486

Yang, S.Y., Bittman, R. and Schulz, H. (1985) J. Biol. Chem. 260, 2862-2868